OPTIMAL FITTING AND VALIDATION OF COMPUTER SIMULATED PROBABILITY OF DETECTION CURVES FROM ULTRASONIC INSPECTION

Mariana Burrowes Moreira Guimarães

Dissertação de Mestrado apresentada ao Programa de Pós-graduação em Engenharia Metalúrgica e de Materiais, COPPE, da Universidade Federal do Rio de Janeiro, como parte dos requisitos necessários à obtenção do título de Mestre em Engenharia Metalúrgica e de Materiais.

Orientadores: Gabriela Ribeiro Pereira
Luís Marcelo Marques Tavares

Rio de Janeiro
Julho de 2018

OPTIMAL FITTING AND VALIDATION OF COMPUTER SIMULATED PROBABILITY OF DETECTION CURVES FROM ULTRASONIC INSPECTION

Mariana Burrowes Moreira Guimarães

DISSERTAÇÃO SUBMETIDA AO CORPO DOCENTE DO INSTITUTO ALBERTO LUIZ COIMBRA DE PÓS-GRADUAÇÃO E PESQUISA DE ENGENHARIA (COPPE) DA UNIVERSIDADE FEDERAL DO RIO DE JANEIRO COMO PARTE DOS REQUISITOS NECESSÁRIOS PARA A OBTENÇÃO DO GRAU DE MESTRE EM CIÊNCIAS EM ENGENHARIA METALÚRGICA E DE MATERIAIS.

Examinada por:

_____

Prof[a]. Gabriela Ribeiro Pereira, D.Sc.

_____

Prof. Luís Marcelo Marques Tavares, Ph.D.

_____

Prof. Daniel Alves Castello, D.Sc.

_____

Dr. Romeu Ricardo da Silva, D.Sc.

RIO DE JANEIRO, RJ – BRASIL

JULHO DE 2018

Guimarães, Mariana Burrowes Moreira

Optimal Fitting and Validation of Computer Simulated Probability of Detection Curves from Ultrasonic Inspection / Mariana Burrowes Moreira Guimarães. – Rio de Janeiro: UFRJ/COPPE, 2018.

XV, 101 p.: il.; 29,7 cm

Orientadores: Gabriela Ribeiro Pereira

Luís Marcelo Marques Tavares

Dissertação (mestrado) – UFRJ/ COPPE/ Programa de Engenharia Metalúrgica e de Materiais, 2018.

Referências Bibliográficas: p. 98-101.

1. Reliability 2. Computer Simulated POD Curves 3. NDT. I. Pereira, Gabriela Ribeiro *et al*. II. Universidade Federal do Rio de Janeiro, COPPE, Programa de Engenharia Metalúrgica e de Materiais. III. Título.

The most common way people give up their power is by thinking they don't have any.

Alice Walker

Here's to strong women.

May we know them.

May we be them.

May we raise them.

Unknown

AGRADECIMENTOS

Gostaria de agradecer acima de tudo aos meus orientadores, os professores Luís Marcelo Tavares e Gabriela Ribeiro Pereira.

Ao Professor Luís Marcelo pela sua incansável ajuda, incentivo e orientação não só na metodologia científica do presente trabalho de pesquisa, mas em todos os tópicos que abordam questões de análises estatísticas e design de experimentos. Sem sua sabedoria e altruísmo em compartilhar conhecimento, esse trabalho científico seria impossível de ser concluído; ou sequer começado...

À Professora Gabriela pela sua amizade, encorajamento e por suas palavras de esperança todas as vezes que foram necessárias, pela oportunidade que me deu de desenvolver o trabalho que meu coração e mente me ordenavam e pela liberdade de fazê-lo sem amarras ou preceitos.

À colega de trabalho e amiga Priscila Duarte de Almeida pelo seu apoio não só cedendo seu ombro quando foi preciso, mas por toda a sua assessoria de especialista em ensaios ultrassônicos. Sem seus conselhos e sem sua consultoria, nada faria sentido. Literalmente.

Ao meu avô Leon Algamis que me fez acreditar, ainda criança, que eu era minimamente capaz e que me ajudou a soprar as nuvens e fazê-las caminharem no céu.

Resumo da Dissertação apresentada à COPPE/UFRJ como parte dos requisitos necessários para a obtenção do grau de Mestre em Ciências (M.Sc.)

CALIBRAÇÃO E VALIDAÇÃO DE CURVAS DE PROBABILIDADE DE DETECÇÃO SIMULADAS DERIVADAS DE INSPEÇÃO POR ULTRASSOM

Mariana Burrowes Moreira Guimarães

Julho/2018

Orientadores: Gabriela Ribeiro Pereira
Luís Marcelo Marques Tavares

Programa: Engenharia Metalúrgica e de Materiais

Com o objetivo de verificar e assegurar a integridade estrutural de componentes industriais, curvas de probabilidade de detecção (POD) são usualmente utilizadas para quantificar a confiabilidade de um ensaio não destrutivo (END). Dada sua natureza estocástica, curvas POD são dependentes do fenômeno físico que rege a técnica de END e de fatores probabilísticos como os parâmetros de incerteza, que requerem a um intervalo de confiança específico. Para tanto, é necessário grande número de dados experimentais, além de um sofisticado controle de tamanho de defeitos e suas localizações em um corpo de prova, o que pode ser um processo dispendioso. Curvas POD simuladas têm o potencial para reduzir esses custos e reduzem a necessidade de tantos dados experimentais. A dissertação valida curvas POD simuladas usando o software CIVA comparando-as com curvas experimentais provenientes de inspeções por técnicas ultrassônicas automatizadas em tubos do tipo API 5L X-65. Além disso, mostra como calibrar as simulações computacionais revelando os parâmetros virtuais mais significantes. Concluindo, a dissertação ainda testa a calibração anterior em um subconjunto de dados experimentais de diferente configuração de inspeção, demonstrando que tal transferência quando feita por simulação necessita de estudos complementares para ser melhor compreendida.

Abstract of Dissertation presented to COPPE/UFRJ as a partial fulfillment of the requirements for the degree of Master of Science (M.Sc.)

OPTIMAL FITTING AND VALIDATION OF COMPUTER SIMULATED PROBABILITY OF DETECTION CURVES FROM ULTRASONIC INSPECTION

Mariana Burrowes Moreira Guimarães

July/2018

Advisors: Gabriela Ribeiro Pereira
Luís Marcelo Marques Tavares

Department: Metallurgical and Materials Engineering

In order to verify and ensure the structural integrity of industrial components, probability of detection curves (POD) are often used to quantify the reliability of a particular nondestructive testing (NDT) technique. Given their stochastic nature, POD curves are dependent not only on the physical phenomena that governs the NDT technique but also on other factors, known as uncertainty parameters (UP), which leads to a normally requested 95% confidence level. Therefore, to satisfy a 95% confidence level, it is necessary to gather a large number volume of experimental data, besides a sophisticated control of sizing and location of defects in a test piece, which is very costly. It is already well stablished that Model-Assisted POD (MAPOD) have the potential to reduce those costs by generating data through numerical modelling, leading to a prediction of the POD curve using, many times, computer simulation in the process. This study demonstrates how simulations can be optimized, shedding light on the most significant parameters that result in better agreement between simulated and real POD curves. Further, it validates simulated POD curves using the software CIVA by comparing them to industrial ultrasonic inspections on API 5L X-65 pipes. Finally, using a different subset of experimental data, demonstrates the difficulty on transferring optimized fitting.

Sumário

LISTA DE TABELAS

LISTA DE FIGURAS

1 INTRODUCTION

The constant efforts to prevent failure on equipment and industrial components resulted in a variety of methodologies to assess structural integrity. The set of procedures and techniques that guarantee structural integrity without damaging the component is known as nondestructive evaluation (NDE) or nondestructive techniques (NDT). Nondestructive techniques are responsible to characterize the materials nature under many aspects (acoustic properties, magnetic properties, microstructure components, among others). Besides, NDT can detect, locate and size possible defects on the structure.

Normally NDT is carried on according to a certain procedure, using one or more piece of equipment and conducted by a human being, either directly or not. Therefore, it is only logical to infer that, with so many variables, these techniques present some unreliability. In fact, there are two major aspects to consider about NDT in order to assure structural integrity (CHAPIUS *et al.*, 2018): reliability and accuracy. Reliability can be understood as "*the ability of the technique to detect defects under realistic conditions of application*" and accuracy as "*the effectiveness of the technique to size the defect*".

According to MÜLLER *et al.* (2013), reliability (R) can be expressed in a modular model that states the following:

$$R = f(IC, AP, OHF) \tag{1}$$

The initials IC stand for the intrinsic capability of the inspection system while AP refers to application parameters used to perform the inspection. The OHF initials stands for human and organization factors. With the intention of evaluate the reliability of a certain inspection scenario, these three factors must be taken into account. As can be seen, reliability brings with itself physical aspects of the technique and defects (IC), procedures variability (AP) and a part that is almost subjective (OHF). Having said that, it is natural to realize that reliability is part ruled by deterministic aspects and probabilistic factors.

The efforts made to build a quantification approach for reliability culminated on a stochastic method that involves predicting the Probability of Detection (POD) Curves. If a certain NDT is defined, the inspection procedure is carried on by one defined operator on a certain

component with defined characteristics and that contains necessarily a defect with size *a*, what is the probability of detecting, under these circumstances, this particular defect? This is the question that a reliability study through POD curves intents to answer. In other words: *the probability of detecting a crack in a given size group under the inspection conditions and procedures specified* – GEORGIOU (2006). This statement declares clearly that POD is specific to a certain scenario and if any essential parameter changes, the original modeled POD cannot be transferred, at first, to a new scenario.

Historically, the first POD curves traced to quantify NDT reliability were only based on experimental data following the binomial approach and in order to associate POD with a suitable confidence level, which is often required 95%, many inspections must be carried out by several inspectors on a coupon carefully design to present a minimum number of defects with different ranges of size defects, locations and types. This kind of campaign is extremely sophisticated, time consuming and expensive, which makes reliability studies through POD curves sometimes prohibitive. For example, designing the experiment in order to perform a reliability study involves answering key-questions such as those described by GEORGIOU (2006):

- What geometrical aspect of the flaw will be used? Length, height, projection area?
- How to establish the range of sizes that will be investigated?
- How many flaw size ranges are necessary?

The advances on forecasting POD through Model-Assisted POD (MAPOD) brought a new possibility on quantifying reliability, according to THOMPSON and SCHMERR (1993). Using mathematical models, POD curves could be predicted with less experimental data, lowering the costs of the campaign. There are many definitions regarding MAPOD concepts, but the most accurate can be found in MIL-HDBK-1823A (2009):

"*Methods for improving the effectiveness of POD models that need little or no further specimen testing*"

The most important model was designed by BERENS (1989) where he presented two different modeling approaches: Hit/Miss and a vs $\hat{a}$. The Hit/Miss approach is mostly applied on NDT that provides binary results, meaning that the possible existing defect is detected or

not detected. Usually, this approach is used when NDT like radiography, visual inspection, liquid penetrant testing, magnetic particle testing among others, are considered. The a vs $\hat{a}$ approach takes into account the signal response and correlates it with the defect size a. It is a continuous distribution of results and is typically applied for NDT that provides inspection results in a signal form such as ultrasonic testing (UT) and eddy current testing (ET). More detailed information on Berens approaches will be presented in the course of this dissertation.

Although MAPOD made quantification of reliability more accessible, there is still need to further reduce the demand for experimental data in developing POD curves for a particular application. Therefore, the ultimate improvement would be that POD curves could be simulated and only based on virtual data, provide the reliability forecast with agreement with experimental campaigns. However, the present efforts still did not reach that goal (CHAPIUS *et al.*, 2018). Instead, simulated POD curves have already been developed and, along with some experimental data, can predict reliability behavior. Simulation of POD curves could be used in several possible ways such as (CHAPIOUS, 2018):

- *NDT performances assessment at feasibility stage*
- *Optimization of the design of experiment*
- *Quantification of the effect of the variability of additional parameters*
- *Identification of parameters for improvement POD results*
- *Complement experimental data by simulated one to compute a full POD curve with better reliability*
- *Provide technical justifications when minor changes of the procedure occur*
- *Design an inspection procedure with an objective in terms of POD*
- *Worst case identification*
- *Training and evaluation of operators' performance.*

Nevertheless, there are many difficulties concerning simulating POD curves and it is a process that requires great deal of expertise. Regarding the modular model for reliability evaluation, the simplest term is the intrinsic capability (IC). Several NDT physics-based models are well stablished and validated due to the deterministic behavior of each phenomena that rules most NDT. The AP term involves the variability of parameters that are unknown or not specified during inspection such as defect orientation or its positioning. The term that

involves human and organizational is just not taken into account in simulated POD curves. Having said that, it is clear that properly simulating a POD curve is not an easy task.

It is important to shade light on the term *simulated POD* in order to correctly understand the presented scenario. The POD curve is considered to be simulated when the data used to build the POD curve come from virtual inspections. The POD curve may or may not be built by the same software that was used to generate simulated inspection data.

The present study uses 2016 CIVA version as the software that simulates not only the virtual inspections but also it is the software that predicts POD curve. CIVA is a closed semi-analytical NDT software that was developed by CEA LIST along with partners and it is distributed worldwide by EXTENDE since 2010. Regarding the experimental data, a large set of data from automated ultrasonic (AUT) inspections on API 5L X-65 tubes will be used, including a calibration one that presents several ranges of defect locations, sizes and types, which were inserted artificially. The fact that the inspections were automated reduces drastically the human and organizational effect on the inspection, which leads to most realistic POD curve simulations. Being the experimental data coming from ultrasonic inspections and allied with the fact that CIVA's UT module is very well stablished, these are the reasons that explain why ultrasonic testing is used as the principal technique in this dissertation.

One of the main goals of the present study is to perform a sensitivity analysis on CIVA software to stablish, in a systematic way, the most relevant parameters that effect simulated POD curve behavior. Based on these results, the next step is to optimize the fitting of a simulated POD curve regarding a specific inspection configuration in order to enhance agreement between the resulting simulated POD and experimental POD. The final approach is to verify the simulated POD curve behavior when the same set of parameters used in the optimizing step is transferred to a different inspection configuration. Usually, the efforts on transferring a specific reliability study based on a particular set of data to a different inspection configuration are carried on using transfer functions, as shown in Figure 1. Therefore, the proposal of this final approach is to verify the suitability on transferring virtual parameters to a different configuration through CIVA.

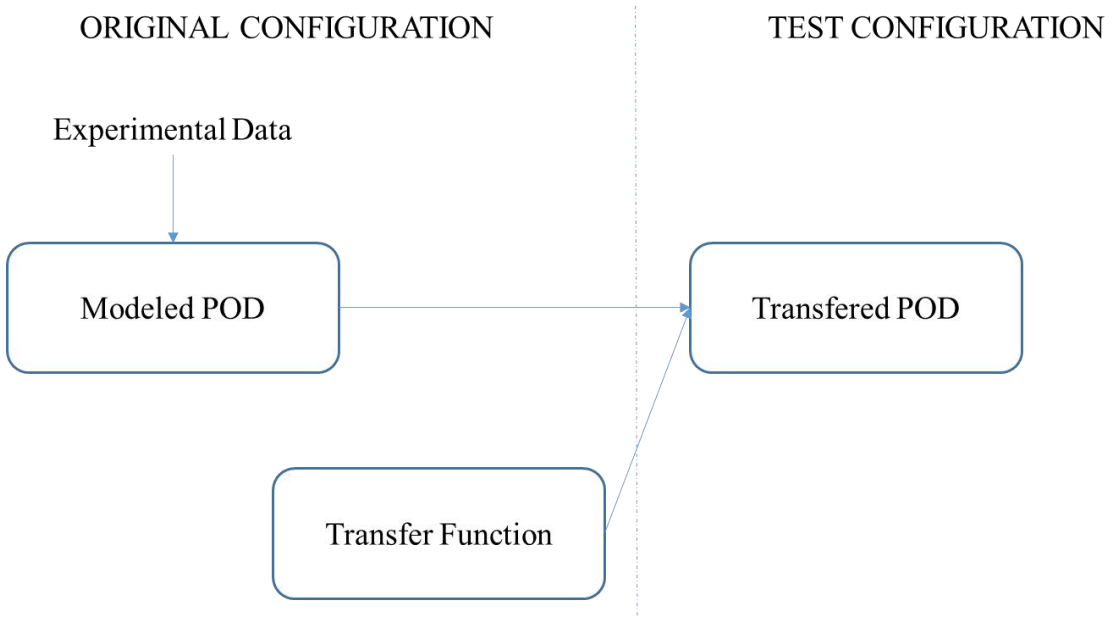

Figure 1: Description diagram on the process of transferring reliability to a different configuration

2 LITERATURE REVIEW

In order to present the state of art on simulation of POD curves, it is at least worthwhile to mention the pioneers that first developed the basics on model-assisted POD (MAPOD), followed by the late productions on the matter. Hence, since the present dissertation approaches mainly simulated POD curves, this particular topic will be predominant in the following literature review reaching specifically efforts on POD curves that were obtained by computational simulation.

Starting with a little bit of history of model assisted POD curves, FERTIG and RICHARDSON (1983) made part of the preliminary efforts on the topic of computer simulations of POD curves. While working for the Rockwell International Science Center, they developed an integrated model that was able to evaluate the performance of a certain ultrasonic inspection (UT) on detecting internal flaws. Of course, their work was based on a number of other works that described the wave propagation phenomena as well as the noise mechanisms but they were able to consider all that background and develop a routine that enhanced the inspection performance by designing the experiment. Attempting to design the best performance transducer, the authors set up an ultrasonic simulation code that presented four different types of approaches: Energy transfer, flaw state, noise process and decision algorithm. FERTIG and RICHARDSON were also able to describe their mathematical model precisely and proposed a different way of determining POD curves: through modeling with some experimental data confirmation.

It is impossible to discuss modeling of POD curves without mentioning the work of BERENS *et al.* (1989). In his paper, Berens presented two approaches intending to formulate a POD(a) function: Hit/Miss and a vs $\hat{a}$. Prior of choosing which approach could be used in a certain data set of results, the paper stated three indications that would influence all future work in this particular field:

- The chances of detection are correlated with crack sizes a
- Different cracks of the same size can significantly present different crack detection probabilities, as can be seen in Figure 2
- Factors other than size are affecting the chances of detection.

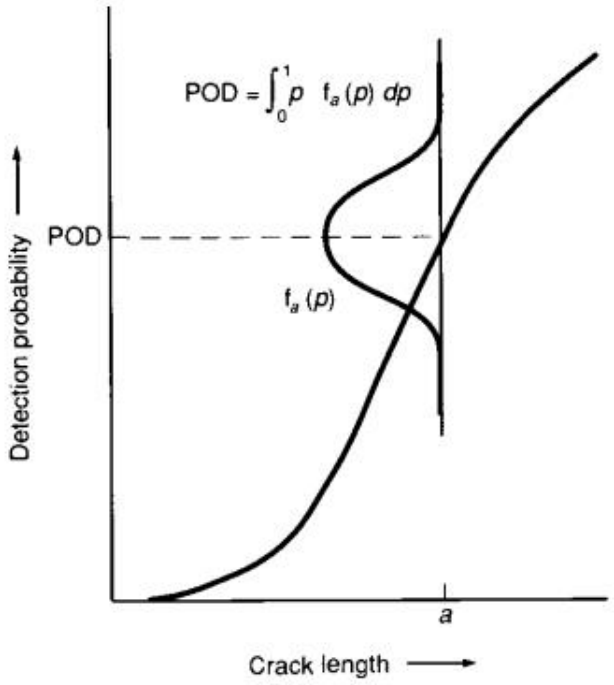

Figure 2: Probability of detection distribution considering a fixed size of defect (Berens, 1989)

They also stated that, depending on the nature of the prior inspections, it is more efficient to use one approach instead of other. NDE techniques that provide results in the detected/not detected form, that is, binary NDE responses, may require a Hit/Miss analysis and, the data set of the inspection would be a set of 0 (not detected) and 1 (detected). In order to draw an S-shaped curve that quantifies the reliability, Berens proposed, for Hit/Miss approach, the following logistic function:

$$POD(a) = \frac{1}{1+\exp(-\beta_1-\beta_2 a)} = \frac{\exp(\beta_1+\beta_2 a)}{1+\exp(\beta_1+\beta_2 a)} \quad (2)$$

Equation 2 involves two parameters, β_1 and β_2, that are not related to the physical model of the used NDE. These parameters are often assessed through maximum likelihood estimation (MLE) from fitting the curve to empirical data. Figure 3 shows the difference of a log odds plot and a cumulative log normal model, both presenting mean = 0 and standard deviation = 1.

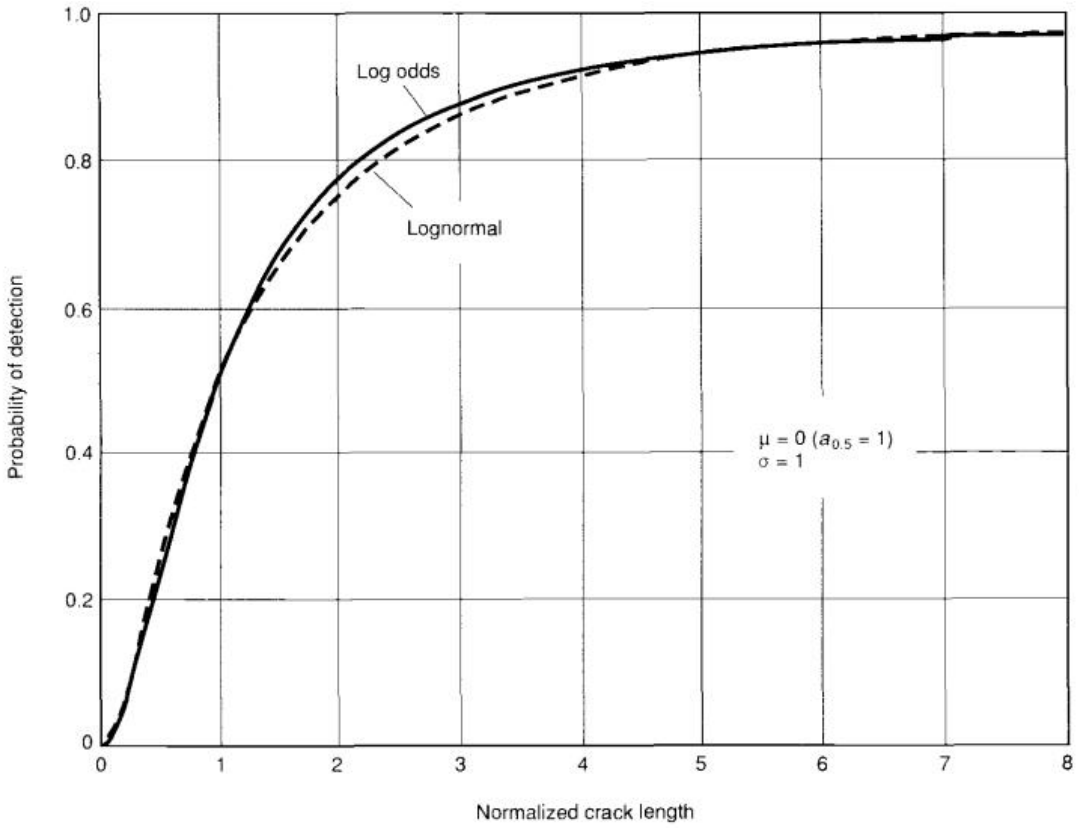

Figure 3: Probability of detection curves – log odds vs cumulative log normal distribution functions (Berens, 1989)

On the other hand, if the NDE results come out as a continuous distribution of signal responses, such as the ones from UT or ET inspections, then an a vs $\hat{a}$ approach is needed and the POD is given by:

$$POD(a) = \Phi\left(\frac{\ln(a) - [\ln(\hat{a}_{th}) - \beta_0]/\beta_1}{\sigma_\delta / \beta_1}\right) \tag{3}$$

The function above is a cumulative log normal distribution with mean and standard deviation of log crack length as following:

$$\mu = \frac{\ln(\hat{a}_{th}) - \beta_0}{\beta_1} \tag{4}$$

$$\sigma = \frac{\sigma_\delta}{\beta_1} \tag{5}$$

The term $\hat{a}_{th}$ refers to the signal response of a certain flaw size a that correspond to the threshold or decision value. Any signal major than $\hat{a}_{th}$ is considered a real inspection

indication; otherwise, it is treated as noise. The terms β_0, β_1 and σ_δ are also determined by maximum likelihood methods.

Just one year later, NAKAGAWA *et al.* (1990) described a model to determine the reliability of an automated eddy current system. Basically, they turned the inspection automated and based on measures of inspectability, ROC (Receiver Operating Characteristic) curves (which allows the characterization on the sensitivity of an inspection system) and POD curves were plotted. They were able to produce an amount of data that was satisfactory to develop a reliability study. However, in addition to that, what can be seen in NAKAGAWA work is that there was no prediction of reliability based on routines or computational simulations. Instead, the POD curves were mathematically modelled.

In the early 1990s, RAJESH *et al.* (1993) also modelled POD from eddy current inspections in order to detect surface cracks. In this particularly case, they used a finite element routine to reconstruct the eddy current technique (ET) inspection, which was successful. However, being a deterministic model, it could not take into account perturbations of the inspections system and, therefore, the POD curve associated to this inspection procedure could not be experimentally validated.

Later on, THOMPSON and SCHMERR (1993) pointed out that model-based probability of detection curves were being rapidly improved not only by computing advances but also by the capability of describing and modelling the physical phenomena that runs NDE techniques. Besides, they stated many uses for model-based POD curves such as optimizing procedures and designing of a variety of NDE techniques, defining its system performance capabilities, developing standards and calibrations for NDE systems, among others.

Meanwhile, in the Harwell Laboratory in Oxford, OGILVY (1993) were also interested in predicting POD curves behavior through modeling. Based on ultrasonic pulse-echo inspection on planar buried defects, the team were able to predict a theoretical POD through a mathematical routine. The main idea was to build a physically-based model to describe the scattering from UT combined with noise theory model in a numerical evaluation package to leave the deterministic scenario and try to predict POD. Adding uncertainty to the physical modeling, he could study some parameters that were capable of increasing uncertainty to the inspection such as roughness, orientation of the defects or flaw depths. The unique aspect of

OGILVY's work was that he not only quantified the uncertainties, but he also put some effort to take false alarm in consideration in his model.

Still in the matter of probability of false alarm (PFA) and at the same institution, Harwell, WALL and WEDGWOOD (1994) presented a review were the authors call for attention on the costs involving PFA and that this type of probability of detection required attention. In addition to that, the authors claimed that PFA could be linked to human factors and that this kind of subjective factor was, in that point, impossible to be modeled. The most important conclusion of their work was that models and databases must be developed in order to increase performance on sensitivity, speed and reliability of NDE inspections.

The following year, CHIOU *et al.* (1995) reported on a model that could predict POD from UT inspection of flat-bottom holes in Ti alloy engine billet material. The parts were characterized not only by physical modeling but also experimentally. As for the modelling part, the authors combined the method of optimal truncation as a plane wave scattering solution with the high-frequency Kirchhoff approximation along numerical integration and a simplified reciprocity relationship for special cases. The Kirchhoff model is useful for the modelling of echoes due to specular reflections. Since the UT theory is not the main topic of the present review, further reading can be found on BO LU *et al.* (2012). In 1996, CHIOU, *et al.* (1996) enhanced the developed model by modeling volumetric defects UT inspection besides flat-bottom holes.

In the following year, WALL (1997) reviewed in detail the state-of-the-art in NDE modeling, but this time he was able to approach human factors as well. According to MATZKANIN *et al.* (2001), Wall listed seven different approaches available to predict POD curves:

- Physical models for POD and PFA;
- Signal/noise models;
- Image classification model (visual POD);
- Inspection simulations;
- Statistical Models (curve fitting);
- Human reliability models and
- Expert judgment.

It is important to say that the corrections proposed by Wall regarding human factors were based on experimental observations and, in that point, Wall himself stated that the modeling of such source of uncertainty was very complex and not available. Wall concluded that modeled POD should definitely be a part of industrial and research day-by-day because:

- Modelling POD would reduce the number of experimental samples required;
- It would gain acceptance and familiarity for the modeling approach in general;
- It could provide validation and improve database for corrections and predictions methods for understanding external factors as humans and environmental.

At the same year, SCHMERR and THOMPSON (1997) presented a paper enlightening the importance of modeling in NDE Standards and made recommendations that, from that point on, any future work regarding modeling of NDE data should comprehend (MATZKANIN *et al.*, 2001):

- The use of models to design, validate and extend the measurements process;
- The use of models to calibrate and quantify the capability of NDE hardware;
- The use of model to train and educate NDE personnel;
- The validation of models themselves.

In that way, it was inaugurated the beginning of the mature modeling era. From this moment on, sophisticated statistical tools sometimes combined with computational tools, became more actively used.

MEEKER *et al.* (1998) proposed a new methodology in their paper on how to improve modeling to determine the reliability on UT inspections that were designed to detect hard alpha inclusions in Ti engine billet materials. They were able to describe the effects that changes in UT scanning velocity and gate width have on the probability of detection. The team calculated the POD for several flaw sizes as a function of threshold values to stablish the effect of scan speed and gate width. Nevertheless, the conclusion was that they needed to investigate this scenario with real hard alpha inclusions, since they used synthetic ones.

Still on titanium engine components, THOMPSON (1999) also presented updates on his previous research and obtained what he thought were the three main sources of variability during automated Ti aircraft billet inspections: microstructural parameters, instrumentation

& scanning procedures and flaw morphology variability. Based on each parameter role, the paper describes a POD/PFA modeling methodology.

TOW and REUTER (1998) were also facing this quite philosophical question: how to take into account real inspection results in a probabilistic model of reliability of a certain structure. They proposed the use of a probabilistic fracture mechanics (PFM) model for pressure vessels reliability and considered the applied stress as the variability source maintaining all others parameters deterministic. The stunning outcome is that they were able to use inspection results and POD curves to determine the probability distribution function (PDF) for the flaws as well as the distribution of flaws among the various size ranges. Along with the PFM model, the PDF were used to stablish the probability of failure (POF) of the component in which flaws has been detected by NDE. They concluded that whenever the inspection performance increased, the probability of failure decreased.

Also in 1998, SIMOLA and PULKKINEN (1998) added a great contribution on POD modeling by examining models for flaws sizing on the basis of statistical logarithmic or logit transformations. That was the moment that POD was modelled as a function of flaw depth and length based on statistical logarithmic or logit transformations of flaw sizes along with models for Bayesian for updating of flaw size distributions. The Bayesian approach enables to take into account prior information of the flaw size and combine it with measured results.

Thus, several efforts have been made on modeling POD curves since the early years and a huge progress on this specific area of reliability studies came out as a result. However, it was in the beginning of the 2000s that the term MAPOD was spread through the scientific community. Researchers of the Iowa State University and the National NDT Centre in Harwell Laboratory in Oxford formed the Model Assisted POD (MAPOD) working group with collaboration of the US Air Force, the Federal Aviation Administration and NASA. The main goal was to explore computational POD opportunities and so it did.

THOMPSON *et al*. (2009), enlightened that MAPOD approaches were initially categorized as Transfer Function (XFM) and Full Model Assisted (FMA). In the XFM approach, the idea is to leverage a prior POD curve based on a certain scenario and then, change only one significant controlling parameter and understand how that change affects the resulting POD. That procedure could be carried out experimentally under restricted and controlled

circumstances or through physics-based computer simulation. Regarding FMA approach, the factors that disturb variability control are tested in a systematic way. Using physics-based models the signal response is estimated as well as the variability due to well-understood physical phenomena. All the variability that comes from unknown sources have to be determined empirically. Having said that, Thompson defined what is understood nowadays as "unified approach" which is a merge of XFM and FMA, such that all factors that governs variability on an inspection scenario can be divided in two groups:

- Those that must be assessed empirically
- Those that are governed by well-understood physical phenomena.

Several authors, while describing their efforts on building MAPOD, don't specify exactly how they combined the information used for estimating POD under MAPOD concepts. MEYER *et al.* (2014) suggested a simple categorization between Non-Bayesian and Bayesian Approaches in order to review MAPOD literature. This present dissertation focuses on simulated POD curves, which are built on CIVA. CIVA code probability of detection mode is based on the parametric functional form of Berens approach (BERENS, 1989) and does not take into account either prior and posterior information in order to predict POD curves, which is the main characteristic of Bayesian approach: "*posterior information equals prior information plus new evidence*" (KENZLER, 2015). Bayesian approaches usually requires many rounds of calculations allowing that the studied scenario learns more information in each round. Since the Bayesian approach is not applicable to the present dissertation, it will be left out from this literature review.

Regarding Non-Bayesian (NBA) and FMA approaches, SMITH *et al.* (2007) and THOMPSON *et al.* (2009) studied MAPOD as a tool for estimating POD applied on fatigue cracks that growth from aircraft wings fastener holes inspected by ET. The modeling part in this case was used to determine the influence of fatigue cracks growing outwards from the mentioned holes under ET inspection while the influence of variability due to geometry was determined empirically. THOMPSON *et al.* (2009) also presented a study on the effect of microstructural variability on POD in various alloys for engine disks. In this case, the effect of grain size on NDE noise level was evaluated through computational simulation while system variability was assessed empirically.

Still regarding the XFM approach, the work by THOMPSON *et al.* (2009) discussed application of MAPOD on ET for detection of fatigue crack on complex engine component. Due to the difficulty on growing fatigue cracks on that kind of geometry, the POD for electro-discharged machined notches was determined and used as the baseline POD curve. Meanwhile, physics-based model was used to study the influence of fatigue cracks versus notches on this baseline curve.

HARDING *et al.* (2009) carried out another very interesting work following the XFM approach. The group studied estimation of POD for fatigue crack around fastener holes in aircraft wings by UT. Their model used data from field and laboratory experiments taking into account the effects caused by: structural geometry, natural variability in fatigue cracks and human factors during inspection. Since they used three sets of experimental data, they opted for the XFM in order to put all the sets of data together and estimate POD. These three sets came from fabricated flaws in the real structure, real flaws in a simplified structure and fabricated flaws in a simplified structure. The authors used a linear regression model to take the parameters from the three data sets to the target scenario and called this "quadrant" approach.

Several studies were carried out on MAPOD applications using the non-Bayesian approaches. From this point on, this literature review will focus on papers that uses CIVA in the process of POD evaluation, starting from the year of 2010, which was the year in which CIVA software was released to the international market.

REBOUD *et al.* (2010) highlighted on their paper the difficulty on inspection on riveted structures and its consequent effort on stablishing the reliability of the used NDT. The team concluded that ET was the best NDT for this kind of structures, when there is no magnetic limitation due to the nature of the material. The paper brings the possibility of using CIVA to improve the inspection procedure through design of experiments (DOE) techniques. In the second part of the paper, the authors presented two POD curves: one based on Hit/Miss approach and the other based on a vs $\hat{a}$ approach, but that did not carried out validation based of experimental data was done. All POD curves were based strictly on simulated data from the virtual ET inspection.

The year of 2012 was a busy one concerning MAPOD application to forecast POD. CARBONI and CANTINI (2012) applied MAPOD to UT inspection of defects located in railway axles. In their work, both approaches were used to evaluate POD: FMA and XFM. They used CIVA to simulate the UT inspections performed by first and second legs methods. The first leg corresponds to the signal response coming from the incident beam while the second leg corresponds to the signal coming from the reflection beam. The FMA approach was used to simulate the experimental variability such as probe location, while the FMA approach was applied to compare the second leg results to experimental data from the first leg. It is important to mention that CIVA was used only to simulate the inspection. No POD curve was simulated by CIVA and no experimental validation of the results were presented.

DEMEYER *et al.* (2012) used the XFM approach to study POD regarding the inspection by UT on Ti plates to detect fatigue cracks. CIVA was used to generate inspection data results for notches on titanium and aluminum plates. Based on these simulation results along with experimental results from inspection on Ti plates, the data gathered was extrapolated to estimate POD results for Al plates. As well as the prior work cited, the authors did not simulate the POD curve, only the inspection results.

REVERDY *et al.* (2013) studied the struggle to inspect aerospace turbine components using phased array technique. The main idea was to validate the virtual inspections performed by CIVA comparing with experimental data. After the experimental validation of the simulation, POD curves were built in order to optimize the virtual inspection process. No POD curve was simulated in the process. Although, the authors state that once the virtual inspection is validated against experimental results, all POD analysis coming from that simulated results are valid, which is highly questionable. It is important to say that the POD curves were generated by CIVA considering 60 values of defect height and for each height, five inspections were made, totaling 300 inspections. The same number of inspections (experimental and simulated) were used in the present dissertation. The simulated value of $a_{90/95}$ were compared to the one predicted by the pertinent standard and it came out that the simulated value was smaller than the one predicted in standard as being critical. Therefore, based only on simulated POD curve, the aerospace structure would not be in any danger of failure.

ANNIS *et al.* (2013) reviewed reliability studies carried out until that point and concluded that, among other things, nuclear industry requires more controlled NDT reliability than aerospace industry. Therefore, producing coupons that provide a higher confidence level that represent nuclear components become extremely costly. Besides, quantifying the artificial defects to ensure a statistical variability on these types of components and confidence requirements it is a sophisticated task. They presented a mathematical model that relies on the Monte Carlo (MC) Method in order to produce random values that could illustrate inspection variability and then create a set of data statistical representative to build POD curves. Unfortunately, the modeling exercise itself was inconclusive and the computational cost of generating those random data was extremely high.

Aiming to bypass the computational cost, the authors suggested the application of a Quasi-Monte Carlo approach (CAFLISCH, 1998). The main idea is to accelerate convergence for MC quadrature using quasi-random or low discrepancy sequences. These sequences are deterministic compared to purely random or pseudo-random sequences. The singularity of it is that these numbers generated by quasi-MC are correlated and allow the system to become more uniform. Considering a Hit/Miss approach, both hit and miss receive a weight corresponding to their prior likelihood generating a Bayesian network.

Results on ANNIS *et al.* (2013) using quasi-MC showed that parameters such as number of defects, number of inspections, range of defect sizes, among others, are correlated to the POD curve. ANNIS *et al.* (2013) is considered one of the most important papers regarding modeling of POD but it was purely mathematical and strongly corroborated many predictions made by BERENS (1989).

As a result of a partnership with the French Oil & Gas company Technip, the CEA team presents in CHAPIUS *et al.* (2014) a set of POD curves generated by CIVA based on AUT (automated ultrasonic testing) on orbital welding. The inspection procedure was based on recommendations by DNV (Det Norske Veritas) and ASTM (American Society for Testing and Materials) best practice guide. The inspections were carried out virtually using CIVA with the virtual solid representing a reference block and the simulated results were used to draw the POD curves. However, no experimental results were used to validate either the simulated POD curves or the virtual inspections.

One of the main motivations of CALMON *et al.* (2015), study elaborated by CEA team along MAPOD Working Group and European Project PICASSO, was to predict multivariable POD considering not only the defect size but its positioning and furthermore, evaluate how those two parameters combined affect the behavior of POD when ET inspections are performed. All ET virtual inspections were performed by CIVA. Moreover, the group intended to establish the set of conditions that enables the cumulative log-normal distribution function which forces, therefore, the use of non-parametrical regression regarding the Hit/Miss approach. Whilst the topic addressed was extremely interesting, the POD curves were not simulated by CIVA. No experimental validation was carried out by the authors.

Concluding, the present literature review clearly shows that this dissertation can shed new light into the study of simulated POD curves. It is extremely hard to find, if at all available, a work that at least consider approaching the following steps based on plane scientific methodology:

- Consider significant amount of experimental data with industrial variability;
- Develops a sensitivity analysis of the software;
- Uses the same software to build the virtual inspections and to estimate POD curve;
- Attempts to optimize the fitting of POD curves in order to improve agreement with experimental results;
- Performs some validation of simulated POD curves comparing to experimental data and
- Tests the achieved optimal fitting on a different set of configurations.

3 METHODOLOGY

In general, the main steps that describe this dissertation Methodology are the following:

1. Stablish a correlation between simulated POD curves and an experimental POD curve built by non-laboratorial experimental set of data;
2. Perform a sensitivity study on the software performing over 80 virtual variations;
3. Compare simulated POD curves considering a new approach of estimating variability of simulated data;
4. Identify the virtual parameters that induce more impact on the simulated POD curve;
5. Apply adjustments on the original virtual scenario in order to optimize the fitting of the simulated POD curve and compare with the experimental one to verify improvements;
6. With the set of adjustments that was used in the optimization step, apply the same set of parameters changes on a different inspection scenario and verify if this optimization set could be transferred to other virtual scenarios.

Since one of the key goals of this dissertation is to optimize the fitting of simulated POD curves in order to get them close to experimental ones, it is necessary to describe both sets of data: experimental data coming from real inspections and the simulated data coming from virtual inspections. Therefore, the Methodology section is divided in two subsections: experimental and simulated data.

3.1 EXPERIMENTAL DATA

The experimental inspection results were kindly shared by LNDC – Laboratory of Nondestructive Testing, Corrosion and Welding that is part of the Metallurgical and Material Engineering Department of the Federal University of Rio de Janeiro. Having Reliability Analysis as one of the most important lines of research, LNDC was hired for a well-established, but undisclosed, pipe manufacturer to analyze its automated ultrasonic

inspection system through POD curves. In order to do that, a coupon was specially built consisting in a 12 m long API 5L X-65 pipe with a longitudinal weld made by SAW (Submerged arc welding). In the welding region and adjacencies, 99 artificial defects were inserted respecting a 100mm distance between each one of them. The defects differ from each other based on geometry, location and type. Regarding their types, as shown in Table 1, six different kinds of defects were artificially inserted: regular longitudinal cracks, longitudinal crack on the HAZ area, two different kinds of transverse cracks, lack of fusion and lack of penetration.

Table 1: List of defects inserted in the API 5L X-65 pipe used in experimental AUT inspections

		Sizes of Defects (mm)		
Types of Defects	Number of Defects	Heights	Lenghts	Depths
Lack of Fusion (LF)	9	0.35 - 2.10	1.5 - 12.0	0.5 - 24.0
Lack of Penetration (LP)	14			
Cracks on HAZ	20			
Transverse cracks type A	12			
Transverse cracks type B	24			
Longitudinal cracks	20			

Each group of defect was produced following a distribution of different and known lengths and heights. The projected heights presented a range from 0.35 mm to 2.1 mm while the lengths varied from 1.5 mm to 12 mm.

The defect insertion technique was based on simulating a real defect by adding size-controlled graphite pieces into the weld region. To do so, cavities were made in the pipe by gouging and the graphite pieces were carefully positioned inside those cavities in specific locations and depths, as shown in Figure 4. At the end of the described process, all cavities were covered by SMAW (Shielded Metal Arc Welding), as can be seen in Figure 6.

Figure 4: Gouging of the pipe to insert artificial defects in the welding region

The graphite technique may be assumed to be an efficient way of simulating real defects because it causes an interference in the ultrasonic wave propagation inside the material due to its different properties. Having a graphite structure inserted in a metal, the ultrasonic wave will be affected as a real defect because the graphite presents different acoustic properties from the metal. The graphite insertion method was properly validated experimentally by LNDC team through macrography as can be seen in Figure 5 and and NDT techniques.

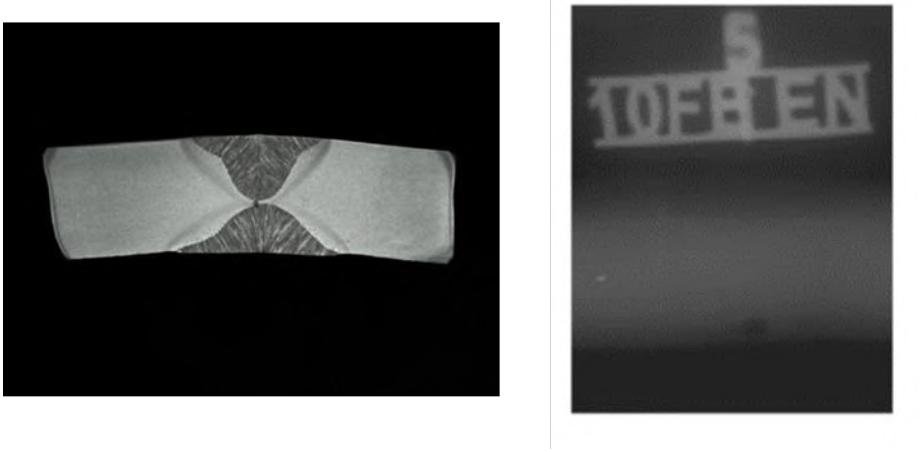

(a) (b)

Figure 5: The figure (a) shows a macrography of a defect inserted in the weld region by graphite technique and figure (b) shows its location through radiography test

Figure 6: Covering of the gouged areas with Shielded Metal Arc Welding

After the insertion of the 99 defects, it was necessary to verify if their location were still the same as projected because the SMAW process could have moved them to a different spot. For that, manual ultrasonic inspection was carried out and all pipe was mapped according to the real and final locations of the defects after the closing process. It is important to mention that only the longitudinal position of the flaws could be confirmed by UT inspection at this point, but not the depths.

Once the coupon pipe was ready, it was transported to the manufacturing plant to be inspected by the automated UT system. The client's system consisted of 12 steady probes working in pairs while the pipes to be inspected pass beneath them. The probes couple stablishes contact with the pipe surface using water as coupling medium. Each pair of probes is designed to inspect a certain area and depth of the pipe. As such, at least in theory, every region of interest nearby the welding area was covered. It is worth mentioning that the UT signal from the inspections were considered to be real defects signals instead of noise each time the they overcame 50% of the screen, stablishing this value as the threshold value.

The client's main concern was if the probes were being efficient regarding the detectability of potential defects. Besides that, they wonder if these probes were detecting what they do not need to detect. In the same way, the client was interested in knowing if the AUT system were failing to detect indications that are crucial for the integrity of the pipe. To answer these

and other important questions, they were right to recognize that a reliability study through POD curves was necessary.

What is important to the present dissertation is not the result of the mentioned reliability study. This dissertation will take advantage of the 1.188 experimental data resulting from real inspections that took place on the industrial plant, which were influenced by all sources of variability made on a 99 well-known defect pipe. From all this valuable data generated, the present work will focus only on a subset that was found to be representative. Since the main propose of this work is only achieved performing a large number of computer simulations, it was necessary to choose a certain configuration of probe and type of defect instead of considering all configurations. Once this chosen subset is studied, expanding the procedure to the full set of data is a trivial, but time-consuming task, which is beyond the scope of the work.

For all further analysis, the configuration that will be considered regards defects that represent cracks on the HAZ (heat-affected zone). One of the main outcomes of the reliability study that was carried out previously was that the probability of detection does not strongly depend on the defect length but on its height. Having said that, for this point on, all POD curves will be based on a fixed length of 12mm and the geometric parameter for the analysis will be the defect height.

The experimental POD curve concerning the subset of HAZ defects was build using the software mh-1823 version 4.2.4, which is a free code written in R that was developed following the MIL-HDBK-1823A (2009) recommendations. This particular software was used in this dissertation since it is the same code implemented on CIVA's POD curve module. In order to compare properly experimental to simulated results, it is important to be as systematic as possible, that is, use the same code, the same data set size (300 results) and the same mathematical approach. The curve can be seen in Figure 7 and shows the main parameters that are taken into account to evaluate a POD curve, which are the a_{90} and $a_{90/95}$ values and the covariance matrix which is composed by parameters that will stablish the σ and μ modeling.

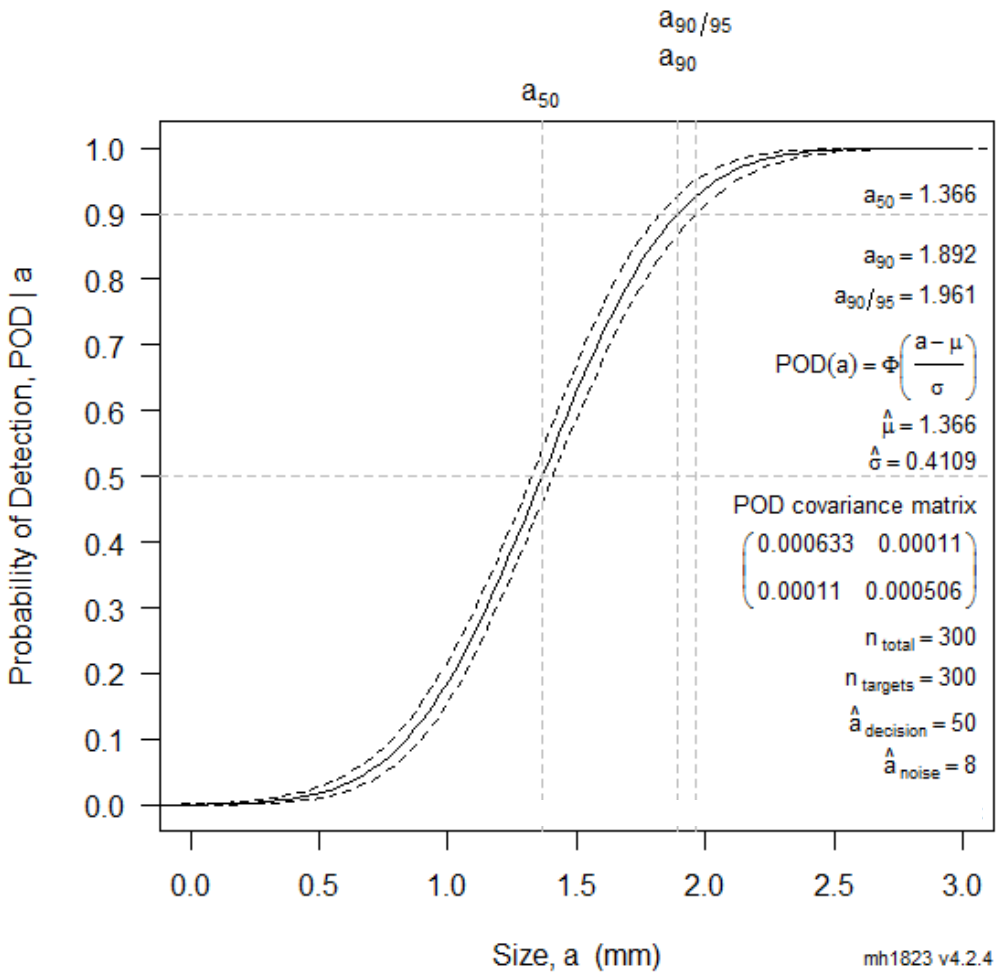

Figure 7: POD curve from experimental data inspection of AUT on HAZ defects

Figure 7 shows the a_{90} and $a_{90/95}$ values being 1.892 mm and 1.961 mm respectively and it is important to emphasize that the axis concerning flaw size is, in fact, its **height**. The a vs $\hat{a}$ approach was selected, as well as a linear distribution of defect heights and a confidence bound of 95%. Aiming to compare the experimental a_{90} and $a_{90/95}$ values with simulated results, the same scenario but virtual, had to be developed.

3.2 SIMULATED DATA

The software used to simulate not only the inspections but also the POD curve was CIVA version 2016. CIVA, as mentioned before, is a well stablished semi-analytical physical-based software used to perform virtual inspections through NDT techniques and to predict reliability through simulated POD curves; among many other functions. CIVA has four major modulus regarding NDT: an ultrasonic module, guided waves module, eddy current module and radiographic module. This dissertation only makes use of the ultrasonic module, specifically the inspection simulation part. The POD analysis is a specific kind of file generated from the simulation file or independently.

For the propose of this work, the inspection simulation was carried out with the experimental configuration of the chosen subset and computational results could be verified associating the signal responses with the experimental ones; the results showed satisfactory agreement. From that point on, it was possible to stablish the virtual model as a suitable representation from the experimental configuration. Therefore, POD files regarding flaws height could start being produced. This original curve, the one built from the experimental model, was called CONTROL and all others curves will consider the CONTROL one as the POD curve base for comparison. All parameters set up in the CONTROL modeling are presented in Table 3 at the end of this section, including the defect geometry as shown in the schematic Figure 8.

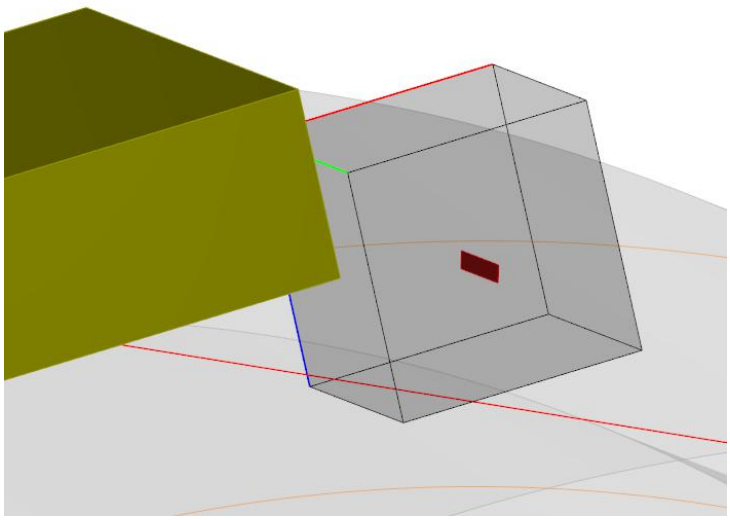

Figure 8: Scheme of the rectangular defect used to simulate the crack on the HAZ

It is important to understand certain aspects on how CIVA performs probabilistic studies to build POD curves. The inspection simulation in a deterministic model. The POD curve can only begin to exist when uncertainty parameters are considered. CIVA calls those parameters as "uncertain parameters" but this dissertation will refer to them as uncertainty parameters or just UP. The users have to define which inspection parameters are uncertain. In the present work, three aspects were defined as uncertain: skew, tilt and disorientation of the flaw. That means that there is no certainty regarding the orientation of the defect. Furthermore, the uncertainty parameters have to follow a given probability distribution function (PDF) which is also defined in the virtual environment. All three uncertainty parameters assumed a normal PDF, which is a perfect acceptable premise, according to expert's analysis (REVERDY *et al*., 2013).

Once the uncertainty parameters (UP) and their PDF are defined, the software is able to describe the variability necessary for the probabilistic study. The mentioned variability is achieved through a Monte Carlo routine that provides a random sampling with null mean value and standard deviation = 1.

When the code gathers the random data sampling sets, it applies the calculated variability to simulate all scenarios respecting the physics-model computation. The result is a set of signal responses for every scenario coming from the combination of each random value calculated for each UP applied on the deterministic model. Based on the resulting set of signal responses, corresponding to 300 inspection results, POD curves can be extracted. The curve is extracted according to Berens approach and it can be analyzed in many ways: Hit/Miss or a vs $\hat{a}$ approach, linear or logarithmic model and variable confidence level among others. The involving parameters are calculated according to MIL-HDBK-1823A (2009) approach. The analysis also provides the data table with all a sizes and all corresponding values attributed to the UP and the maximum signal response (maximum amplitude). Results on CIVA are also presented graphically as data plot of flaw sizes vs signal response, a data plot of residuals and de POD red curve along with the confidence level blue curve, as it shown in red in Figure 9.

After performing the virtual inspections, the resulting data is exported and the POD curve that corresponds to CONTROL configuration is built through mh-1823, as it is shown in

Figure 10. This figure shows the a_{90} and $a_{90/95}$ values being 1.623 mm and 1.664 mm. As well as the experimental POD curve, the simulated POD curve considered the a vs $\hat{a}$ approach, the linear distribution of defect heights model and a confidence bound of 95%.

An initial comparison between experimental and simulated results of a_{90} and $a_{90/95}$ is presented in Table 2.

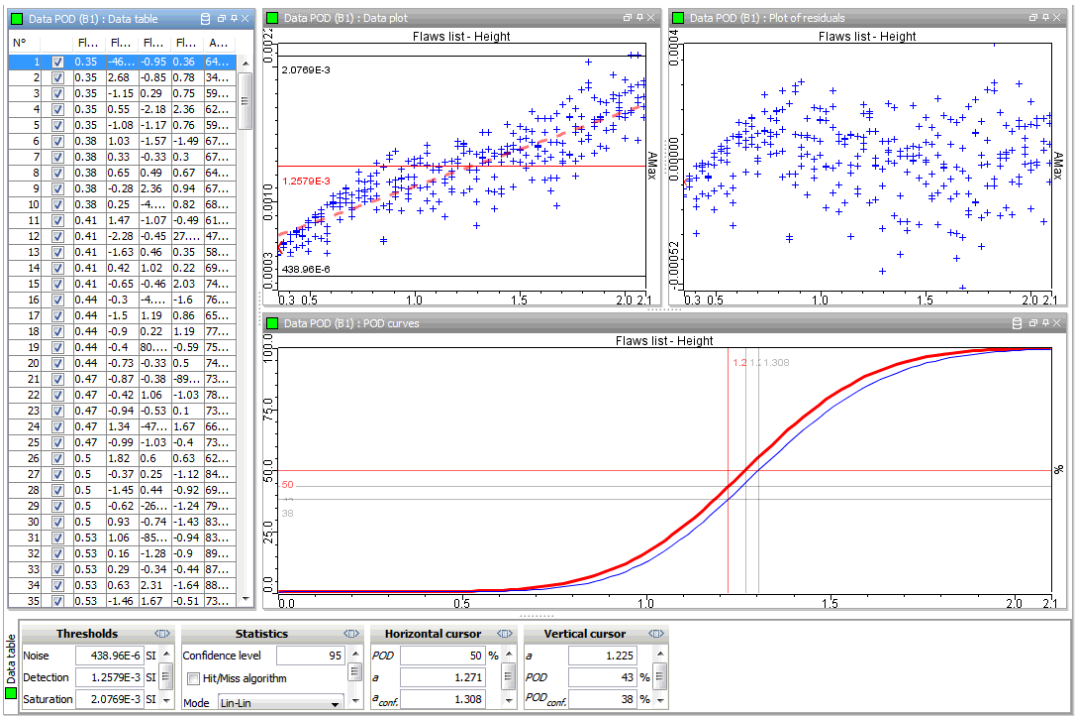

Figure 9: Example of POD analysis results coming from CIVA software

It can be seen that the corresponding values differ, of course, but they remain in good agreement, which allows follow-up studies to be done.

Table 2: Comparison between experimental and simulated data for a_{90} and $a_{90/95}$ values CONTROL regarding configuration

	a_{90}	$a_{90/95}$
Experimental	1.892 mm	1.961 mm
Simulated	1.623 mm	1.644 mm

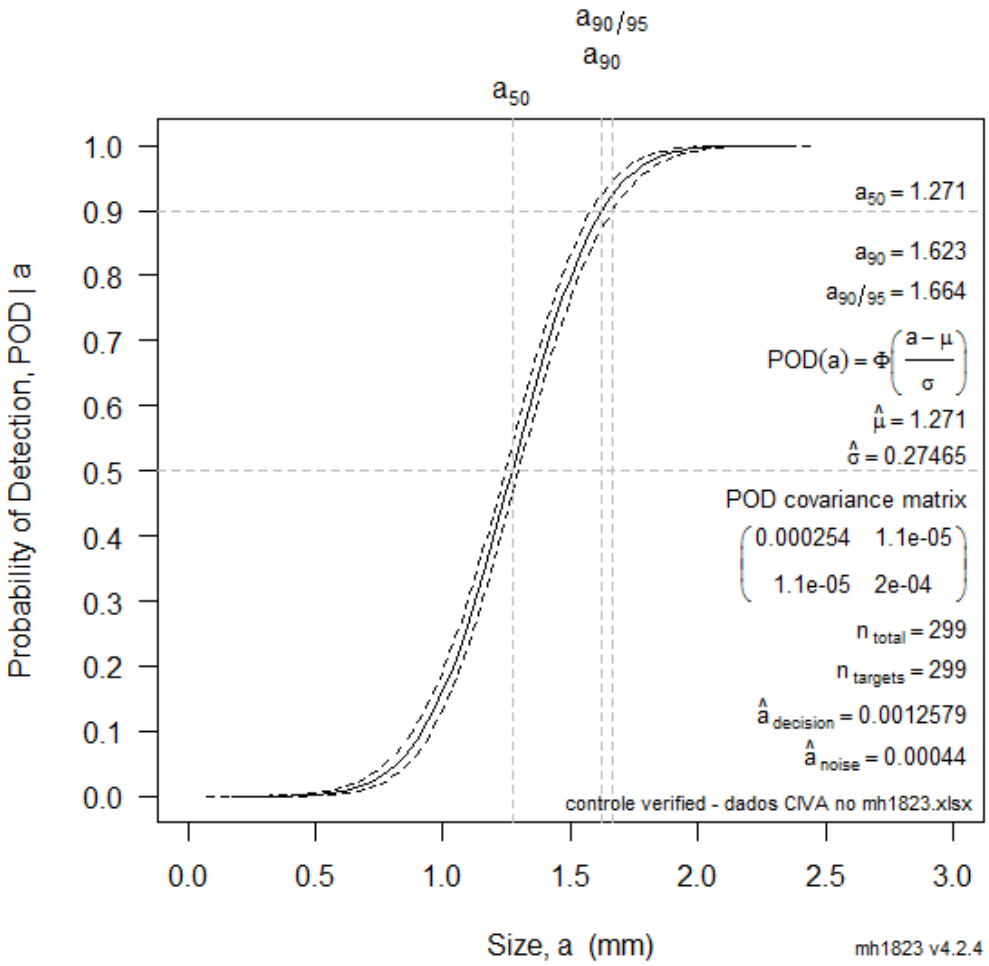

Figure 10: POD curve from simulated data inspection of AUT on HAZ defects

	a_{90}	$a_{90/95}$
Experimental	1.892 mm	1.961 mm
Simulated	1.623 mm	1.644 mm

Table 3: Simulation parameters used to model CONTROL scenario through CIVA

CONTROL PARAMETERS					
Simulation Settings	Initialization	Computational configuration	advanced definition		
		Involved modes	transversal waves		
	Interactions	Specimen echoes model	Kischhoff		
		Backwall skip activated			
		Number of half skips	1 max		
		Flaws model	Kirchhoff & GTD		
		Sensitivity zone	Enabled		
			Dimensions	x	30 mm
				y	30 mm
				z	30 mm
			Positioning	arbitrary	
				coordinate system local	
				Cartesian	
				depth direction	along local normal
			Local Cartesian coordinate	x	59 mm
				y	0
				z	8 mm
	Options	Compuitation type	3D		
		Field reflector interaction	plane wave		
		Accuracy	Field	1	
			Defect	1	
	Other Options	Account for attenuation			
		No creeping waves			
		Mode identification	Activated		
		Number modes to return	5		
		Calibration	No		

Probe		Contact with wedge		
	Crystal shape	Single element pattern		
		Geometry	Rectangular	
		Width	8 mm	
		Length	9 mm	
		No apodization		
	Focusing	Flat (surface type)		
	Wedge	Geometry	L1	34 mm
			L2	34 mm
			L3	68 mm
			L4	30 mm
		Crystal Orientation	Refraction angle	60°
			Incident angle	50.14°
		Other Angles	Squint angle	0
			Disorientation	0
		Wave Type	Transverse	
		Material	Plexiglas	
		Attenuation type	Modal	
		Longitudinal wave attenuation	power	
		Transversal wave attenuation	none	
		Structural noise	none	
	Signal	Imported reference signal		
		Sampling	number of points	512
			temporal position	1.707 mm
			frequency	4 MHz
	Case	Unabled		

Flaws	Shape	Rectangular defects		
	Geometry	Length	12 mm	
		Height	0.35 - 2.1 mm	
	Positioning	Options	Length along rotation axis	
		Position mode	from surface to bottom	
		Ligament calculation	outer	
		Center coordinates	y	150 mm
			Θ	0
			R	228.6 mm
		Orientation	tilt	0
			skew	0
			disorientation	0
		Ligament	0.5 mm	
		Translation direction	along normal direction	
Specimen	Geometry	Diameter	457.2 mm	
		Length	300 mm	
		Thickness	28.32 mm	
		Inner Radius	200.28 mm	
		Angular Sector	180°	
		Roughness	20 mm	
	Material	Carbon Steel		
		Density	7.8 g /cm^3	
		Longitudinal wave	5900 m/s	
		Transversal wave	3230 m/s	

Inspection		Single transducer		
	Configuration	Inspection plane	perpendicular to rotation axis	
		Inner/outer	external	
		Scanning direction	positive	
		Matched contact	NO adapted probe	
	Positioning	Choice or reference point	wedge center	
		Reference point coordinates	offset y	140 mm
			offset Θ	-15°
			offset R	9.614 mm
		Reference point in the CIVA reference frame	y	140mm
			Θ	-15°
			R	238.214 mm
	Coupling medium	water		
	Bottom medium	air		
	Scanning	Θ rotation	step	0
			number of steps	0
		Translation along the axis	step	0.1 mm/deg
			number of steps	190
		Choice of scanning modes	No increment	
			Scanning reversed	
			Increment skip	raster

PoD	Variables	Number characteristic Values	60	
		Number of samples	5	
		Charasteristic Value	Height	0.35 - 2.1 mm
		Step value	0.03	
		Type	Linear	
		Uncertain Parameters	skew	PDF Normal
			tilt	PDF Normal
			disorientation	PDF Normal
	Extraction	Type of Amax	ABS	
		No signal processing		
		No calibration		

4 RESULTS AND ANALYSIS

This section is divided in four major topics, illustrated in Figure 11, which are: Sensitivity Analysis, Simulated Relevant Parameters, Optimal Fitting of Simulated POD Curves and Optimal Fitting Transfer to a Test Set of Data.

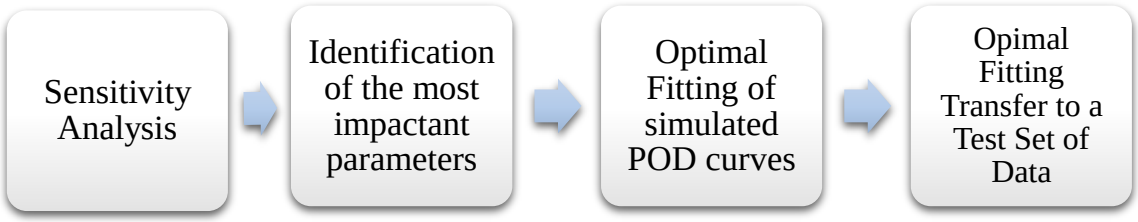

Figure 11: Flow chart of the main steps covered in the Results and Analysis section

It is important at this point of the dissertation, to stablish the terms for all virtual inspection configurations that will be addressed to. Each process brought up by Figure 11 has specific inspections configurations and the correspondent names and descriptions are as follow:

- CONTROL Configuration: is the virtual configuration coming from the experimental data regarding HAZ defects, showed in Table 3,
- OPTIMAL Configuration: is the CONTROL configuration after changes on the virtual setting under the sensitivity analysis guidelines,
- TEST Configuration: is the virtual configuration coming from the experimental data regarding Lack of Fusion defects,
- TRANSFERRED Configuration: is the TEST configuration after changes on the virtual setting under the same optimized parameters used in the OPTIMAL configuration.

4.1 SENSITIVITY ANALYSIS

The present section addresses the simulation parameters that may affect the simulated POD curve behavior when performed by CIVA software. To do so, the configuration CONTROL

showed on Table 3 will suffer systematic modifications changing one parameter at a time while the others remains constant. Therefore, the subsection will show graphic representations comparing two POD curves: CONTROL and the curve resulting from changing the parameter of interest. The results are divided in two categories: Computational Parameters and Physical Parameters. In order to inform the reader about which parameters names are being used literally as they are in CIVA, most parameters are presented in quotes in the first time that they are mentioned.

4.1.1 Assigning Variability to Simulated Data

As the probabilistic part of the simulated POD curve is based on a random set of numbers attributed to the uncertainty parameters, it is obvious that every POD built will differ from each other. Comparing two POD curves in a raw way will give the impression that all parameters modification affect the original curve (CONTROL). Therefore, if the intention here is precisely to stablish which parameters affect the most the POD behavior, it is important that an *error bar* is applied to the curves in order to distinguish from each other and compare them.

Well, the question is how to assign an error value to simulated data? For that matter, a method to do just that was proposed by the author of this dissertation to assign variability to simulated POD curves for comparison proposes.

As previously mentioned, being the POD curve a stochastic way to quantify reliability, there is a deterministic part and a probabilistic part. In CIVA, when a certain configuration is simulated and the POD curve is drawn, if there are no changes in any parameter, the generated curve will remain unchanged. It states that the software presents repeatability, which is expected. In that way, it presents no direct variability between two simulations. However, CIVA presents a functionality that is to randomize the uncertainty parameters (UP). In other words, all parameters remain constant but a new set of UP is produced. The result showed in Figure 12 is a different POD curve based on the randomized set of UP.

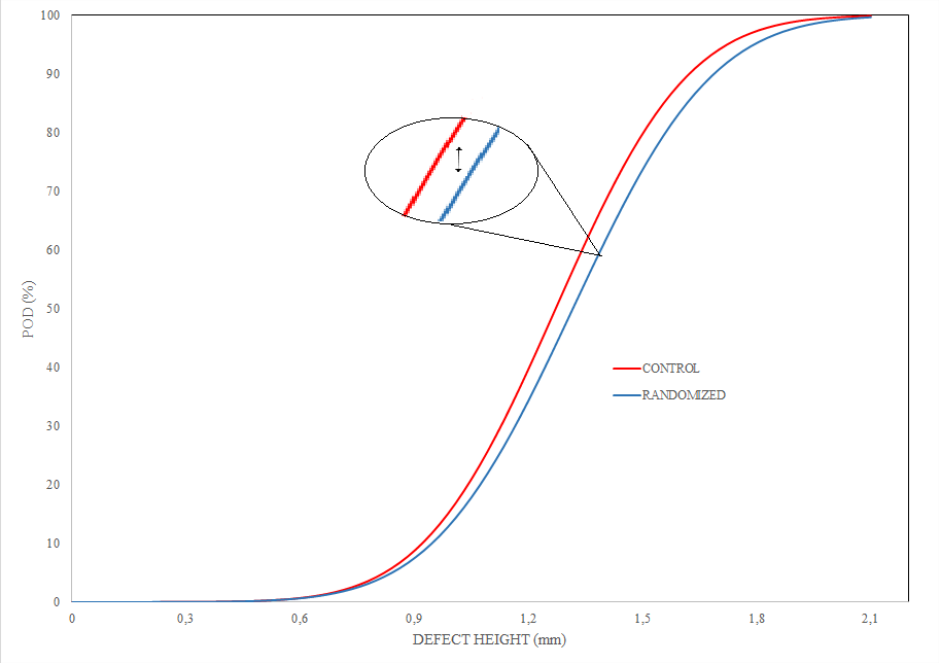

Figure 12: POD curve from CONTROL configuration before and after randomization of UP

The next step was to subtract the CONTROL POD values from the randomized curve. The result from the subtracting operation is a distribution of values that vary mostly in the transition area of the curve, tending to 0 when POD approaches the origin and when it approaches the 100% baseline. These subtraction values are then put on a decreasing order and the upper quartile of numbers were selected. Calculating the mean of the upper quartile, it was possible to get to a constant value of 6.03793% which is, from this point on, considered as simulated data error or as variability of simulated data. The unit is % because the value came from the subtraction of two probabilities values.

Therefore, all simulated POD curves in the sensitivity analysis section will present two auxiliary curves attached, as shown in Figure 13 – one above and another below the POD curve - varying the original probabilities values in a range of +/- 6.03793% in order to compare different configuration curves.

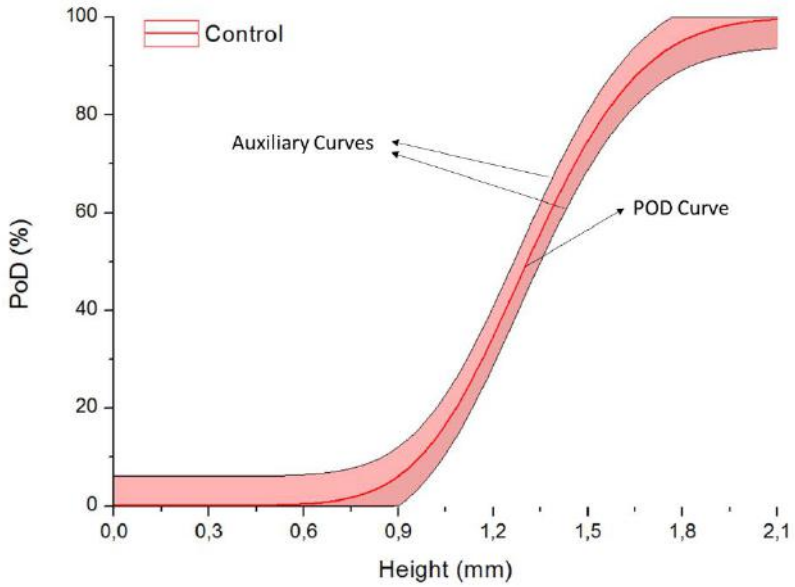

Figure 13: Auxiliary curves attached to the CONTROL POD curve representing the variability assigned to simulated data

Idealistic, it would be preferable is the variability assigned to the simulated data was not a constant value but a function that increases in the middle region of the POD curve and decreases at both extremes of it. For an initial approach, a constant value was used but further consideration on that matter in future works must be paid attention.

4.1.2 Computational Parameters

This subsection will report all parameters that do not represent direct physical meaning regarding UT, being mostly parameters that changes the computational configuration and premises. Setup of computational parameters is located on the "Simulation Settings" tab on CIVA and the parameters classified in five major categories: Initialization, Interactions, Gates, Options and Calibration. Each category presents a variety of parameters that can be set. Over twenty parameter change analyzes were performed and will be investigated as follows.

4.1.2.1 Computation Configuration

Computational configuration allows the user to choose between many ways to compute the simulation such as easy setting, direct, half skip, full skip, advanced definition and others. For the user that does not have experience on UT or CIVA, it is best to choose the "easy setting" option whilst the user that is more acquainted with the tool can choose the "advanced definition".

The CONTROL configuration assumes the advanced definition and the changed one was the easy setting. In fact, as Figure 14 shows, there is no impact on resulting POD curves when the easy setting is chosen as both curves are superimposed. Instead, there is one important advantage of using the easy setting: the computational cost is lower. While the advanced definition takes around 8 hours of simulation time, the easy setting take almost 3 hours, always using an Intel Xeon CPU E5-2620, 2 processors (2 GHz). Therefore, if the user does not need the advanced definition, it is strongly recommended that the easy setting be used.

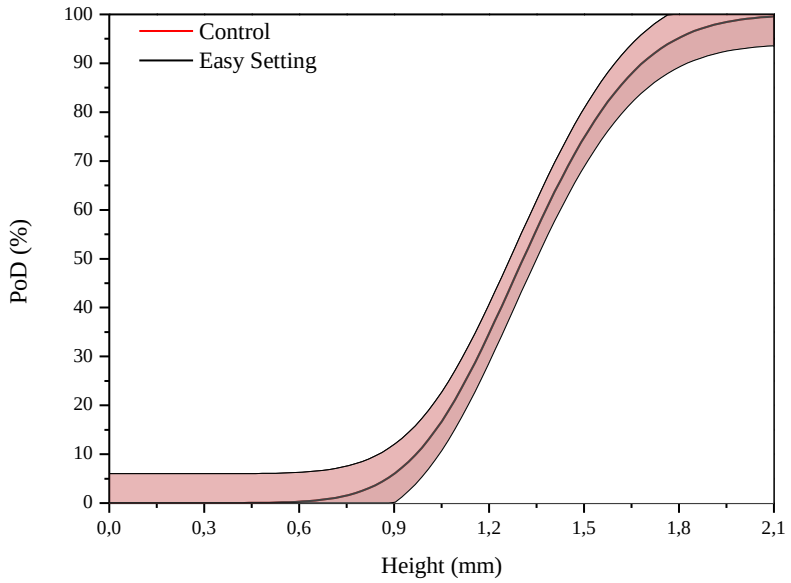

Figure 14: Effect of computational configuration on simulated POD: curves superimposed showing no difference between CONTROL (Advanced Definition) vs Easy Setting behavior regarding POD curves

4.1.2.2 Involved Modes – Longitudinal and Transverse Waves

"Longitudinal waves", "transverse waves" and "account for mode conversions" are the options of the "involved mode" configuration. The user can choose more than one mode to set the simulation. On CONTROL configuration, the transverse mode was selected and the changed configuration accounted for both transverse and longitudinal waves and no difference between the two configurations could be detected on the POD curve. Regarding the "account for mode conversion" option, this is a typical example that if the user does not need the simulation to compute all modes conversions, this option definitely should not be enabled. While the CONTROL configuration takes 8 hours to me simulated, the one that accounts for mode conversion takes 54 hours and the POD curve based on this last model is exactly the same as the CONTROL.

4.1.2.3 Specimen Echoes

Regarding the "specimen echoes model", the user can choose between a "specular" model and a non-specular model: the "Kirchhoff" scattering, which was used in CONTROL configuration. In the case of the present particular configuration, there was no difference on the POD results between the two echoes models.

Concerning which echoes are taken into account, the user can select among front echoes, back wall echoes, interface echoes and side echoes. CONTROL configuration enables the "back wall echoes" and once the corresponding POD is simulated, it shows no difference from the simulated POD for back wall echoes disabled. The time for computing the simulation is 3 hours for back wall echoes disabled and approximately 8 hours for "back wall echoes" enabled, so the user might gain some substantial time disabling this particularly option.

4.1.2.4 Skips – Number of Half Skips

While the CONTROL configuration consider one half skip to be computed, the changed configuration assumes five maximum half skips regarding the ultrasonic wave. Skip can be understood as the sound path distance between two successive surface reflections. Therefore, a half skip is half of that distance. Increasing the "number of half skip" is the same as extending the reach of the ultrasonic beam. Simulating the POD for five half skips, results show a POD that display no difference in comparison with the original one (one half skip).

4.1.2.5 Flaw Model – Kirchhoff & GTD

Still on simulation settings, CIVA presents a tab under Interactions that refers to the model that is used to simulate the flaw. The current model is "Kirchhoff & GTD" (BO LU *et al.* (2012)) for the rectangular defect and it is activated in CONTROL configuration. For any planar defect, CIVA uses geometrical theory of diffraction (GTD) and the Kirchhoff approximation for scattering modeling. When this option is disabled, the POD curve cannot be plotted due to calculations errors. The problem is that the software does not inform the error to the user right up front. The error is reported at the end of all calculations, which taken nearly 3 hours to be finalized.

4.1.2.6 Sensitivity Zone

Establishing a "sensitivity zone" (SZ) is equivalent to establishing a ROI (region of interest). In theory, if the virtual inspection configuration is properly set, there should be no difference between defining or don't a SZ. If the probe is at the correct place and the flaw is detectable, the simulated POD for both configurations should be the same. It is only a computational tool to focus computational effort in a certain region; and that in fact could be inferred on the followings comparisons between:

- Sensitivity zone enabled (CONTROL) *vs* disabled

- SZ dimension decreased from 30 mm x 30 mm x 30 mm (CONTROL) to 25 mm x 25 mm x 25 mm
- SZ dimension enhanced from 30 mm x 30 mm x 30 mm (CONTROL) to 35 mm x 35 mm x 35 mm

The resulting simulated POD curves show no difference when compared to CONTROL configuration POD curve. Therefore, settling changes on the sensitivity zone does not enhance nor decrease simulated reliability.

4.1.2.7 Gate

The "gate" in an UT inspection is the window that will provide the signal response for a possible indication. It is extremely important that the gate is set according as part of the inspection calibration system. Regardless, concerning simulated POD curves performed by CIVA, the fact that the gate is enabled or disabled, the resulting POD is not significantly affected. Furthermore, once the option "gate" is enabled, the way that synchronization is stablished is irrelevant to simulated POD curve. The user can set the synchronization by the "echo max absolute" or "first echo" and the simulated reliability presents the same behavior.

4.1.2.8 Computation Type

About the computation of virtual inspection, users have two options available: compute the results through a "3D" model or using a "2D" model. The 2D model is usually used to study the ultrasonic phenomena on a certain section of the virtual solid.

For a full simulation experience using defect inspection module, it is recommended the 3D computation type. Based on the previous information, it is expected that for the changed configuration, which admitted a 2D computation, the reliability result could not be calculated.

4.1.2.9 Field Interaction

There are many ways to compute the UT beam when a virtual inspection takes place. Concerning the field interaction, CIVA provides the "plane wave approximation for incident plane" and "full incident beam". It is logical to infer that one considers mathematical approximations for the beam while the other takes the full beam incidence into account.

The result shown in Figure 15 reveals a completely different POD curve from the original CONTROL. The results show an increase on the detectability resulting in a steeper curve. The computational cost also increases drastically for the full computational mode. While the CONTROL configuration results in an 8 hours simulation process, the full incident beam results in a 36 hours simulation.

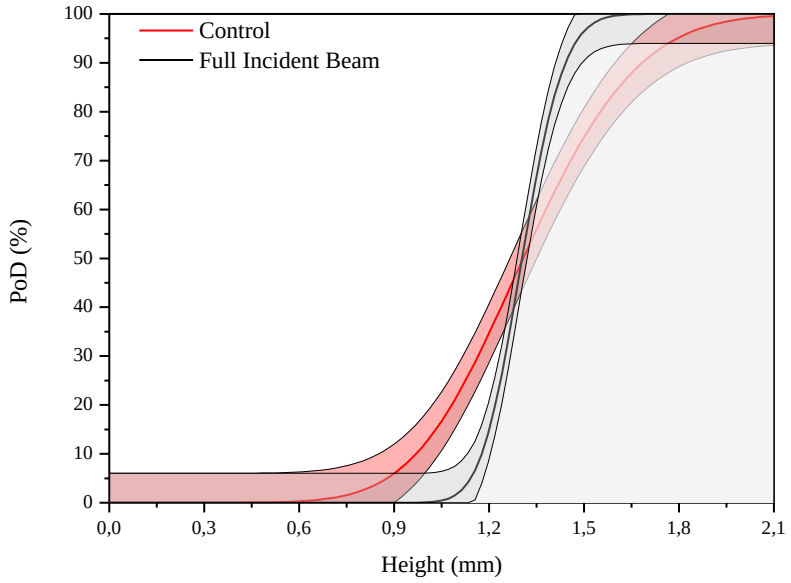

Figure 15: Effect of field interaction on simulated POD: CONTROL (approximation) vs Full Incident Beam

4.1.2.10 Accuracy Field and Accuracy Defect

The software provides an option to change the "accuracy field" and "accuracy defect". Under Options tab on Simulation Settings, the user can change the previous default value, which is one. Both parameters were tested changing the accuracy value to two as an initial attempt to study these variables and the results are shown in Figures 16 and 17. No important changes on the simulated POD for accuracy field change was detected. Although, changes on the accuracy defect cause a decrease of simulated reliability.

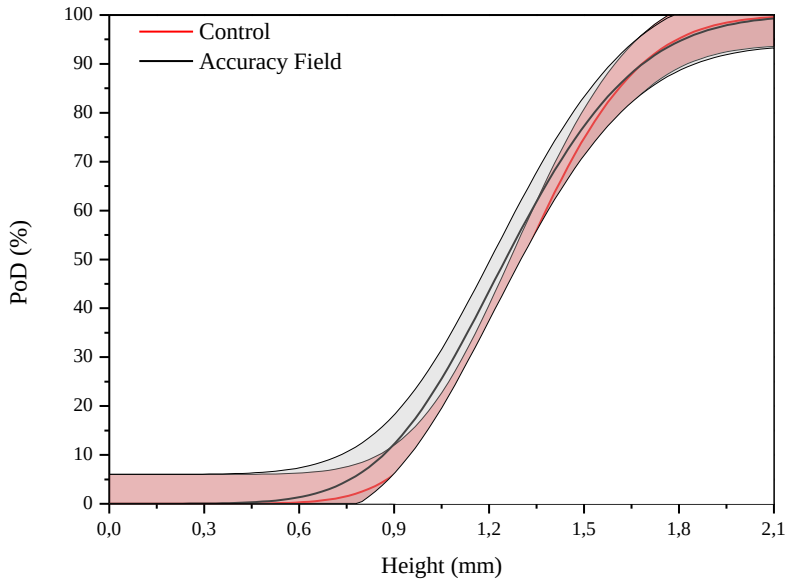

Figure 16: Effect of accuracy field on simulated POD: CONTROL (1) vs accuracy field 2

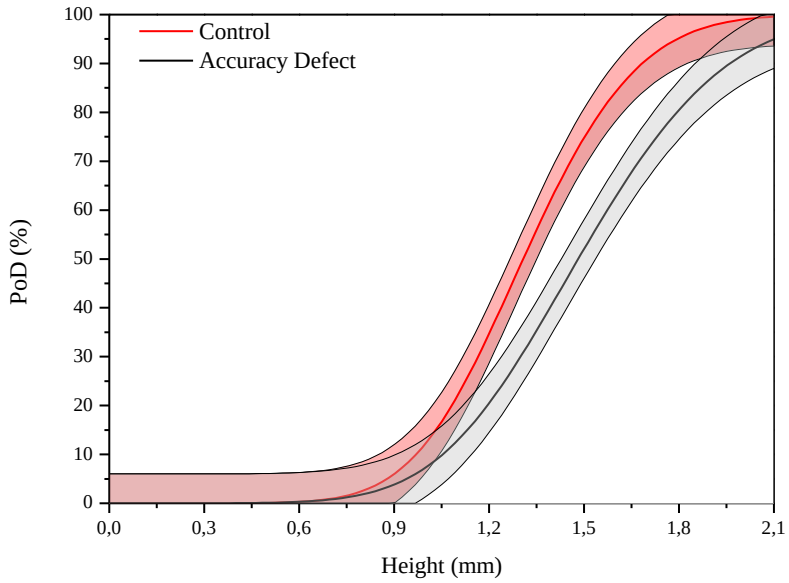

Figure 17: Effect of accuracy defect on simulated POD: CONTROL (1) vs accuracy defect 2

4.1.2.11 Account for Attenuation

It is also possible to "account for attenuation" by checking the correspondent box under Options tab. Since the material inspected is a regular steel, there are no expected attenuation. Moreover, as will be seen on Physical Parameters Section, the material is set up for not to account for attenuation. As expected, no impact on the simulated POD is perceived when this option is disabled.

4.1.2.12 Creeping Waves

"Creeping waves" are a particular phenomenon where longitudinal waves are taken into account (KRAUTKRAMER (1990)). Although, even when only transverse waves are considered, there are mode conversions inside the material and creeping waves can be produced. The base simulation CONTROL only considers transverse waves and besides that, does not account for mode conversions. Therefore, if the user chooses those options, which

are longitudinal waves and uncheck the account for conversion mode box, the option to account creeping waves must be disabled; otherwise the simulation will not be completed.

4.1.3 Physical Parameters

In this present section, the sensitivity analysis concerning physical UT parameters is explored. The analysis of physical parameters is subdivided respecting the categories used by CIVA, which are Specimen, Probe, Inspection, Flaws and POD. The majority of the relevant physical parameters were tested, totaling over sixty POD predictions accounting for more than 700 hours of simulation.

4.1.3.1 Specimen

The tab for specimen specification allows the user to set properties of the material, its dimensions and geometry, among other parameters. CIVA provides options to insert homogeneous and heterogeneous materials, add new materials to the already extended material library, insert attenuation and structural noise and account for depressions. At this point, it is worthwhile reviewing the settings used in CONTROL regarding the specimen set up:

- Geometry: Cylinder
- Outer Diameter: 457.2 mm
- Thickness: 28.32 mm
- Material: Carbon Steel
- Roughness: 20 μm
- No attenuation / no structural noise / no depressions

4.1.3.1.1 Outer Diameter

The actual pipe used in all experimental inspections has 457.2 mm of "outer diameter". This comparison aims to stablish what influence an increase on the outer diameter would have on the probability of detection of defect from HAZ type. In order to do so, an increase of 10 mm (~2%) on the outer diameter was performed virtually and the corresponding POD was built. Figure 18 shows that, regarding a_{90} and $a_{90/95}$ values, there was no effect by increasing the outer diameter, whereas the probability of detection increases for flaw sizes between 0.6 mm and 1.4 mm. For instance, flaw sizes of 1.2 mm, for example, are detected with a probability of 45% regarding the CONTROL configuration while the same flaw size is detected with over 70% POD when the outer diameter is increased.

4.1.3.1.2 Thickness

Just like the outer diameter analysis, the original "thickness" value was increased in approximately 2% from the original value and the possible impact on POD is evaluated comparing the increased thickness with the POD regarding the original configuration (CONTROL). Figure 19 shows the lower values of probability of detection due to the incremental increase on thickness value.

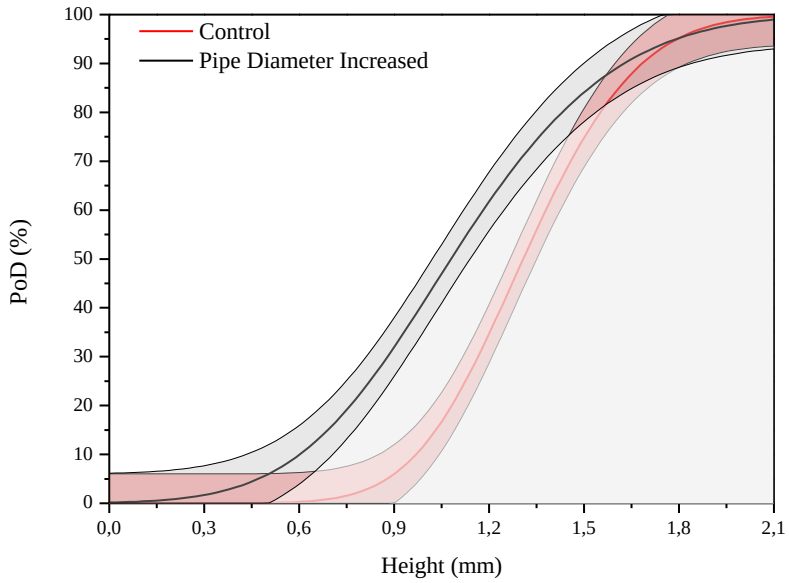

Figure 18: Effect of outer diameter on simulated POD: CONTROL (457.2 mm) vs Outer Diameter Increased (467.2 mm)

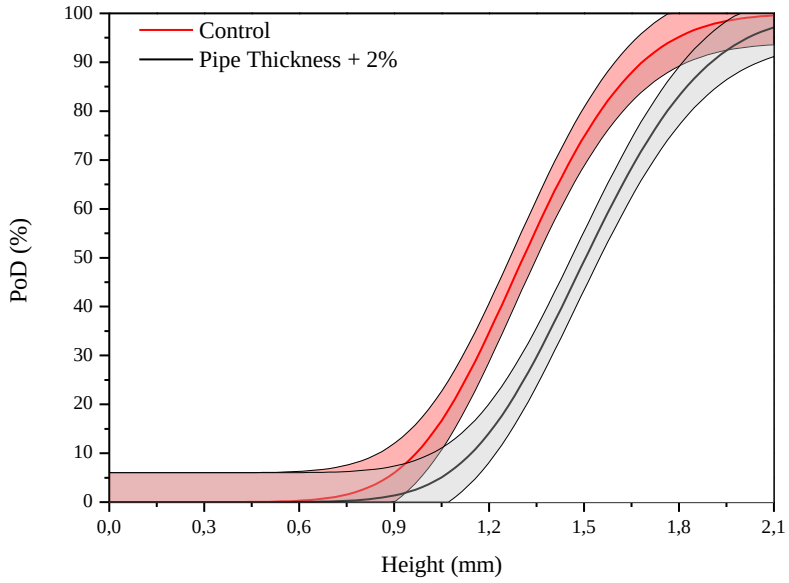

Figure 19: Effect of thickness on simulated POD: CONTROL (28.32 mm) vs Thickness Increased (28.88 mm)

4.1.3.1.3 Roughness

According to HONEYWELL (2009), the surface "roughness" of a steel oil pipe is around 45 μm. In CONTROL modeling, the roughness used was 20 μm and this value was attributed to the experimental pipe empirically. No formal tests were used to stablish the exact roughness value. It could be considered that the value used in the CONTROL simulation is near the predicted by HONEYWELL (2009). However, it could also differ from the expected value due to fabrication conditions. The experimental pipe presented a rather irregular surface and it is possible that the simulated roughness value was underestimated. For that reason, the changed POD prediction considered a roughness of 100 μm and Figure 15 shows that the 100 μm roughness resulted in lower probabilities of detection.

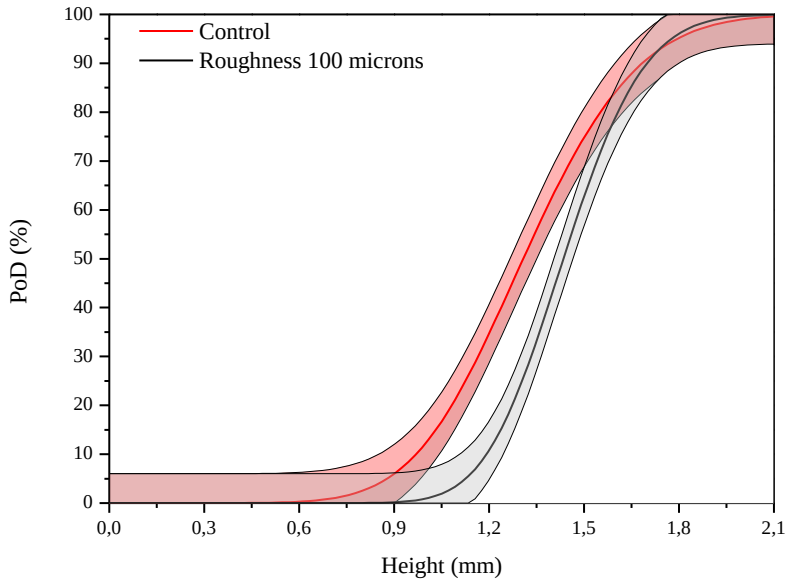

Figure 20: Effect of roughness on simulated POD: CONTROL (20 μm) vs Roughness of 100 μm

This result is expected since a higher roughness makes coupling of the probe on the surface pipe more difficult. Nevertheless, the roughness of 4 μm was also tested to predict the POD behavior when the surface is more polished. Results shown at Figure 21 enlighten that no

significant difference on POD is perceived. This means that under a certain value, the roughness does not impact the probability of detection.

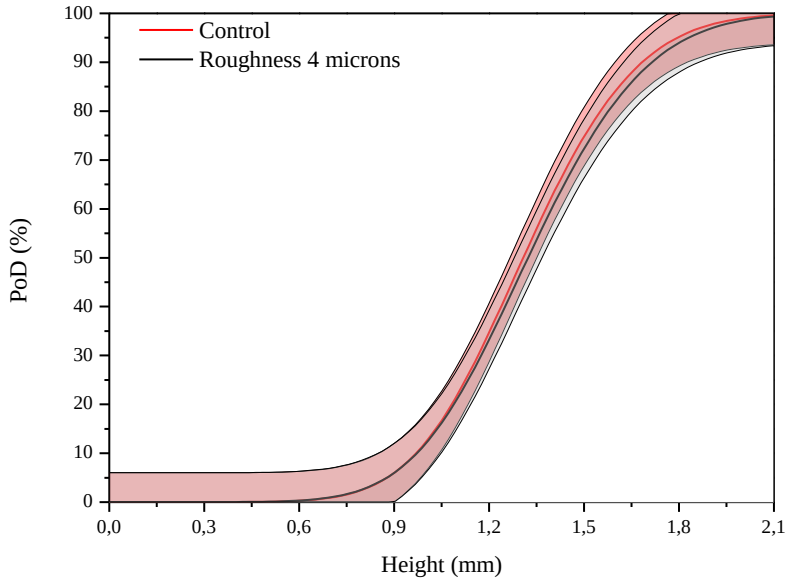

Figure 21: Effect of roughness on simulated POD: CONTROL (20 μm) vs Roughness of 4 μm

4.1.3.1.4 Material

CIVA contains an interesting variety of materials on its library. They are divided in four major groups: anisotropic materials, composites, isotropic and polycrystalline materials. The experimental pipe is a regular API 5L X-65 which is usually produced for oil transport. Since CIVA does not provide this particular option, the configuration CONTROL assumed the pipe material as being regular steel which shows similar characteristics compared to API 5L X-65 regarding longitudinal and transverse wave velocities. To test the material impact on POD, two different materials were considered in the changed configuration: 410 and 302 stainless steel. Figure 22 compares reliability results between regular steel and 410 stainless steel while Figure 23 shows the results for 302 stainless steel. On the comparison between regular steel and 410 stainless steel, the simulated reliability decreased, while regarding 302 stainless steel, POD showed no significant difference.

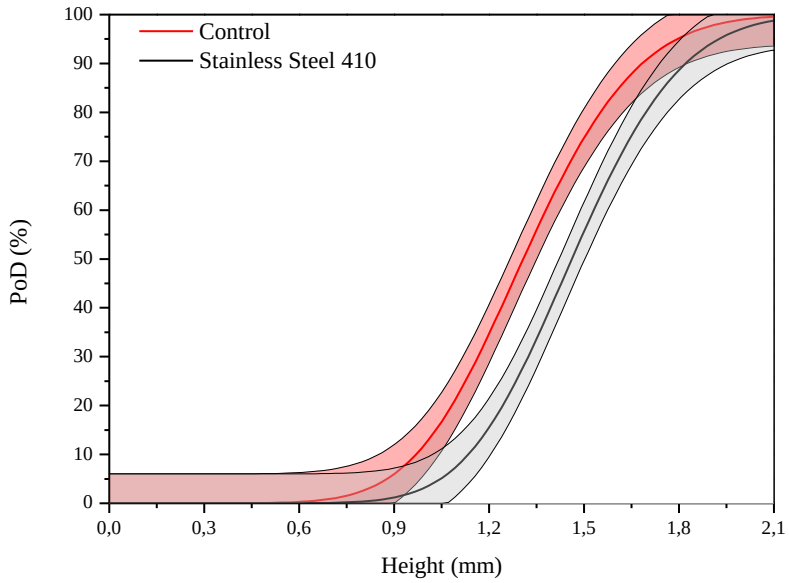

Figure 22: Effect of material on simulated POD: CONTROL (steel) vs Stainless Steel 410

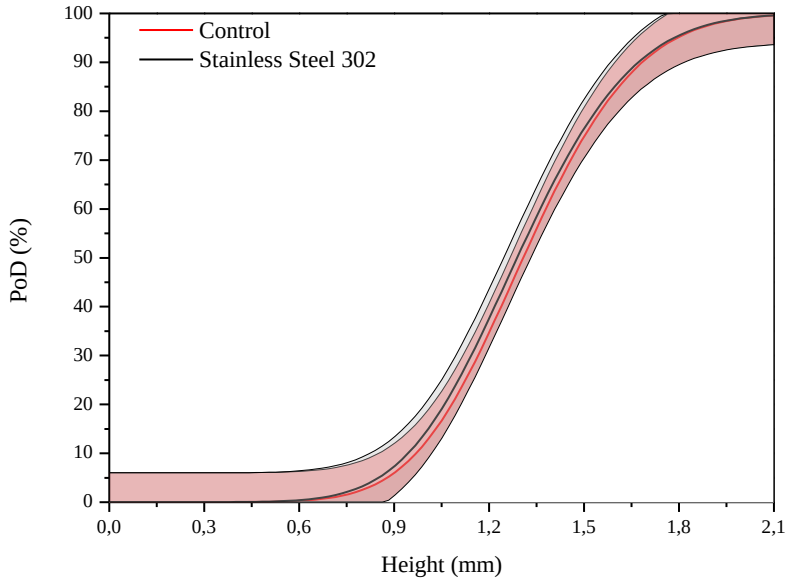

Figure 23: Effect of material on simulated POD: CONTROL (steel) vs Stainless Steel 302

These results are suitable to the sensitivity analysis but they do not show good agreement with real inspections. Usually, stainless steel presents a very unique microstructure where the crystallographic directions of the grains totally differ from one other, scattering the ultrasonic wave (MARK *et al.* (2014)). As such, it was expected that the simulated results would show a drastic drop of reliability which was not observed, because CIVA does not take into account stainless steel microstructure, regarding version 2016.

4.1.3.2 Probe

The Probe tab is divided in five groups being: Crystal shape, Focusing, Wedge, Signal and Case. The probe can be set as contact type, immersion, dual element, flexible, surrounding array, surrounded array and EMAT.

CONTROL configuration admits a contact probe with wedge. Under crystal shape tab, the user can change the pattern of crystal and its geometry. Focusing tab provides options on the surface type being flat, cylindrical, spherical, bifocal, trifocal or Fermat. For the baseline POD curve, a flat surface type probe was selected in CONTROL. The wedge tab allows the user to change wedge configurations as its geometry and material while the Signal tab characterizes the UT signal properties. The Case simply allows the user to consider or not a probe's case visualization.

4.1.3.2.1 Crystal Shape

CONTROL configuration set the crystal geometry as rectangular. The present subsection intents to analyze the impact of changes in geometry on the simulated POD curve. For that matter, the changed configuration admits a circular "crystal shape" and results are demonstrated on Figure 24.

The comparison between the two configurations shows that when the shape of the crystal is modified, the reliability suffers an impact decreasing its behavior, represented by a horizontal shift in the curve.

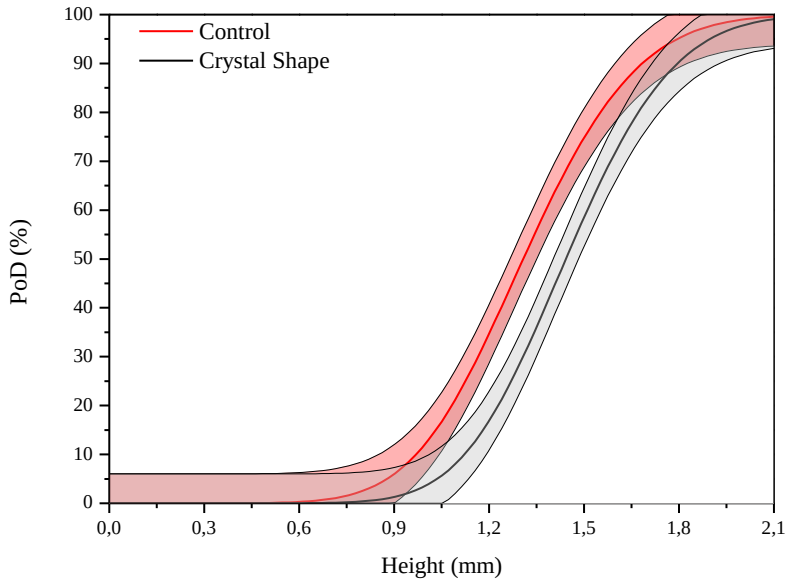

Figure 24: Effect of crystal shape on simulated POD: CONTROL (rectangular) vs circular crystal shape

4.1.3.2.2 Crystal Dimension

The user can also change the dimensions of the probe's crystal. CONTROL set the size of the crystal as being 8 mm of width and 9 mm of length. The changed configuration admitted a crystal size being 9.6 mm of width and 10.8 mm of length.

Results in Figure 25 show a small loss of reliability, especially between defect heights between 0.9 mm and 1.3 mm. However, the changed configuration presented a steeper curve, which is a good result in terms of reliability since it clearly discriminates defects that are and that are not detected.

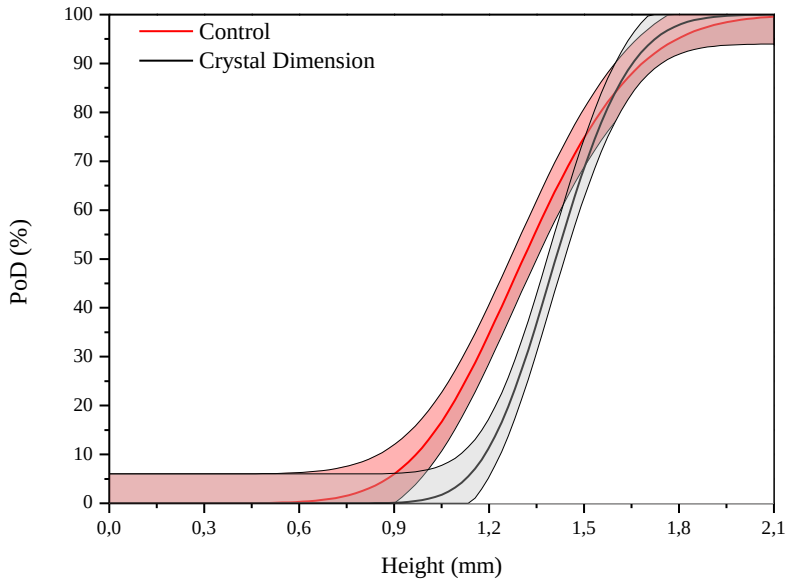

Figure 25: Effect of crystal size on simulated POD: CONTROL (8 mm x 9mm) vs 9.6 mm x 10.8 mm

4.1.3.2.3 Wedge Geometry – Crystal Orientation

Experimental results demonstrate that the wedge is amenable to suffer wear due to constant friction between its surface and the object of inspection. This wear makes the wedge slightly inclined which can affect the direction of the ultrasonic beam. Changing the "crystal orientation" on the simulation environment is an appropriate way to simulate the wedge wear. From the experimental inspections, it could be observed that this wear, on average, is around 2°. Therefore, while CONTROL configuration admits a crystal orientation of 60° for refraction angle, the changed configurations will admit 58° and 62° for refraction angle. Results are shown in Figures 26 and 27 and both demonstrate that there is no significant impact on reliability due the wedge wear regarding CONTROL configuration. Although, they suggest that a reduction in the refraction angle resulted in a shallower POD curve and an increase of the refraction angle result on a steeper simulated curve. Therefore, these parameters effect cannot be undervalued.

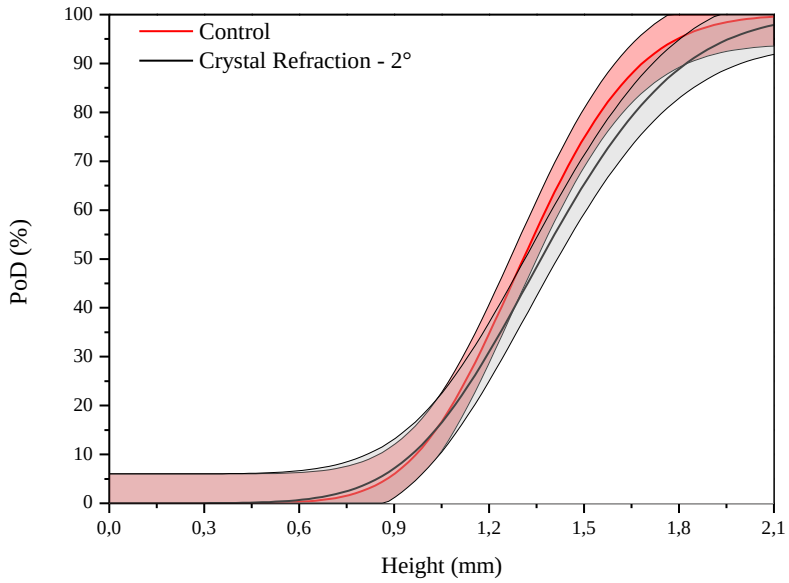

Figure 26: Effect of crystal refraction angle on simulated POD: CONTROL (60º) vs Crystal Refraction -2º (58º)

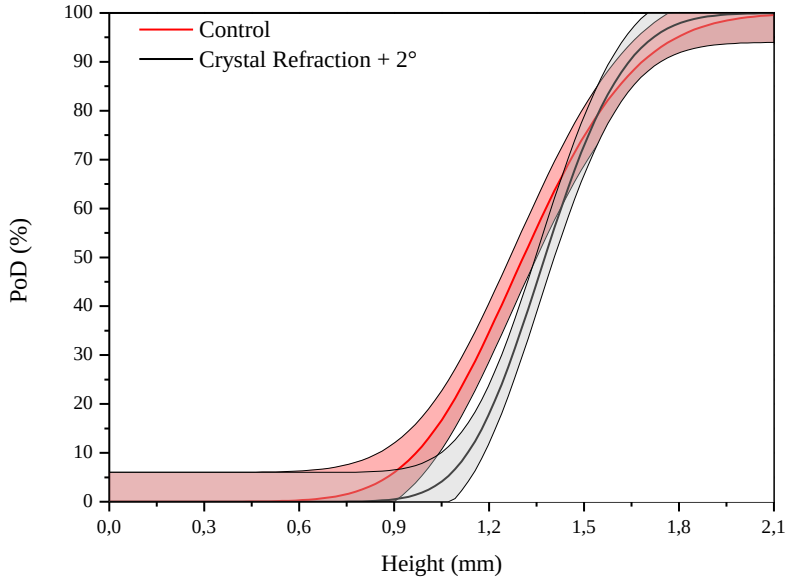

Figure 27: Effect of crystal refraction angle on simulated POD: CONTROL (60º) vs Crystal Refraction +2º (62º)

4.1.3.2.4 Wedge Geometry – Squint Angle

"Squint angle" can be understood as being the measurement on how deviated the ultrasonic beam is related to the probe's axis, as can be seen in Figure 28.

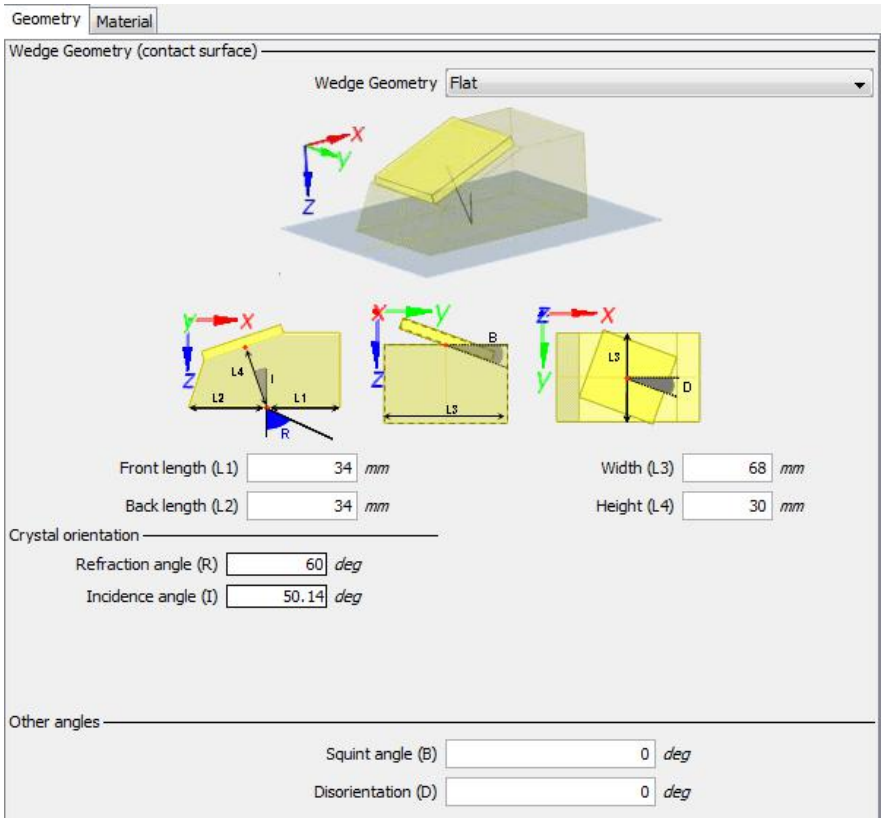

Figure 28: Representation of the Squint Angle (B) and Disorientation Angle (D) according to CIVA software

Probe manufactures try to keep this particular angle always below 2º, although, ideally, it should be zero. In fact, zero was the value used in the CONTROL configuration. The present subsection evaluates the squint angle impact on reliability when it is ± 2º. Results shown in Figures 29 and 30 reveal a significant impact of squint angle on the POD curve and in both cases, reliability decreases.

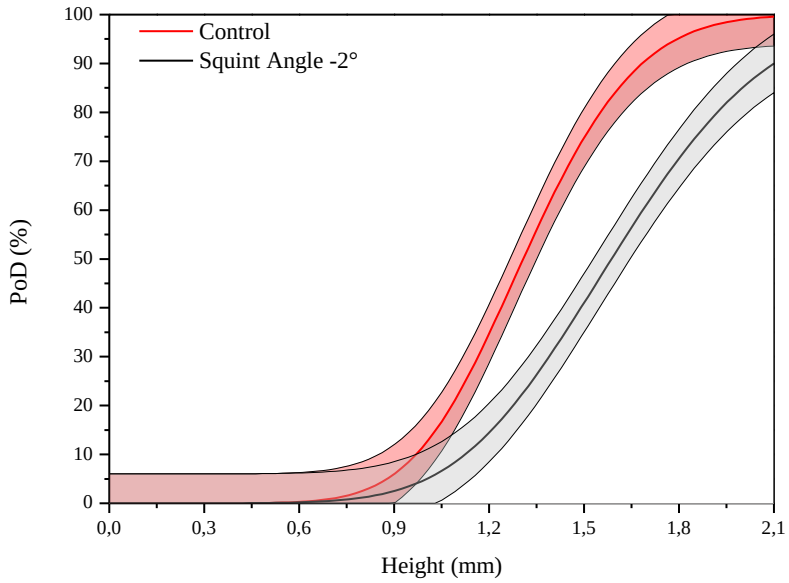

Figure 29: Effect of squint angle on simulated POD: CONTROL (null) vs squint angle -2º

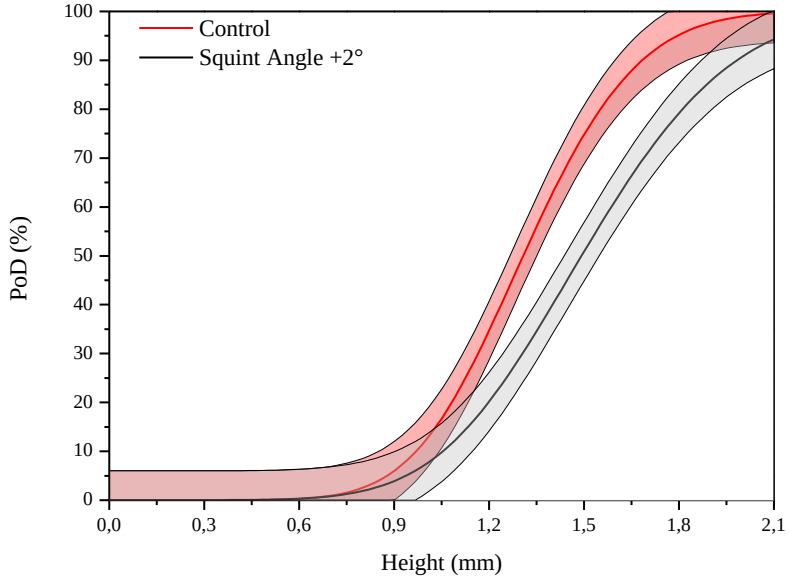

Figure 30: Effect of squint angle on simulated POD: CONTROL (null) vs squint angle +2º

4.1.3.2.5 Wedge Geometry – Crystal Disorientation

"Crystal disorientation" is the angle formed when there is any rotation of the crystal around its own axis, according to Figure 28. Control configuration admits crystal disorientation equals zero, as it should be in practice. The changed configuration will admit a 2º disorientation in order to assess its impact on reliability.

Figure 31 shows that the POD curve suffers a significant impact of the tested parameter, lowering the reliability.

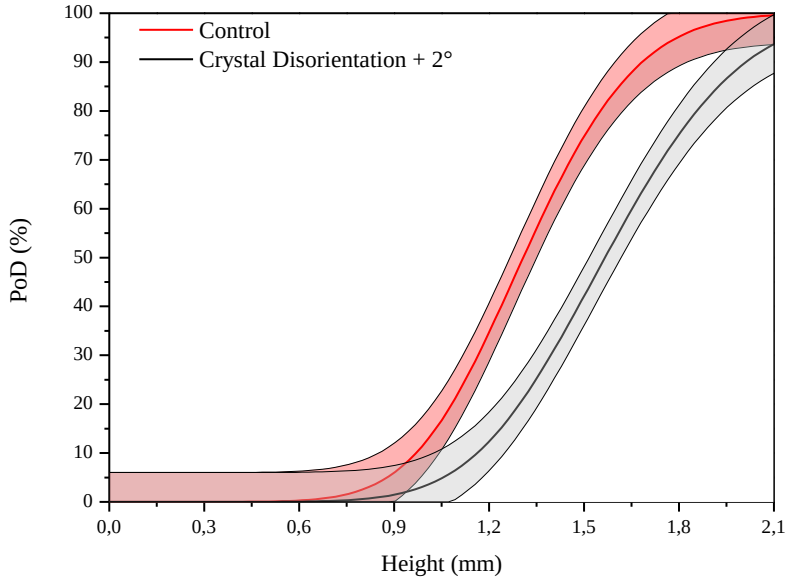

Figure 31: Effect of disorientation angle on simulated POD: CONTROL (null) vs disorientation angle +2º

4.1.3.2.6 Wedge Material

The wedge is usually made of an attenuating material such as a polymer. CONTROL configuration used a "plexiglass" wedge while the changed configuration admitted a "rexolite" wedge. Figure 32 shows that the resulting POD curve remained nearly unchanged, except for two aspects: flaw sizes between 0.8 mm and 1.3 mm have different POD values

and the changed configuration provides a less steep POD curve, which is not good for reliability analysis.

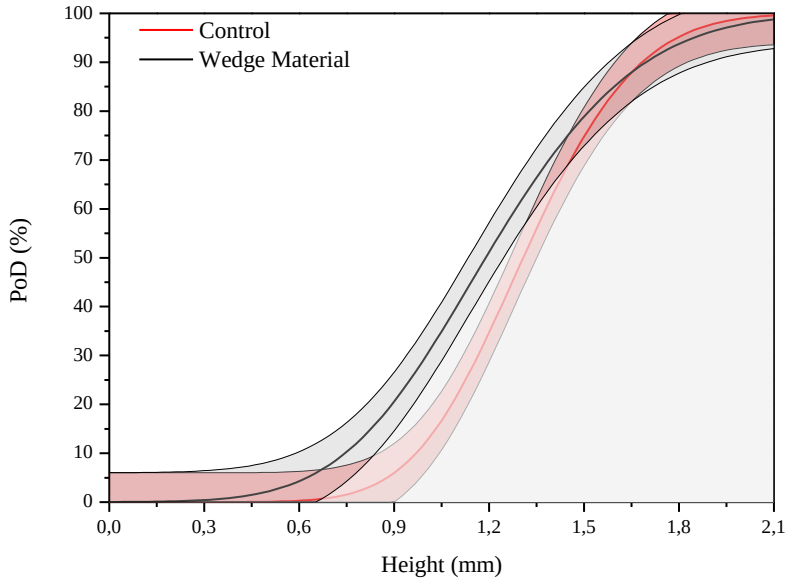

Figure 32: Effect of wedge material on simulated POD: CONTROL (Plexiglass) vs Rexolite

4.1.3.2.7 Signal Choice

CIVA's signal tab allows the user to set up configurations regarding the ultrasonic signal properties. Regarding "signal choice", CIVA presents three possible modes to the final user: Gaussian, Hanning and Imported. CONTROL configuration admits the imported signal but this choice was not based on any prior knowledge on the matter. The changed configuration considered a Gaussian signal choice and the resulting POD curve shows no significant difference between the two configurations.

4.1.3.2.8 Signal Frequency

Every probe has an intrinsic frequency and choosing the right one to perform a certain inspection can provide important enhancements on reliability. The probes used on the experimental inspections were 4 MHz probes.

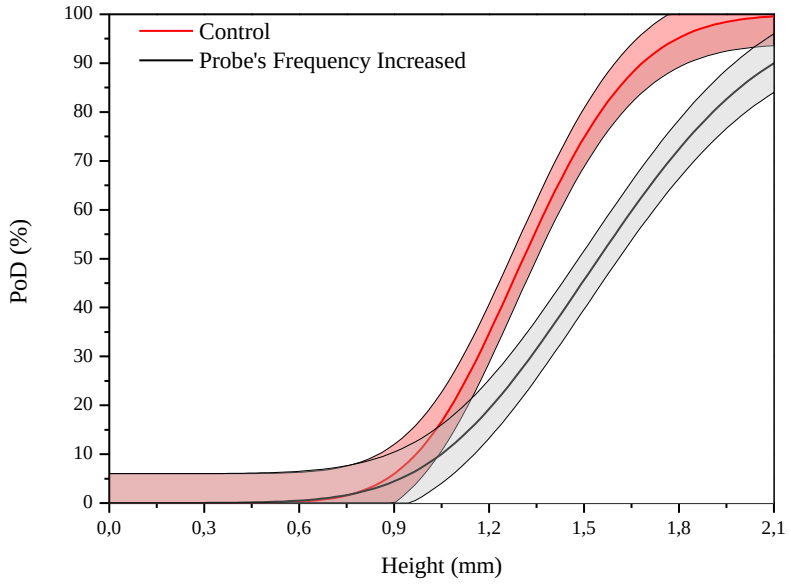

Figure 33: Effect of frequency on simulated POD: CONTROL (4 MHz) vs frequency increased (4.8 MHz)

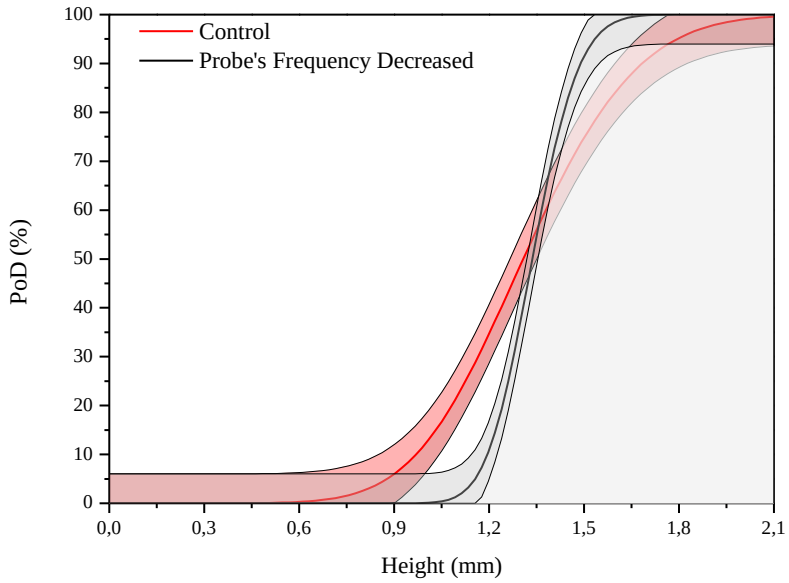

Figure 34: Effect of frequency on simulated POD: CONTROL (4 MHz) vs frequency decreased (3.2 MHz)

Therefore, the frequency set up on the CONTROL configuration was also 4 MHz. The present subsection will assess the effect of this frequency on the POD curve when its value is increased and decreased 20%. Figures 33 and 34 show two different impacts on the CONTROL POD curve. Figure 33 indicates that when there is an increase in 20% on the probe's frequency, the reliability decreases while Figure 34 show the exact opposite: when frequency is decreased in 20%, reliability increases. Indeed, reduction in frequency of the probe resulted in steeper POD curves.

4.1.3.3 Inspection

Inspection tab brings five major capabilities for the user to simulate the reliability analysis, namely: Configuration, Positioning, Coupling Medium, Bottom Medium and Scanning. CONTROL configuration admits a single transducer inspection instead of Tofd or Tandem. This section deals with the evaluation of inspection parameters and their influence on the

probability of detection, analyzing six major aspects involving: scanning, coupling and bottom medium and adapted probe.

4.1.3.3.1 Adapted Probe

Under the configuration tab, the user can set the matched contact enabling the "adapted probe" option. Adapted probe disregards any difficulty in respect to the coupling of the probe onto the inspected surface. It is, however, an ideal approach that cannot be reproduced fully on experimental inspections. CONTROL configuration disables the adapted probe in order to better reproduce experimental results. However, aiming to proceed with the sensitivity analysis of the software, the changed configuration enables the adapted probe and the resulting effect on reliability is shown in Figure 35. As expected, the resulting POD curve shows that probability of detection is increased with adapted probe.

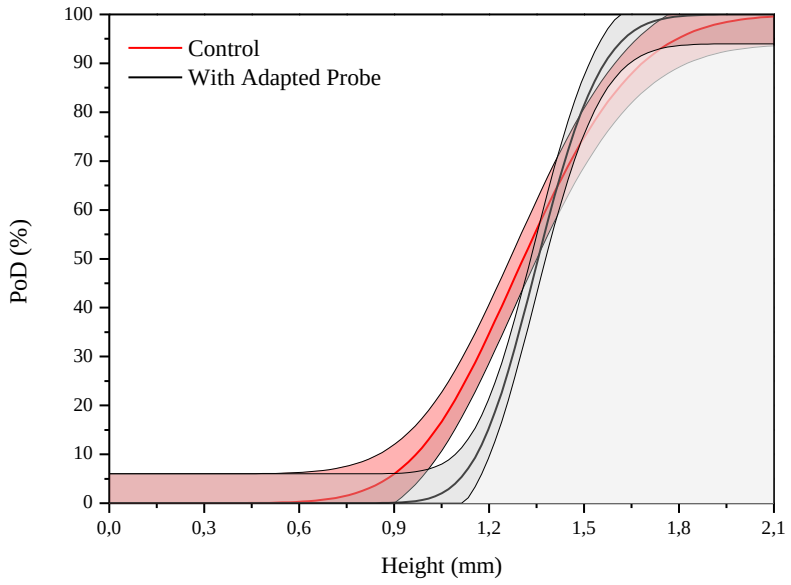

Figure 35: Effect of adapted probe on simulated POD: CONTROL (disabled) vs Adapted Probe Enabled

4.1.3.3.2 Coupling Medium

Since the experimental inspections were performed as being contact inspections, it is important to analyze the influence of the medium used to couple the probe to the pipe surface. In the CONTROL configuration water was used as the "coupling medium". The changed configuration will analyze the impact on changing water to glycerin. Figure 36 shows a resulting steeper curve and a better probability of detection, especially for flaw heights over 1.3 mm.

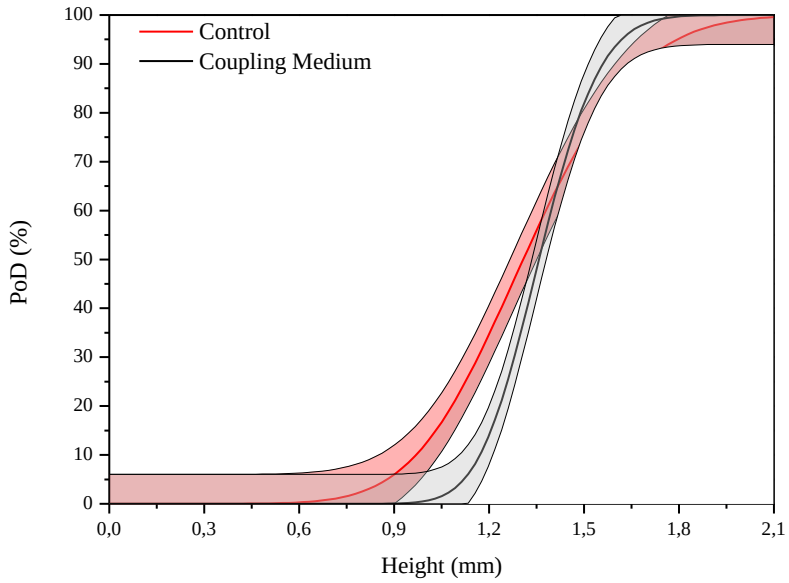

Figure 36: Effect of coupling medium on simulated POD: CONTROL (water) vs Glycerin

4.1.3.3.3 Bottom Medium

In this subsection, the effect of the nature of "bottom medium" is analysed. The experimental pipe was an oil pipe but at the moment of the inspection, it was empty. Therefore, the bottom medium is air and this characteristic was transferred to the CONTROL configuration. The changed configuration declares a bottom medium as oil as if the pipe was filled. After simulating the POD curves, results showed no significant difference between CONTROL and changed configuration regarding reliability.

4.1.3.3.4 Scanning

Scanning parameters on a simulated inspection are some of the most important parameters, so they must be analyzed carefully. The present subsections will analyze two scanning options: “number of steps” and one “scanning choice mode”.

The inspection step along the number of steps on the inspection axis gives an idea on how the inspection is being judicious. For instance, if the simulation takes an inspection value every 2 mm instead of every 0.1 mm, it means that there are regions that are not being inspected.

Moreover, if only 10 measurements of signal response are made, instead of 200, it is logical to infer that the resulting simulation will be less effective. With these arguments in mind, it is easy to understand the importance of inspection scanning. The CONTROL configuration admits 190 steps with a step of 0.1 mm/degree. The changed configuration admits only 19 steps and the resulting POD curve is shown in Figure 37.

As expected, the simulated POD curve for 19 steps reveals a less refined probability of detection. This subsection also tested a change in the “scanning mode”. CONTROL configuration disabled both software’s options: “increment” and “scanning reversed”, which means that the movement that the probe carries out is straight forward on the inspection axis predefined.

The scanning reverse admits a back and forward scanning regarding the probes movement on the inspected area. Regarding this parameter, enabling scanning reverse mode has no effect on the resulting simulated POD.

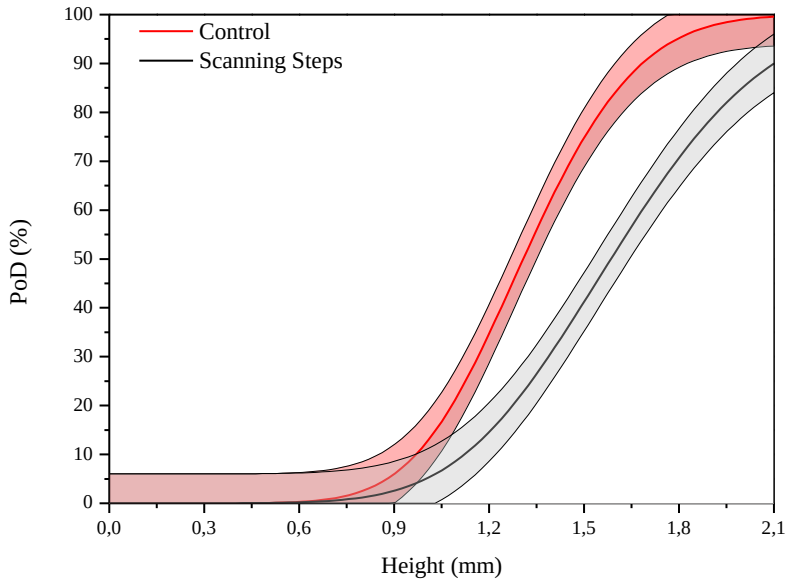

Figure 37: Effect of scanning steps on simulated POD: CONTROL (190 steps) vs 19 steps

4.1.3.4 Flaws

Regarding the Flaws section, aspects such as their geometry and position will be addressed and their effect on simulates POD curves will be analyzed. Along with basic parameters, sophisticated aspects concerning reliability such as characteristic values and uncertainty parameters and their probability distribution function (PDF) will be discussed. Reviewing some important aspects concerning the CONTROL configuration and the corresponding POD curve, it is worth emphasizing that the heights of the defects were defined as characteristic values and that the orientations of the defects were considered as uncertainty parameters: tilt, skew and disorientation. The geometry of the flaw is considered to be rectangular, which is suitable for a defect type as crack. The flaw length is considered 12 mm for all simulations in the present dissertation and will not be changed; otherwise, it would be impossible to compare the PODs. Indeed, in order to keep the CONTROL as the reference configuration, flaw length must not be altered. The height of the flaws varied from 0.35 mm to 2.1 mm, as already mentioned before in the Methodology Section.

4.1.3.4.1 Flaw Positioning

CIVA allows the user to position the flaw in three major ways: with its length along the rotation axis, perpendicular to the rotation axis or in an oblique way. CONTROL assumes the "flaw position" with its "length along the rotation axis" and this subsection will analyze the impact on the POD curve of changing this position to "oblique".

Figure 38 show how the probability of detection decreases when the flaw is in an oblique position. This result was expected since the probe was set to detect the flaw directly. If the flaw is in an oblique position, its reflection area decreases and the ultrasonic sees the flaw as being considerable smaller than in reality it is.

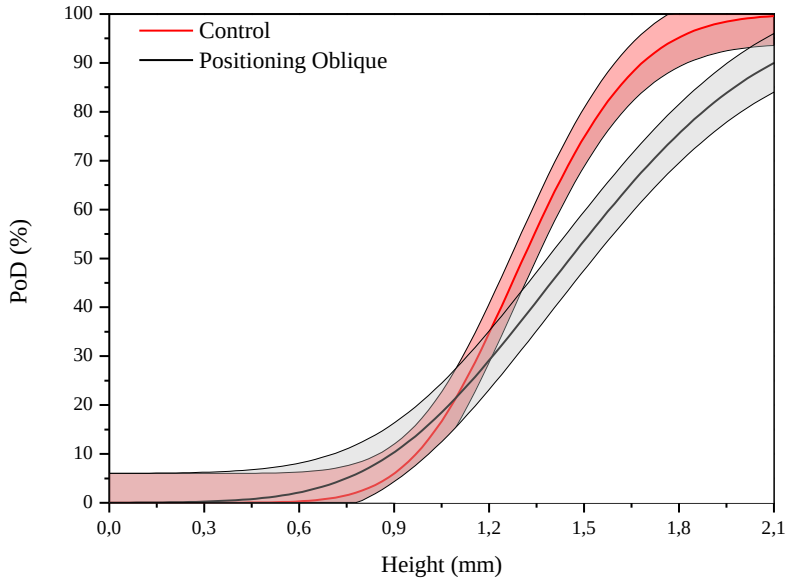

Figure 38: Effect of flaw positioning on simulated POD: CONTROL (length along rotation axis) vs oblique position

4.1.3.4.2 Center Coordinates

It is also possible to establish the positioning of the defect regarding its "center coordinates". CONTROL considers the flaw's positioning center in 150 mm regarding the axial direction and 0 degrees regarding the θ coordinate. The changed configurations evaluate the change of axial positioning to 160 mm and θ equals to ± 3º. Figure 39 presents results concerning changes on center coordinates on y and shows no important effect on the simulated POD curve, although the changed configuration results on a POD less steeper. Figures 40 and 41 show, respectively, the simulated POD curves for θ + 3º and -3º and present two different behaviors. While the result for θ + 3º indicates a loss in reliability, the results for θ - 3º seems to present no significant change on reliability, but the curve presents a flatter behavior suggesting a slight loss of reliability.

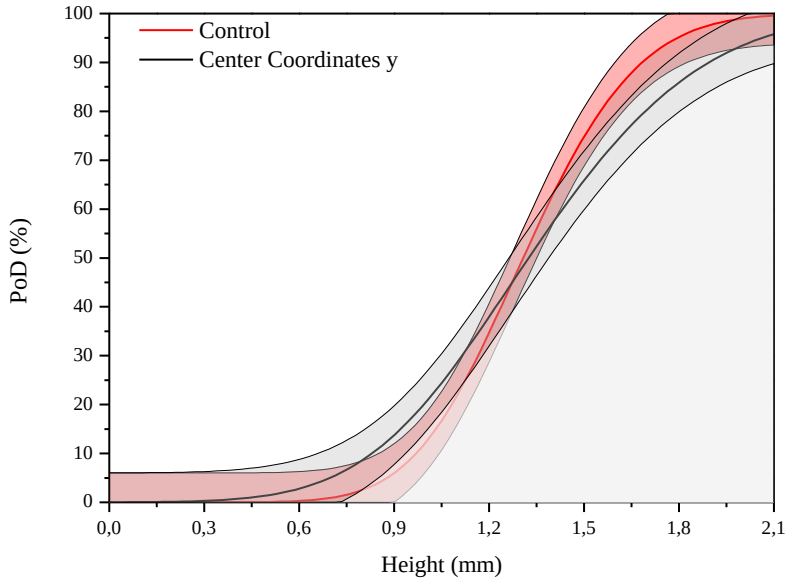

Figure 39: Effect of center coordinates *y* on simulated POD: CONTROL (150 mm) vs axial position = 160 mm

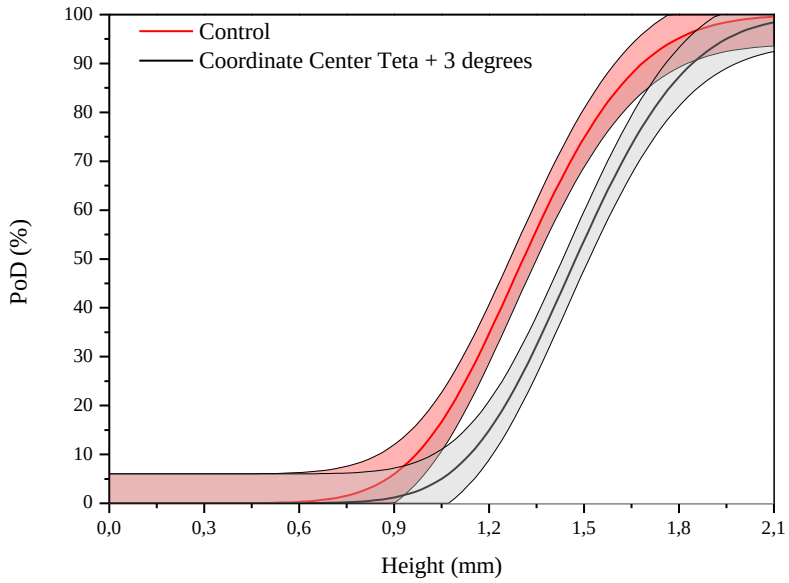

Figure 40: Effect of center coordinates θ on simulated POD: CONTROL (θ=0) vs θ + 3º

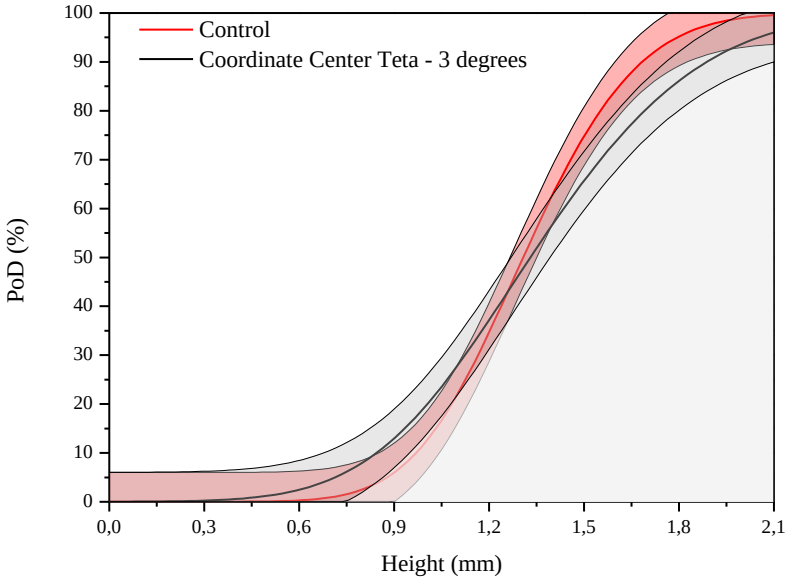

Figure 41: Effect of center coordinates θ on simulated POD: CONTROL (θ=0) vs θ - 3º

4.1.3.4.3 Orientation

There are three possible "orientations" that the rectangular flaw can admit: "tilt", "skew" and "disorientation". Disorientation can be understood as being the defect orientation regarding *x* axis as illustrated on Figures 42 while tilt is the orientation regarding *y* axis and skew is the orientation regarding *z* axis. As an observation, it is important not to confuse flaw disorientation with the probe's crystal disorientation angle.

In real experimental inspections, it is very difficult to determine the orientation of a certain flaw and, for that reason, the three orientations will be considered uncertainty parameters (UP). Although, it is worth testing the possibility that just one of the orientations is uncertain or two of them are uncertain. CONTROL admits all three being uncertain and states that their PDF is normal. This subsection will analyze first the possibility that not all of them are UP and then, will analyze the impact of changes on the PDF considered. Figures 43, 44 and 45 show the POD curves considering just one orientation as UP but still respecting a normal PDF.

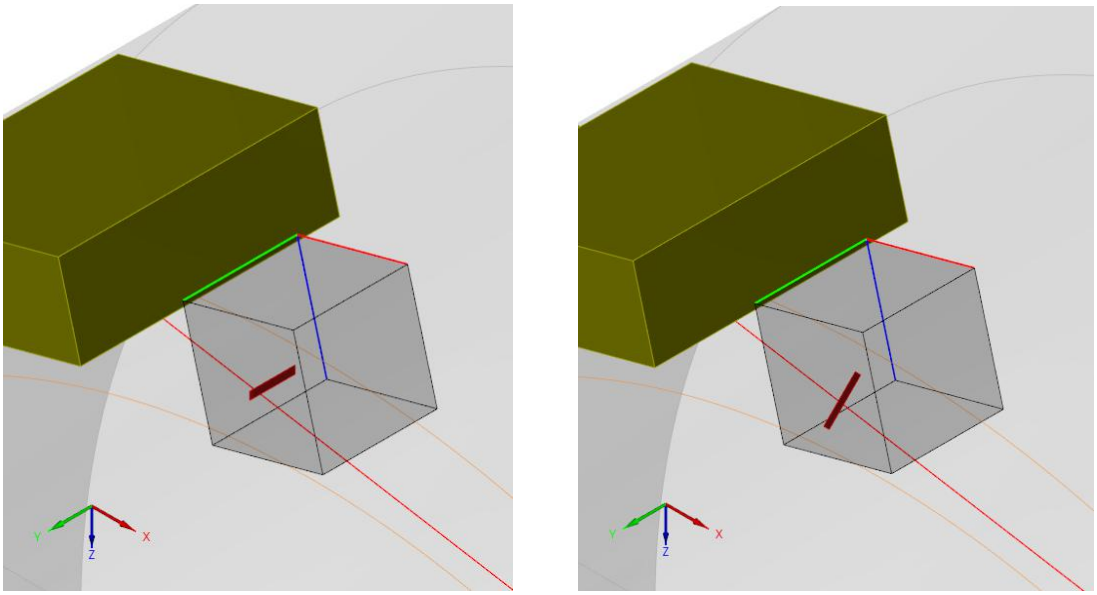

Figure 42: Disorientation representation: rotation on *x* axis

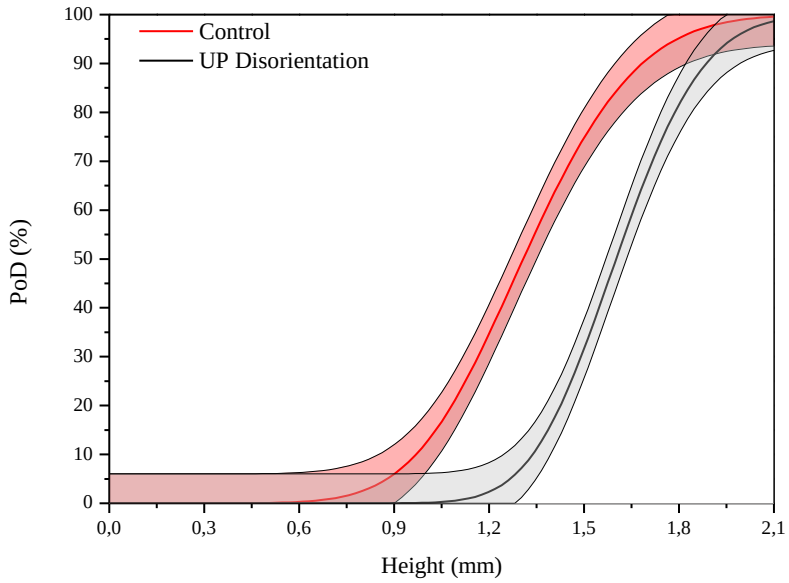

Figure 43: Effect of uncertainty parameters on simulated POD: CONTROL (disorientation + skew + tilt under normal PDF) vs Disorientation (normal PDF)

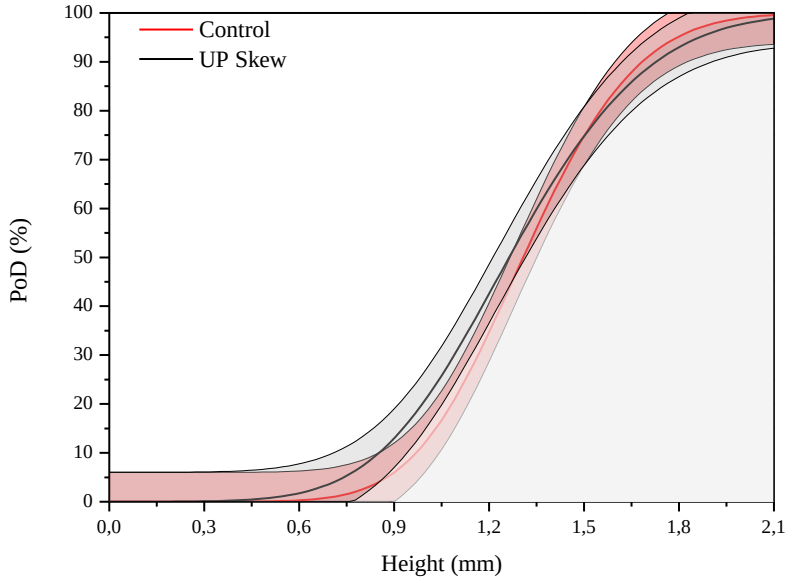

Figure 44: Effect of uncertainty parameters on simulated POD: CONTROL (disorientation + skew + tilt under normal PDF) vs Skew (normal PDF)

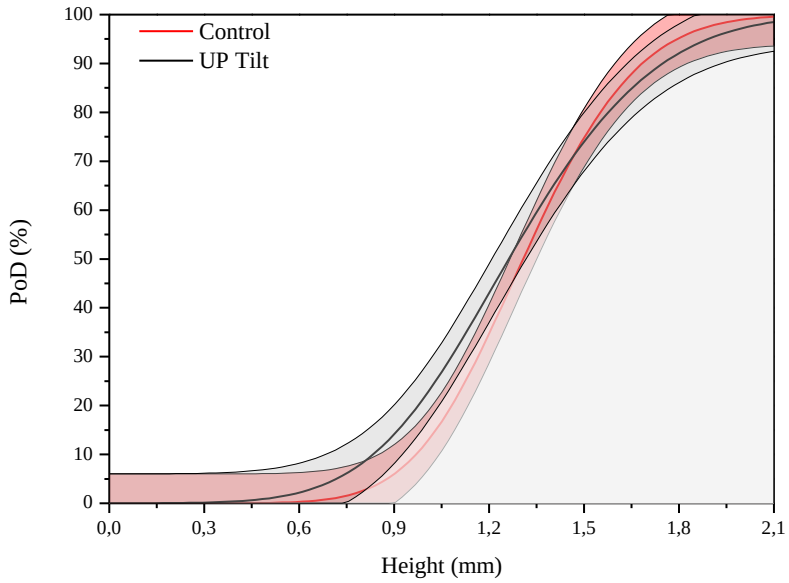

Figure 45: Effect of uncertainty parameters on simulated POD: CONTROL (disorientation + skew + tilt under normal PDF) vs Tilt (normal PDF)

Surprisingly, results show that if only skew or tilt are considered as uncertainty parameter, the resulting reliability presents the same behavior that when skew, tilt and disorientation together are considered. As for the disorientation, when only this type of orientation is chosen as uncertainty parameter, reliability decreases.

The next natural step is to evaluate the combination of the UP compared with CONTROL configuration. In other words, if two of the orientations as UP are considered instead of only one, as used above, and compare those combinations with CONTROL that admits all three orientations as being UP, what will be the effect on reliability? Figures 46, 47 and 48 show the results for those combinations of two UP. Results show a modest loss of reliability in comparison to Figures 46 and 47 but no significant difference on Figure 48.

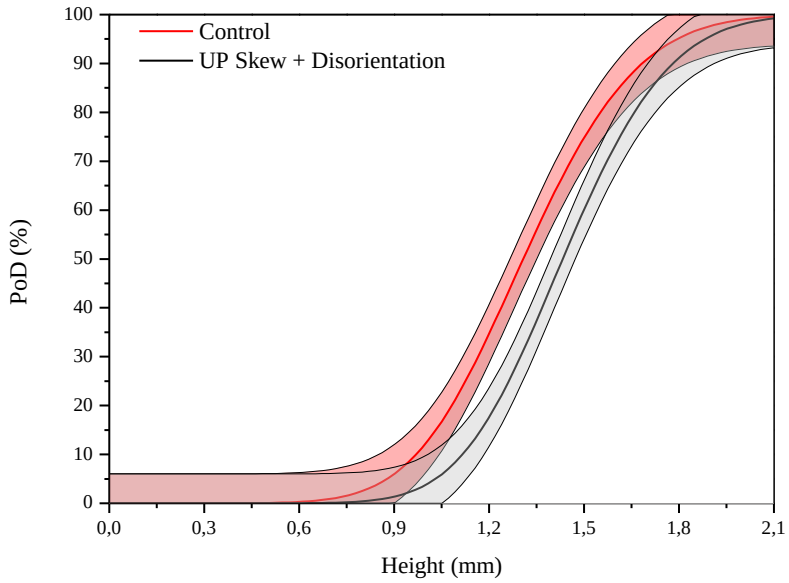

Figure 46: Effect of uncertainty parameters on simulated POD: CONTROL (disorientation + skew + tilt under normal PDF) vs Skew + Disorientation (normal PDF)

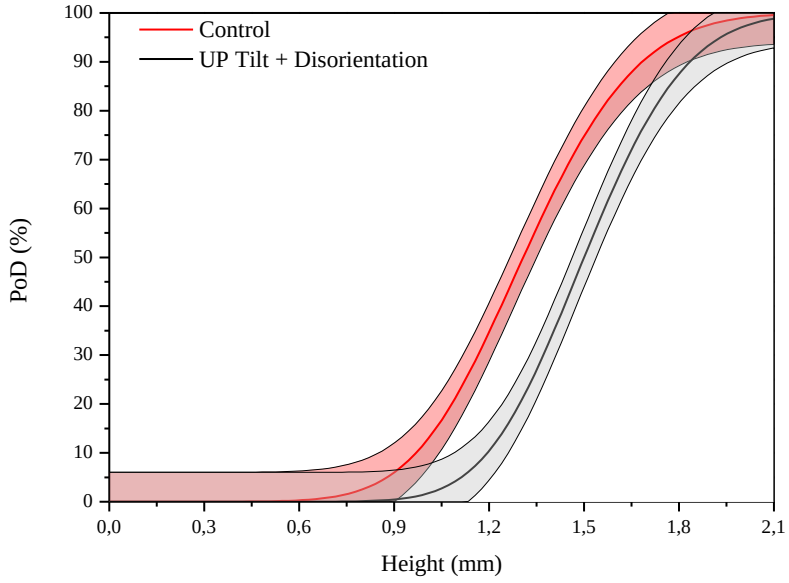

Figure 47: Effect of uncertainty parameters on simulated POD: CONTROL (disorientation + skew + tilt under normal PDF) vs Tilt + Disorientation (normal PDF)

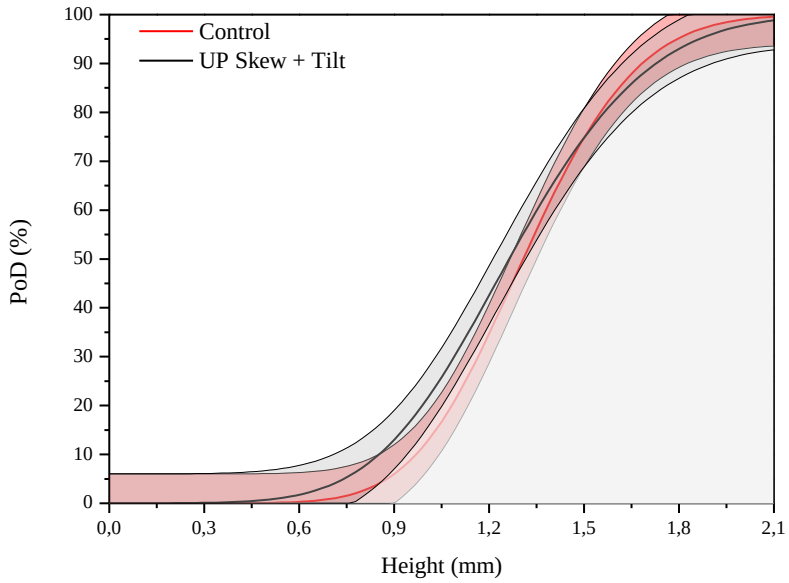

Figure 48: Effect of uncertainty parameters on simulated POD: CONTROL (disorientation + skew + tilt under normal PDF) vs Skew + Tilt (normal PDF)

The presented result could make the user wonder if this behavior is in any level linked to the chosen PDF. In order to evaluate the role of the PDF, the same simulations were re-run but taking into account a uniform PDF for the UP. For that matter, Figures 49, 50 and 51 show the results for single UP presenting a uniform probability distribution function.

Results show that all three POD curves differ from CONTROL, which was expected. The single UP behavior which was unexpected. While the disorientation under Normal PDF was more impacting on reliability when compared to the three UP all together, it was the tilt orientation that provided more impact under a uniform PDF.

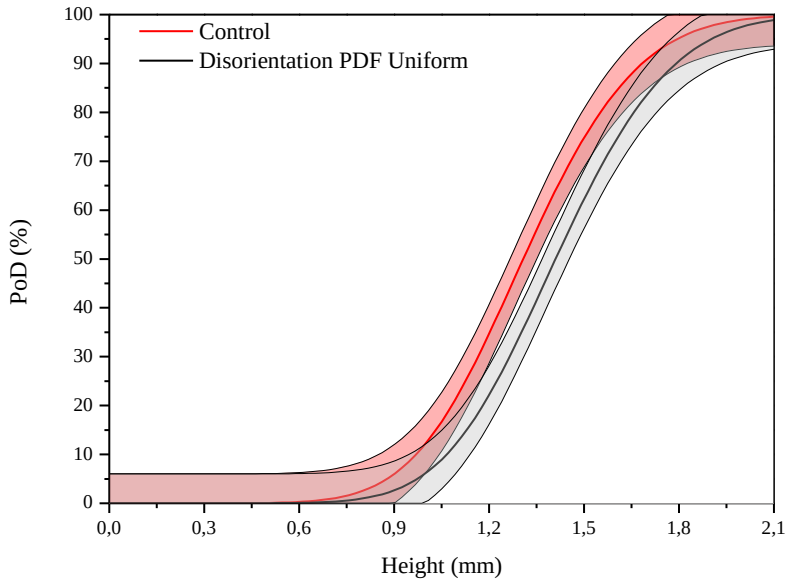

Figure 49: Effect of uncertainty parameters on simulated POD: CONTROL (disorientation + skew + tilt under normal PDF) vs Disorientation (uniform PDF)

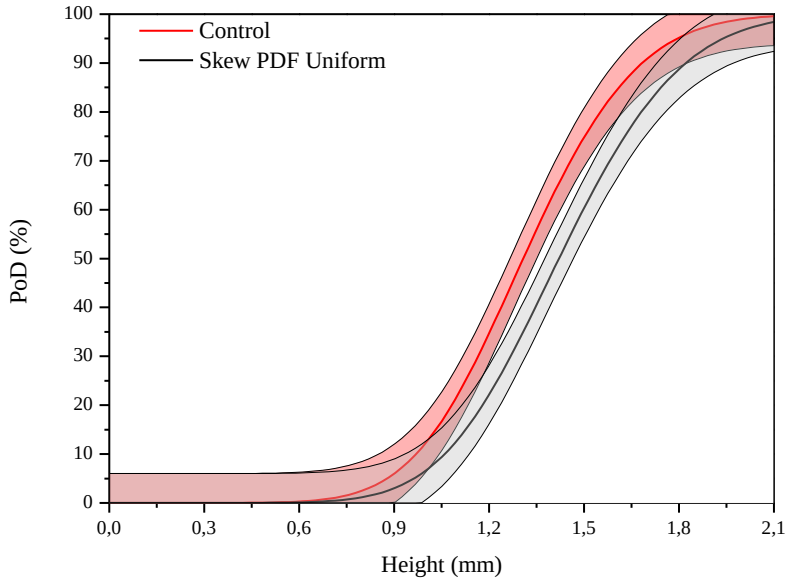

Figure 50: Effect of uncertainty parameters on simulated POD: CONTROL (disorientation + skew + tilt under normal PDF) vs Skew (uniform PDF)

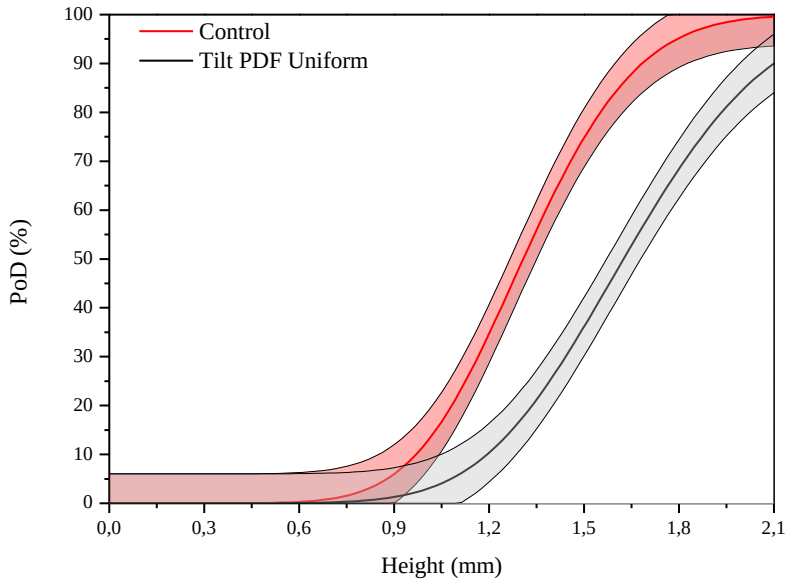

Figure 51: Effect of uncertainty parameters on simulated POD: CONTROL (disorientation + skew + tilt under normal PDF) vs Tilt (uniform PDF)

Once the change of the PDF from Normal to Uniform provided different results for single uncertainty parameters, it was considered worthwhile testing a third PDF type in order to evaluate properly its impact on reliability. Therefore, the same study performed by changing Normal PDF to Uniform PDF was also made changing Normal PDF to Log-Normal. Figures 52, 53 and 54 show complete different results that the ones shown so far regarding PDF. As such, it can be concluded that there an optimal way to establish the PDF for each UP, and that this optimal way has to be evaluated case-by-case considering each inspection variability according to an expert opinion.

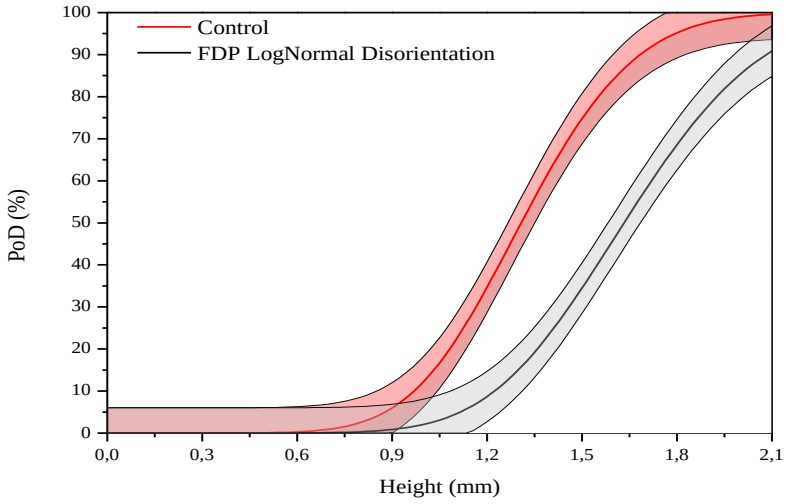

Figure 52: Effect of uncertainty parameters on simulated POD: CONTROL (disorientation + skew + tilt under normal PDF) vs Disorientation (Lognormal PDF)

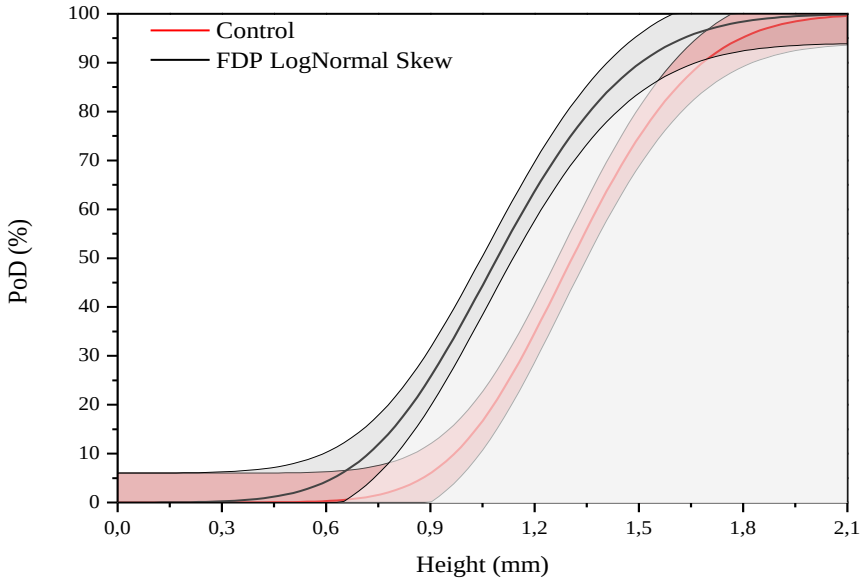

Figure 53: Effect of uncertainty parameters on simulated POD: CONTROL (disorientation + skew + tilt under normal PDF) vs Skew (Lognormal PDF)

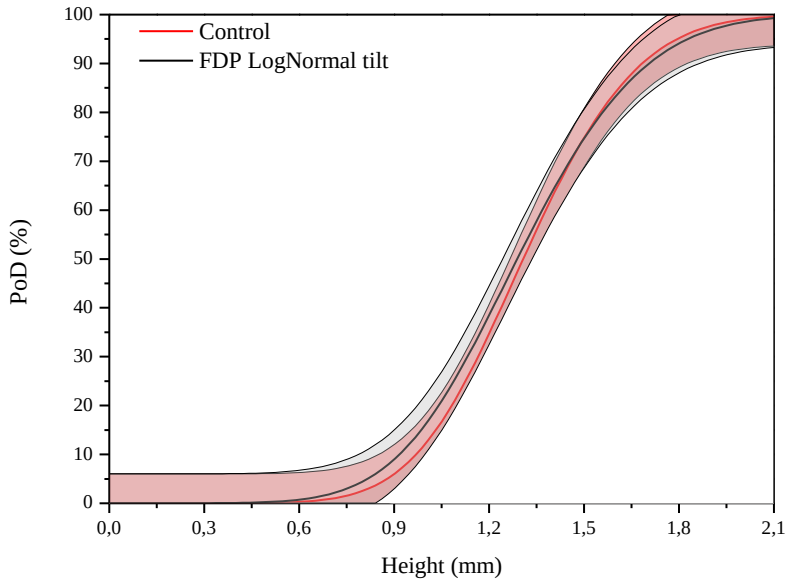

Figure 54: Effect of uncertainty parameters on simulated POD: CONTROL (disorientation + skew + tilt under normal PDF) vs Tilt (Lognormal PDF)

Summarizing the virtual tests presented concerning PDF of uncertainty parameters, here are the studies performed:

- Skew + Disorientation + Tilt under Normal PDF vs Skew under Normal PDF
- Skew + Disorientation + Tilt under Normal PDF vs Tilt under Normal PDF
- Skew + Disorientation + Tilt under Normal PDF vs Disorientation under Normal PDF
- Skew + Disorientation + Tilt under Normal PDF vs Skew + Tilt under Normal PDF
- Skew + Disorientation + Tilt under Normal PDF vs Skew + Disorientation under Normal PDF
- Skew + Disorientation + Tilt under Normal PDF vs Tilt + Skew under Normal PDF
- Skew + Disorientation + Tilt under Normal PDF vs Skew under Uniform PDF
- Skew + Disorientation + Tilt under Normal PDF vs Tilt under Uniform PDF
- Skew + Disorientation + Tilt under Normal PDF vs Disorientation under Uniform PDF
- Skew + Disorientation + Tilt under Normal PDF vs Skew under LogNormal PDF

- Skew + Disorientation + Tilt under Normal PDF vs Tilt under LogNormal PDF
- Skew + Disorientation + Tilt under Normal PDF vs Disorientation under LogNormal PDF

Since each UP parameter was tested in two different PDF, the present analysis requires also to test all three parameters under Uniform and LogNormal PDF. Figures 55 shows the results for skew + tilt + disorientation under Uniform PDF and it can be seen that the tested POD curve reveals a drop on reliability. The simulation of the configuration skew + tilt + disorientation under LogNormal PDF could not be concluded due to calculations errors.

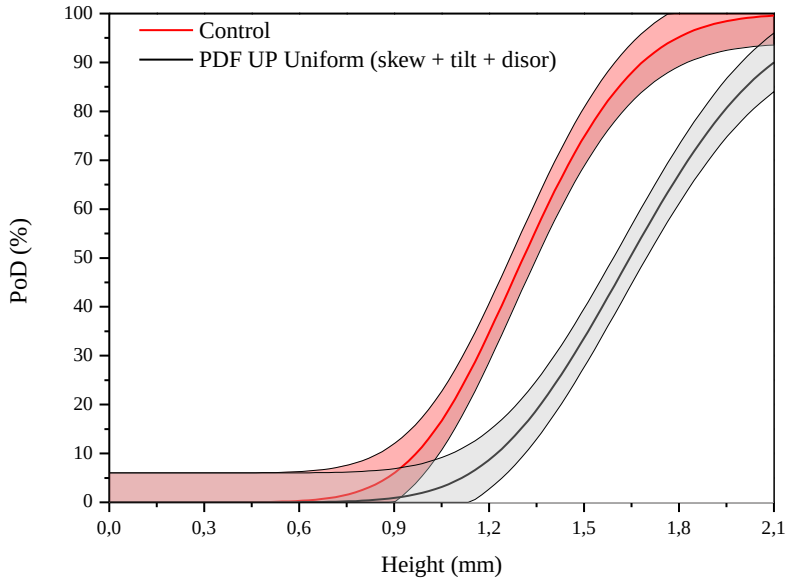

Figure 55: Effect of uncertainty parameters on simulated POD: CONTROL (disorientation + skew + tilt under normal PDF) vs disorientation + skew + tilt under Uniform PDF

4.1.3.4.4 Ligament

"Ligament" is the parameter that defines the distance of the flaw positioning to the specimen surface, as can be seen in Figure 56. In the experimental configuration, the HAZ defect is located in a depth of 0.5 mm below the external surface of the pipe. Therefore, the CONTROL configuration also considered a depth of 0.5 mm. The changed configuration

admits the depth being 1.0 mm, so the ligament also assumes this value. Results shown in Figure 57 suggest that increasing the depth of the defect under the CONTROL's inspection configuration, decreases the reliability and the probability of detection of defects with height between 0.9 mm and 1.7 mm suffers a drop.

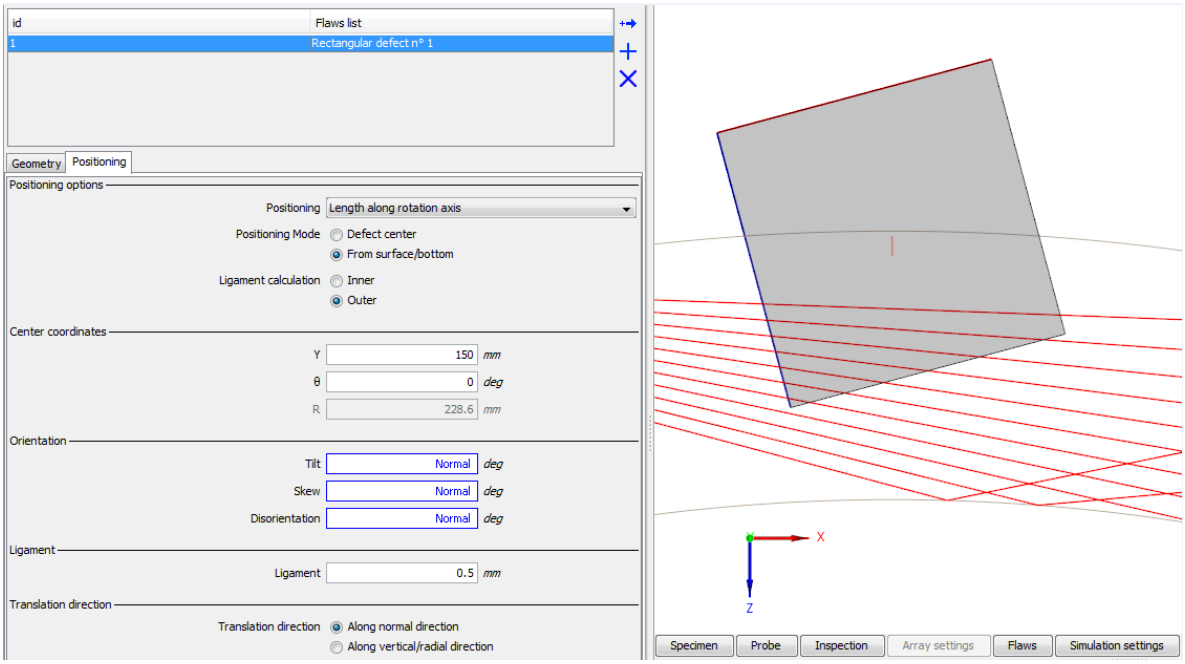

Figure 56: CIVA's representation of ligament as being the distance between the flaw and the pipe's surface (outer or inner)

Another parameter concerning ligament called "ligament calculation" was also tested. Ligament calculation defines which specimen surface is considered when the depth of the flaw is set up: inner or outer surface. The real defect was located 0.5 mm from outer surface, so the virtual model followed this configuration. The changed configuration located the flaw 0.5 mm from the inner surface and computational calculation of reliability was not completed because the flaw just could not be detected anymore.

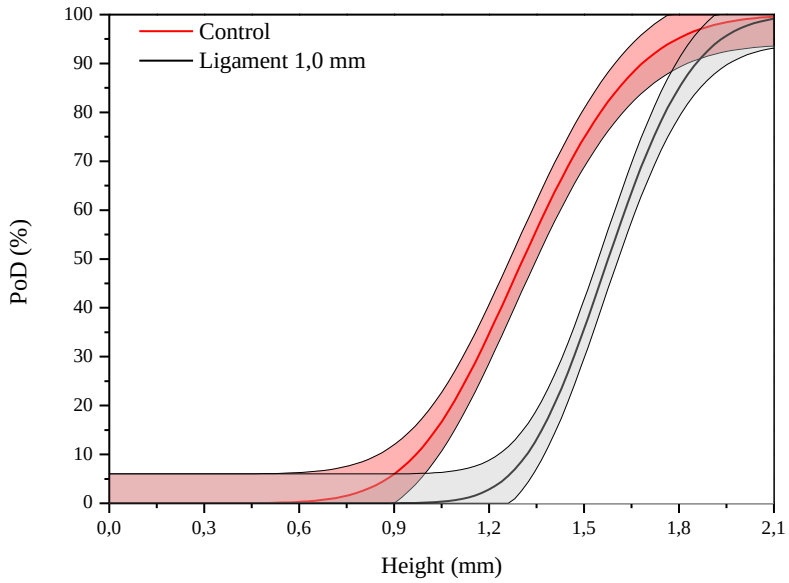

Figure 57: Effect of ligament on simulated POD: CONTROL (0.5 mm) vs ligament of 1.0 mm

4.1.3.5 POD

There are many parameters that can be tested regarding the POD tab in CIVA: variables parameters, extraction and computation options. In theory, every parameter under POD tab should impact in some way the simulated POD curve. The significance of this impact is analyzed in the present section.

4.1.3.5.1 Number of Characteristic Values

The characteristic value is the geometric parameter that is taken into account to build the POD curve. In this case, the characteristic value is the flaw height. Once the height range is established (0.35 mm to 2.1 mm), the "number of character value" represents how many height values are going to be considered, maintaining a fixed step value. In other words, there are 60 height values between 0.35 mm and 2.1 mm which are equally divided. In terms of a reliability study, a large number of characteristic values should increase the quality of the

result, improving the confidence bound. However, this strategy increases costs, not only experimentally but also computationally. Changing the step value and keeping the start and stop values, which are 0.35 mm and 2.1 mm, has the same impact as changing the number of characteristic values, therefore, this analysis will be considered done. This subsection verifies the impact on the POD curve once the number of characteristic values is either increased or decreased. Surprisingly, results shown in Figures 58 and 59 indicate that the reliability decreases in both cases.

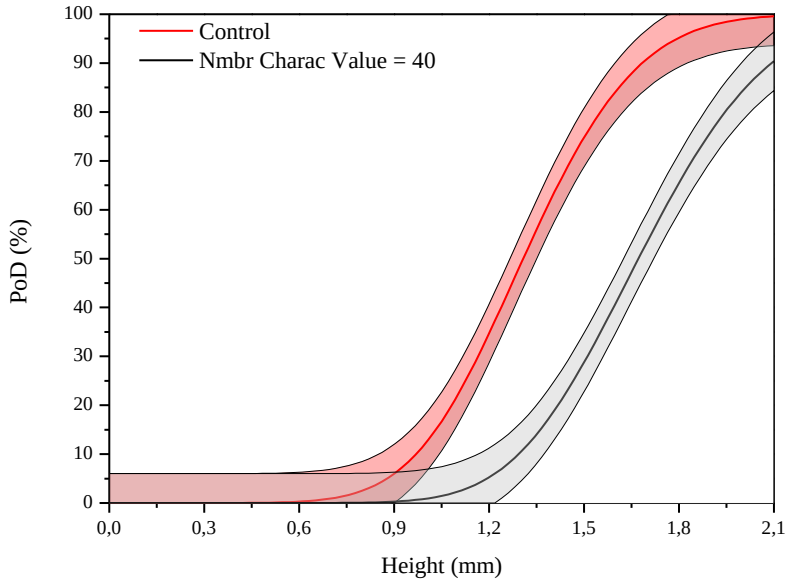

Figure 58: Effect of number of characteristic values on simulated POD: CONTROL (60) vs 40 Characteristic Values

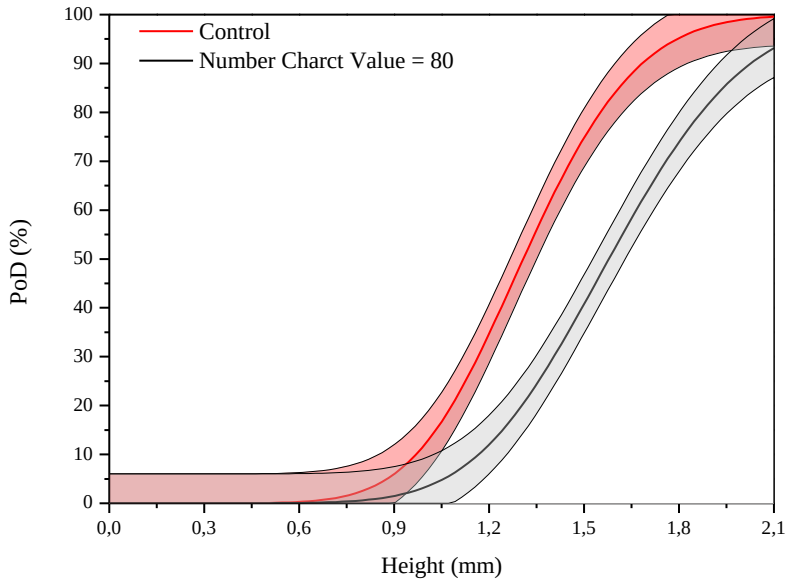

Figure 59: Effect of number of characteristic values on simulated POD: CONTROL (60) vs 80 Characteristic Values

4.1.3.5.2 Number of Samples

The "number of samples" determines how many times each "characteristic value" (parameter explained in the prior subsection) will be inspected. The CONTROL configuration sets up a sample value = 5 which means that all 60 characteristic values will be inspected five times summing a total of 300 inspections which is the same number of experimental inspections. It is interesting to evaluate the effect when the number of samples is either increased or decreased. Figures 60 and 61 present those results, showing the simulated POD curve for 3 and 7 samples, respectively. They show that for a reduced number of samples, reliability remains the same while for an enhanced number of samples, reliability decreases.

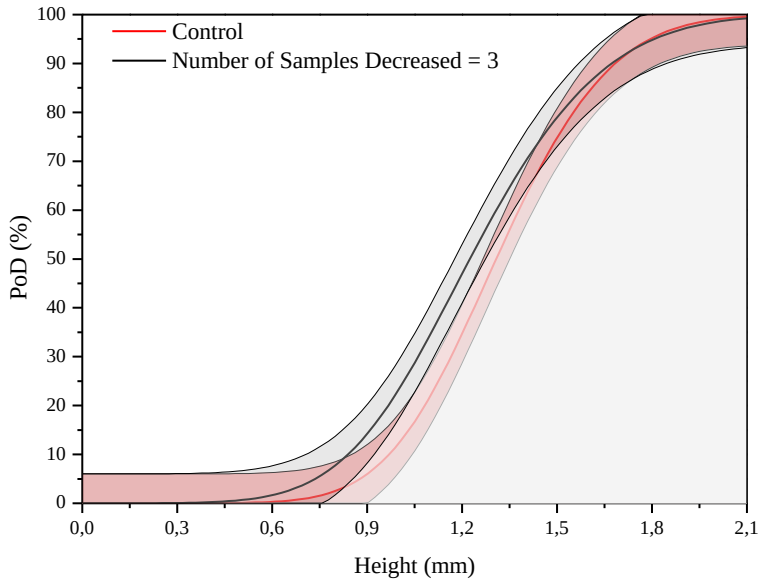

Figure 60: Effect of number samples on simulated POD: CONTROL (5) vs Number of samples = 3

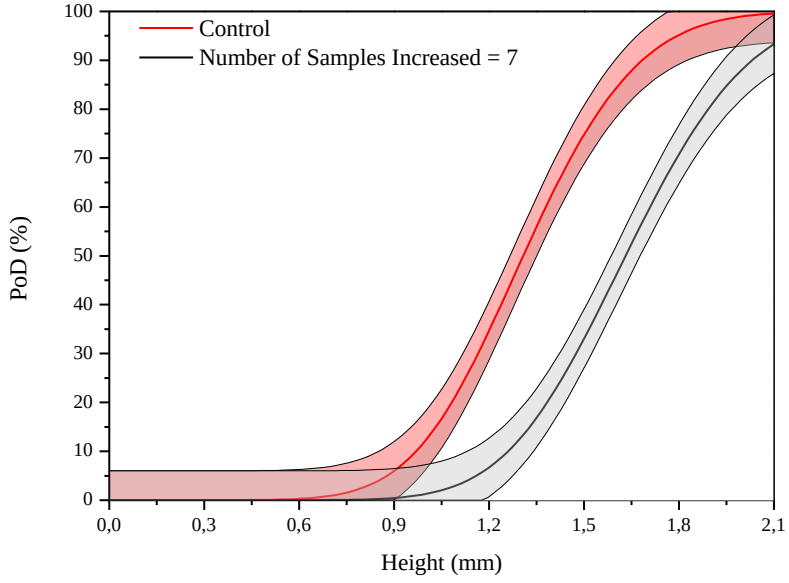

Figure 61: Effect of number samples on simulated POD: CONTROL (5) vs Number of samples = 7

4.1.3.5.3 Number of Classes for Histogram

Regarding uncertainty parameters, CIVA provides a histogram showing the minimum and maximum values considered as well as the mean and standard deviation values. This particularly parameter does not present any physical meaning, but as it is a parameter that can be changed by the user, it is worthy to describe its impact on reliability simulation. It is possible to change the number of classes used in this histogram and CONTROL configuration considered 10 classes while the changed configuration considered 50 classes. Figure 62 shows the impact of increasing histogram number and suggests that the resulting POD curve suffered a loss of reliability.

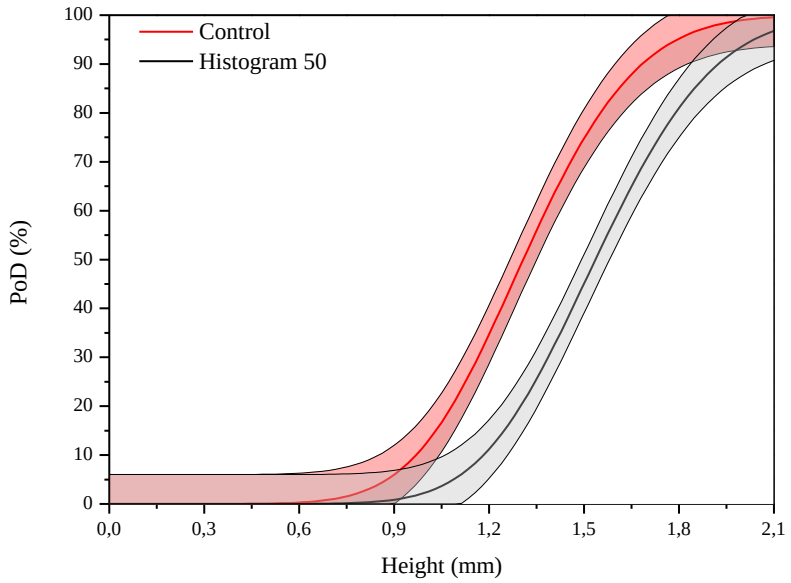

Figure 62: Number of Classes for Histogram: CONTROL (10) vs 50 classes for histogram

4.1.3.5.4 Randomization

As described by the proposed approach to assign variability to simulates data, it is possible to randomize the uncertainty parameters set of data. The resulting simulated POD curve is impacted by this randomization as shown in Figure 63 but not enough to differ from the

original POD curve without randomization. This capability provides certain variability on the UP values but are incapable to change the reliability.

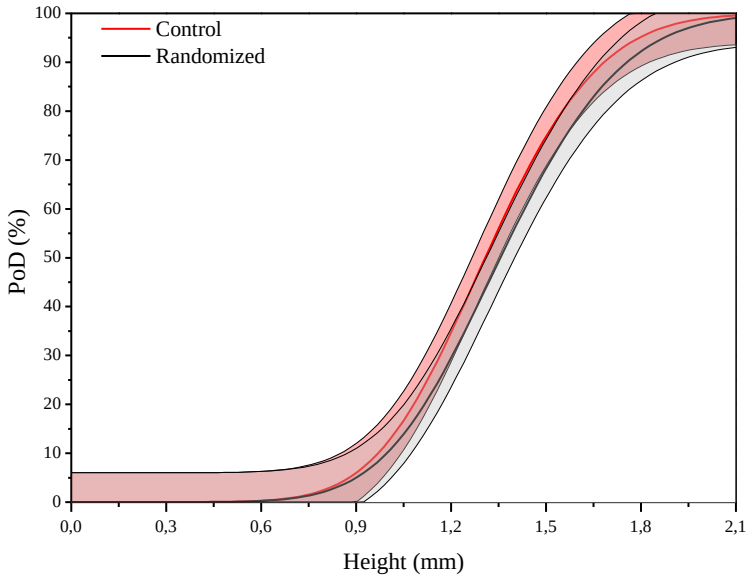

Figure 63: Effect of randomization on simulated POD: CONTROL (no randomization) vs UP randomized

4.1.3.5.5 Extraction of Signal Response

Under the Extraction tab, the user can choose how the signal response values will be considered to build the simulated POD. The amplitude of the ultrasonic signal can be extracted considering the "absolute maximum values", "positive maximum values" or "negative maximum values". CONTROL configuration considered the extraction of all absolute maximum values while the changed configuration considered the positive values. The resulting POD curves and enlighten that no significant difference between them is produced by that parameter.

4.2 SIMULATED RELEVANT PARAMETERS

This section will present the most significant parameters for simulated POD curves. These are the parameters that initial users of CIVA software must dedicate more attention if they aim to simulate POD curves. It is important to mention that the results presented in this section are not final, but relative to the changes tested on the CONTROL configuration. They come from a sensitivity analysis regarding CONTROL configuration and compared with incremental changes. It is a comparative study between two distinct virtual configurations. If the original configuration is completely different from the one used in this dissertation (CONTROL) it is possible that incremental changes would provide a different impact on the simulated POD. The present study must be perceived as a preliminary approach concerning comparing simulated POD curves and as a guideline for users starting to simulate reliability on CIVA.

Having said that, Table 4 shows a list of all tested parameters that, in any level, changed the behavior of the POD curve.

The next natural step is to use the collected information to fit parameters of the CONTROL configuration aiming to reach better agreement of the simulated POD with experimental data. Nevertheless, not all parameters can be changed on prior simulation because it would lose its representativeness regarding experimental inspections.

Parameters such as specimen material or geometry, crystal shape or dimension, coupling medium or probe's frequency are examples of parameters that cannot be modified, otherwise the simulation will not be describing the reality of the physical experiment. The following section addresses some parameters that can be modified in order to optimize the fitting of the simulated POD curve.

Table 4: List of tested parameters that changed simulated POD curve behavior

Module	Parameter	Prior Condition	Tested Condition	Effect on POD
Simulation Settings	Full Incident Beam	Disabled	Enabled	Increases
	Accuracy Defect	1	2	Decreases
Specimen	Outer Diameter	457.2 mm	467.2 mm	Increases
	Thickness	28.32 mm	38.32 mm	Increases
	Roughness	20 mm	100 mm	Decreases
	Material	Steel	Stainless steel 410	Decreases
Probe	Crystal Shape	Rectangular	Circular	Decreases
	Crystal Dimension	8.0 mm x 9.0 mm	9.6 mm x 10.8 mm	Decreases
	Squint Angle	0	+ 2 degrees	Decreases
	Squint Angle	0	- 2 degrees	Decreases
	Disorientation Angle	0	+ 2 degrees	Decreases
	Wedge Material	Plexiglas	Rexolite	Increases
	Frequency	4 MHz	4.8 MHz	Decreases
	Frequency	4 MHz	3.2 MHz	Increases
Inspection	Adapted Probe	Disabled	Enabled	Increases
	Coupling Meddium	Water	Glycerin	Increases
	Scanning Steps	190	19	Decreases
Flaws	Positioning	Lenght along rotation axis	Oblique	Decreases
	Center coordinates θ	0	+ 3 degrees	Decreases
	Ligament	0.5 mm	1.0 mm	Decreases
POD	Number Characteristic Values	60	80	Decreases
	Number Characteristic Values	60	40	Decreases
	Number of Samples	5	3	Decreases
	Number Classes Histogram	10	50	Decreases
	Uncertain Parameters	Skew + Tilt + Disorientation	Disorientation	Decreases
	Uncertain Parameters	Skew + Tilt + Disorientation	Tilt + Disorientation	Decreases
	Uncertain Parameters	Skew + Tilt + Disorientation	Tilt PDF Uniform	Decreases
	Uncertain Parameters	Skew + Tilt + Disorientation	Skew LogNormal	Increases
	Uncertain Parameters	Skew + Tilt + Disorientation	Disorientaion LogNormal	Decreases
	Uncertain Parameters	Skew + Tilt + Disorientation	Skew + Tilt + Disorientaion LogNormal	Decreases

4.3 OPTIMAL FITTING OF SIMULATED POD CURVES

The Sensitivity Analysis carried on regarding CIVA software in order to stablish the impact of changes on the virtual inspections parameters that will or will not affect the simulated POD curve, generated a subset of parameters that were considered the most relevant ones on that matter.

Figure 64 describes the process of optimizing the CONTROL configuration as being an interactive and systematic process that should lead to a more representative simulated POD curve when compared with the experimental one.

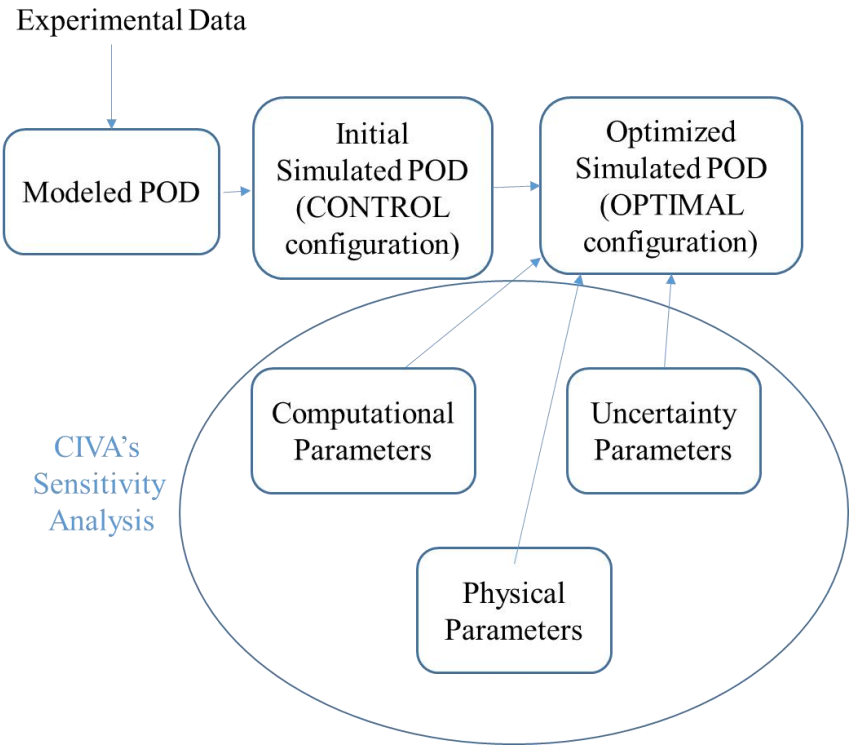

Figure 64: Description diagram on the process of optimizing the fitting of CONTROL configuration

In other words, based on the most relevant parameters that effect the simulated POD curves behavior presented on the previous section, it is possible to set up a new CONTROL configuration, which is called OPTIMAL configuration, aiming to build a simulated POD curve that presents the a_{90} and $a_{90/95}$ parameters that more closely match the experimental ones. Nevertheless, before changing the virtual parameters of the prior configuration, it is important to consider some aspects:

- Not all parameters that effect the simulated POD curve can be changed, as explained in section 4.2;
- It takes only one example of combination of changed parameters to indicate that it is possible to calibrate simulated POD curves;
- The calibration example presented is one combination parameters of the many combinations that possibly could improve the curve behavior.

Improving the simulated curve behavior does not mean that the parameters that are responsible for increasing reliability have to be taken into account in the calibration process. The aim is not to change the behavior of the curve by increasing the reliability, but to more closely match the experimental results. Having said that, the chosen parameters to re-run the CONTROL simulation were parameters that originally decreased the simulated reliability but are perfectly suitable to turn the simulated POD more realistic.

Based on the results presented on Table 4, some of the experimental parameters were reassessed regarding the actual inspected pipe and the AUT system. Therefore, all changed performed on the CONTROL configurations were corroborated by results coming from the sensitivity analysis. The parameters that were reassessed and used as optimal fitting set parameters were: full incident beam, ligament, squint angle, roughness and the crystal refraction angle due to wear.

The full incident beam option was activated to re-run CONTROL simulation instead of plane wave approximation for incident beam because it is natural to think that, in real inspections, the ultrasonic beam doesn't suffer computational approximations being a truly incident beam.

Even though the crystal refraction angle was not elected as one of the most relevant parameters, it is important to take into account the expert's opinion that it is a source of system perturbation and that this parameter combined with the others can result in an effect on the simulated POD curve that cannot be disregarded. After the experimental inspections, a wear measurement was performed on the corresponding wedge. It could be verified that, in fact, evidence existed of wear that resulted on a 2° inclination between the wedge and the pipe surface. Therefore, this inclination value was transferred to the refraction angle of the probe, changing it from 60° to 58° in the OPTIMAL configuration.

In the same way, the original ligament value was considered inaccurate and could be changed on OPTIMAL configuration. This consideration could be made because there is no certainty about the depth of the inserted defect. No destructive test was carried out to verify the exact depth of the graphite piece after the gouging opening and the consequent closing through SMAW. Although, after the Sensitivity Analysis results, inspections on the actual pipe trough phased array techniques suggested that the depth of the considered defect was not 0.5 mm but approximately 1.0 mm.

About the roughness, as the sensitivity analysis suggested, the value was updated to 48 μm, based on specific literature (HONEYWELL, 2009) regarding brand new oil pipes such as API 5L X-65.

Concerning squint angle and its important effect on simulated POD curves, this possible perturbation should be considered by the OPTIMAL configuration. As the squint angle could not be measured at the actual AUT system probes, a medium value was attributed to it on the OPTIMAL configuration. Therefore, at the re-run CONTROL simulation, squint angle was set to 1°.

Table 5: Parameters considered on the optimal fitting process

	Incident Beam	Squint Angle	Refraction Angle	Ligament	Roughness
CONTROL configuration	Approximated	0	60°	0.5 mm	20 mm
OPTIMAL configuration	Full Incident	1°	58°	1.0 mm	48 μm

Figure 65 shows the results for the simulated POD curve regarding the calibration coming from the changes made on the parameters listed on Table 5.

Extracting the results for a_{90} and $a_{90/95}$, Figure 66 demonstrates the clear improvement that the calibration provided on the simulated POD curve, as presented in greater detail in Table 6. It is obvious that calibration procedures could enhance the simulation POD curve results bringing them closer to real results increasing the agreement between simulates and experimental reliability prediction.

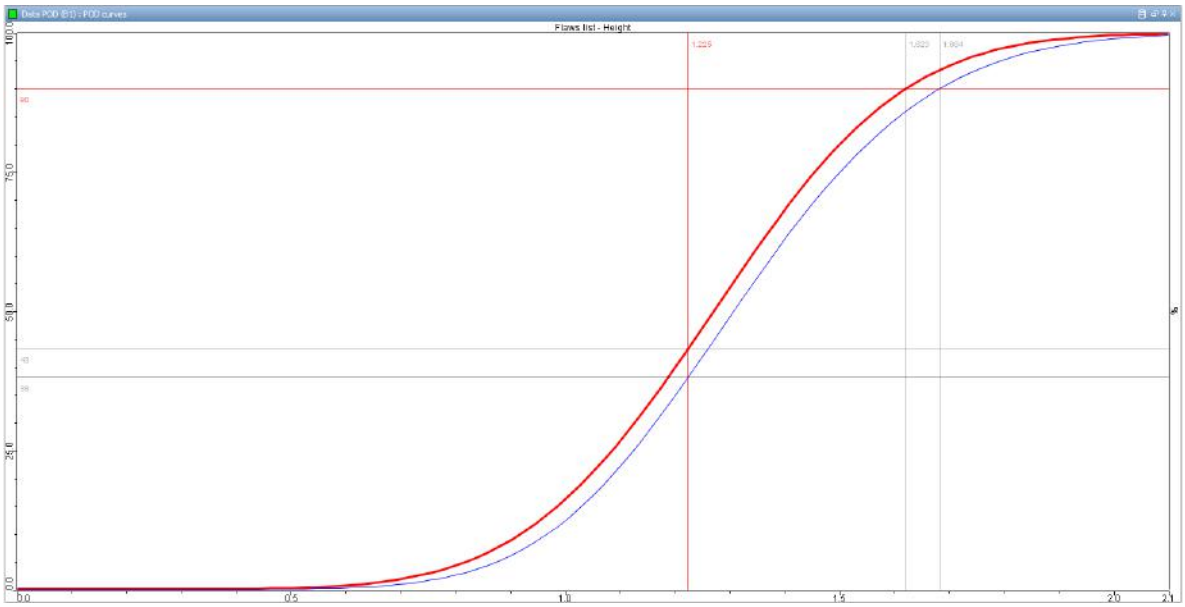

Figure 65: Simulated POD curve after calibration changes were made on CONTROL configuration: OPTIMAL configuration

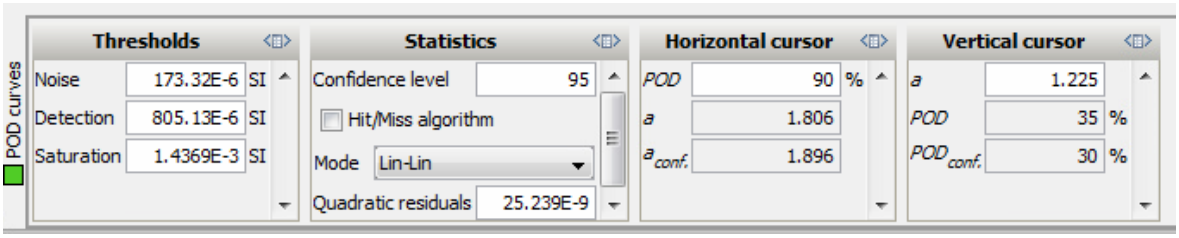

Figure 66: Details of the POD curve parameters values regarding OPTIMAL configuration set up

Table 6: Comparison between experimental and simulates results before and after calibration procedures regarding HAZ defects

	Experimental	CONTROL configuration	OPTIMAL configuration
a_{50}	1.366 mm	1.271 mm	1.359 mm
a_{90}	1.892 mm	1.623 mm	1.806 mm
$a_{90/95}$	1.961 mm	1.664 mm	1.896 mm

4.4 OPTIMAL FITTING TRANSFER TO A TEST SET OF DATA

This section addresses the evaluation of the optimal fitting transfer regarding the selected set of parameters to a similar but different set of experimental data. While the usual method used to transfer reliability involves applying a transfer function to the inspection configuration, as shown in Figure 1, this study will address to that matter in a different systematic and interactive way, as described by Figure 67 below.

Using computational simulation tools, more specifically, CIVA software, it is possible to transfer unfailingly the computational parameters as well as the uncertainty parameters the exact way as they present themselves in the OPTIMAL configuration. The new physical parameters box on the below diagram refers to the differences regarding the TEST configuration as they consider a new type of defect and its positioning.

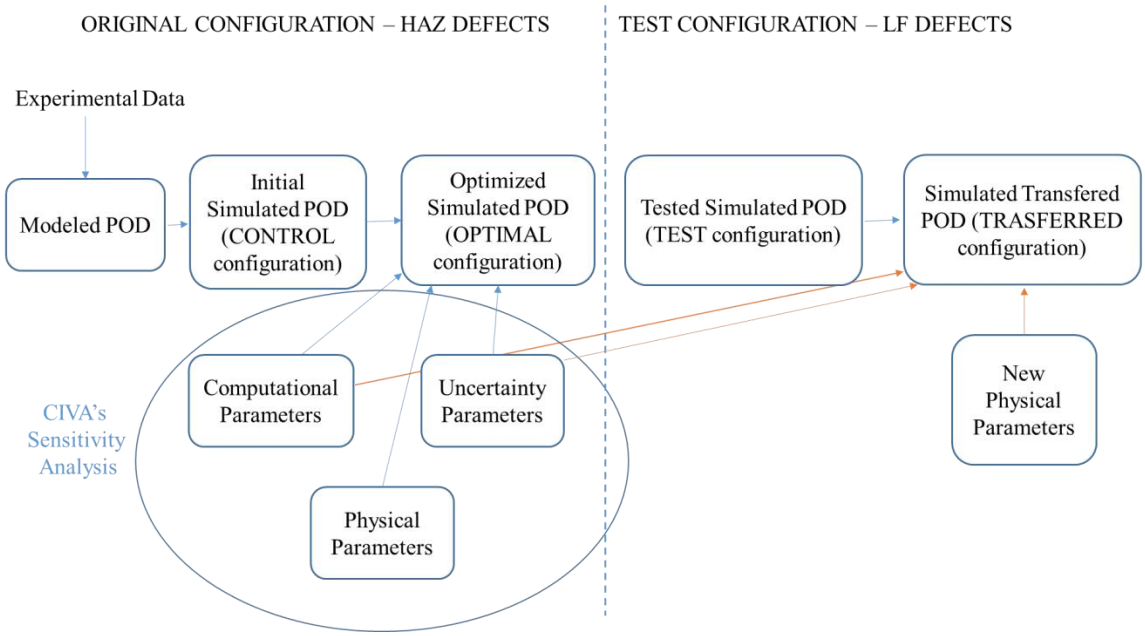

Figure 67: Description diagram on the process of transferring the fitting of OPTIMAL configuration to the TRANSFERRED configuration

The main question that will be analyzed in this section is whether or not it is possible to use the same set of optimal fitting parameters to a different experimental-based simulation and still maintain the improvements that were observed on the original experimental-based simulation.

In order to answer that question, the experimental results were revisited and another subset of defects was chosen. While the first subset of defects and inspections procedures culminated on the CONTROL configuration described on Table 3, this new subset of defects are represented virtually by the TEST configuration. The main difference between the two sets of experimental and simulated data sets is that the first one took into account cracks in the HAZ defects located at 0.5 mm (theoretical value) from the surface and the second subset of defects are the type lack of fusion (LF) in a depth of 7.0 mm from the outer pipe's surface.

The second type of defects and their positioning were inserted in the virtual environment of CIVA and the UT inspection simulations were performed. The resulting POD curve is shown in Figure 68, whereas the a_{90} and $a_{90/95}$ parameters are given in Table 7.

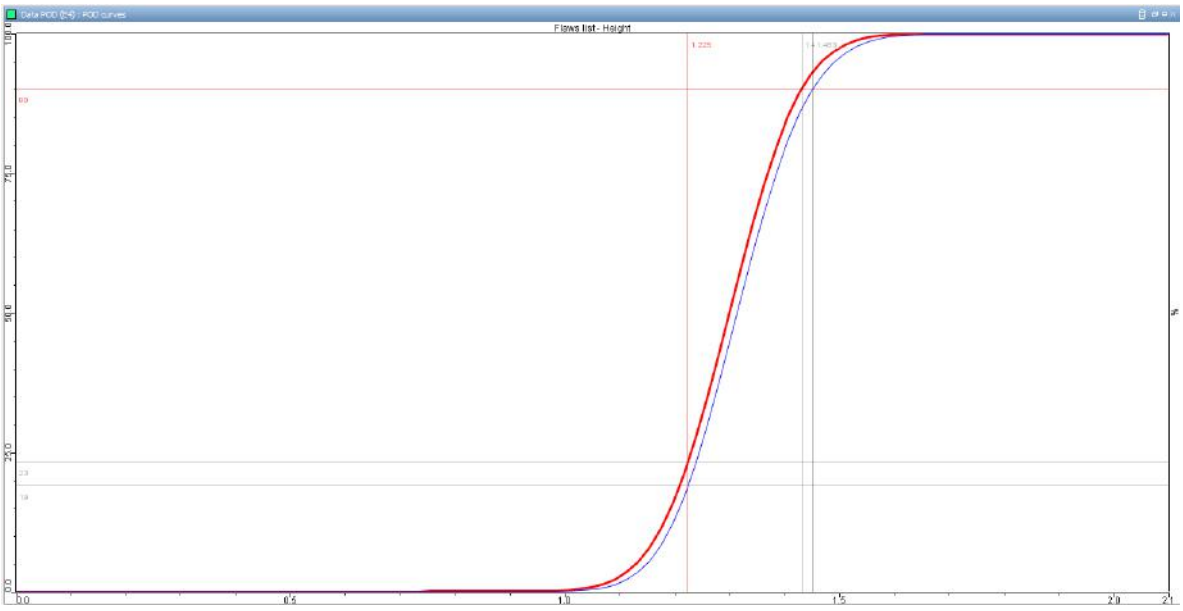

Figure 68: Simulated POD curve regarding TEST configuration: LF defects

Table 7: POD curves values regarding TEST configuration – LF Defects

	a_{90}	$a_{90/95}$
TEST Configuration	1.433 mm	1.453 mm

Reliability analysis coming from experimental inspections revealed a_{90} and $a_{90/95}$ values of 1.26 mm and 1.493 mm respectively, while simulated results were equal to 1.433 mm and 1.453 mm respectively, as shown in the table above. As such, the simulated curve shows an excellent agreement to experimental results. Once the simulated and experimental reliability results for LF defects show enough agreement, the process of trying the optimal fitting applied on HAZ defects on LF defects in order to evaluate its behavior under transference of reliability could proceed.

Thus, Figures 69 shows the simulated curve after the calibration parameters of HAZ defects were applied on LF defects, defining from now on, the TRANSFERRED configuration.

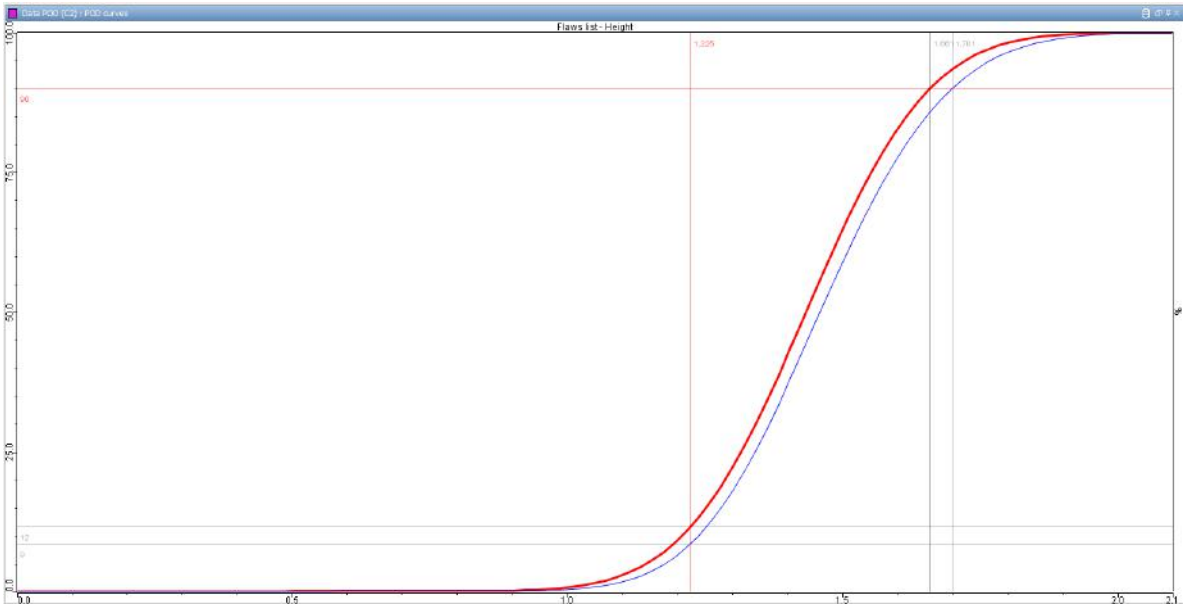

Figure 69: Simulated POD curve regarding TRANSFERRED configuration

Table 8: POD curves values regarding TRANSFERRED configuration – LF Defects

	a_{90}	$a_{90/95}$
TRANSFERRED Configuration	1.661 mm	1.701 mm

The previous results, however, demonstrate that applying an optimal fitting used on a certain virtual inspection configuration to a different one could decrease the simulated result's agreement to experimental ones, which is corroborated by the comparison presented on Table 9.

Table 9: Comparison between experimental results and simulated results before and after transferring HAZ defects optimal fitting procedures to LF defects

	Experimental	TEST configuration	TRANSFERRED configuration
a_{90}	1.260 mm	1.433 mm	1.661 mm
$a_{90/95}$	1.493 mm	1.453 mm	1.701 mm

The analysis made so far concerning transferring optimal fitting to a different inspection configuration demonstrate what the common sense states: if two different virtual inspections are carried on, the results regarding simulated POD curve will be different. Although, the contribution of the present study is to stablish a systematic way to approach the reliability transferring subject and to shade light on the parameters that should be considered in a more careful way.

Nevertheless, it is already possible to infer that there is a certain set of parameters that can be transferred to different inspection's configuration without prejudice of simulated reliability. These parameters are all parameters listed on Table 10 that were tested in sensitivity analysis process and were found not to impact the POD curve behavior.

What can be seen based on the results it that:

- Not all virtual parameters impact on the simulated POD curve;
- There is a subset of virtual parameters that effect the simulated POD curve enhancing or decreasing reliability, which are mostly physical parameters and uncertainty parameters;
- It is possible to perform an optimal fitting on the simulated POD curve addressing corrections on virtual parameters in order to enhance the agreement regarding experimental curves;
- It is possible to transfer virtual parameters to a different inspection condition without impacting on simulated reliability. According to that, the interactive analysis process developed suggests that transferring computational and most uncertainty parameters to a different inspection configuration should be able to optimize the fitting for this different configuration through simulation, but further studies must be carried on.

Table 10: Parameters that can be transferred to a different virtual inspection configuration without impacting on simulated POD curve behavior

Module	Parameter	CONTROL Configuration	Sensitivity Analysis Test
Simulation Settings	Invloved Modes	Transverse Waves	Transverse + Longitudinal Waves
	Account for Mode Conversion	Disabled	Enabled
	Specipen Echoes - Model	Kirchhoff	Specular
	Number of Half Skips	Max. 1	Max. 5
	Sensitivity Zone	Enabled	Disabled
	Sensitivity Zone Dimension	30 mm x 30 mm x 30 mm	25 mm x 25 mm x 25 mm
		30 mm x 30 mm x 30 mm	35 mm x 35 mm x 35 mm
	Gate	Enabled	Disabled
		Echo Max Absolute	Fisrt Echo Synchronization
	Accuracy Field	1	2
	Account for Attenuation	Enabled	Disabled
Specimen	Roughness	20 mm	4 mm
	Material	Steel	Stainless steel 302
Probe	Signal Choice	Imported	Gaussian
Inspection	Bottom Medium	Air	Oil
	Scanning Reversed	Disabled	Enabled
Flaws	Positioning	Lenght along rotation axis	Oblique
	Orientation as UP - PDF Normal	Skew + Tilt + Disorientation	Skew
	Orientation as UP - PDF Normal	Skew + Tilt + Disorientation	Tilt
	Orientation as UP - PDF Normal	Skew + Tilt + Disorientation	Skew + Tilt
	Orientation as UP	Skew + Tilt + Disorientation (PDF Normal)	Tilt (PDF LogNormal)
POD	Extraction of Signal Response	absolute maximum values	positive values

5 CONCLUSIONS

Through the software CIVA, a sensitivity analysis on the POD curve was carried out on both computational and physical parameters. The tested parameters were changed one at a time and their effect on the resulting simulated POD curve was analyzed based on a comparison to a control simulation. This control simulation came from a series of experimental results carried on by UT on API 5L X-65 pipes and used as reference to validate and calibrate the simulated POD curves. The defect considered by the control configuration was a crack on the HAZ.

Based on sensitivity analyzes results, a subset of virtual parameters was selected as being the most relevant ones based on their impact on the resulting POD curve, increasing or decreasing the reliability of the inspection. Thus, these most relevant parameters guided an OPTIMAL configuration by changing some of the virtual inspection parameters, namely: ligament, incident beam, roughness, squint angle and crystal's refraction angle. Adjusting these parameters values on the OPTIMAL configuration and setting up a calibration set, the resulting POD curve could be driven closer to the experimental one, increasing the agreement between simulated POD curves and experimental POD curves.

Regarding transfer function, a different inspection configuration based on a different type of defect (lack of fusion) was selected in order to analyze the feasibility of transferring optimal fitting parameters to a new simulation configuration. The simulated POD curve based on the actual experimental inspections on the LF defect was build showing excellent agreement with experimental POD curve regarding the same type of defect. After applying the OPTIMAL configuration set of optimal fitting parameters to LF configuration, the resulting POD curve showed a loss of agreement comparing to experimental results. Nevertheless, it is possible to stablish that there is a set of parameters that can be transferred based on sensitivity analysis results. Therefore, results suggest that it might be possible to transfer reliability results using CIVA if the interactive process of finding the suitable parameters are optimized and better understood, which implies on further studies on the matter.

In addition to that, the Transfer Function is described by Thompson *et al.* (2009) as a new set of empirical data which will be compared to a baseline POD curve. This new set of data has

to be brought up through careful laboratory experiments and/or physics-based computer simulation. Nevertheless, the present dissertation attempts to compare the reliability of two different sets of data from non-laboratorial inspections using physics-based simulation. In order to perform additional tests regarding the effectiveness of the transfer function, controlled experiments could be necessary.

On the other hand, this dissertation also studied in a systematic way the effects on variability of physical parameters on the resulting reliability through physics-based computer simulation using CIVA. This particularly systematic study characterizes a FMA (Full Model Assisted) approach, described by Thompson *et al.* (2009). Having said that, it is accurate to imply that in this dissertation, the unified approach was carried on successfully.

Finally, it is important to mention that no further comparison with the current state of art status concerning optimal fitting of POD simulated curves and their validation through non-laboratorial experimental AUT data could be elaborated because the present study found no reference regarding all the topics at a single reference.

6 FUTURE WORK

Suggested future work regarding validating and calibrating simulated POD curves using CIVA from experimental UT inspections include:

- The Proposed Method to apply variability on simulated data can be improved by, for example, a non-uniform variation of the variability value along the POD curve.
- Some few CIVA parameters that were not tested on the sensitivity analysis for being considered less important could be tested.
- Combinations of simulation parameters could also be tested by sensitivity analysis. In other words, evaluation of double changes of virtual parameters or different simulation order could be tested.
- Different experimental sets of data could be taken into account to verify if there is any difference on the sensitivity analysis results.
- Different combinations of parameters could be tested in order to optimize the simulated POD curves.
- A second set of experimental data could be taken into account to evaluate the possibility of transferring calibration set of parameters to another experimental-virtual configuration.

REFERENCES

ANNIS, C., GANDOSSI, L., MARTIN, O., 2013, “Optimal sample size for probability of detection curves”, In: Nuclear Engineering and Design, pp. 98-115, USA.

BERENS, A., 1989, NDE Reliability Data Analysis, Nondestructive Evaluation and Quality Control. In: ASM Metals Data Book, Vol. 17, 5th ed., pp. 689–701, USA, December.

BO LU, DARMON, M., POTEL, C., ZERNOV, V., 2012, “Models Comparison for the Scattering of an Acoustic Wave on Immersed Targets”. 10th Anglo-French Acoustics Conference, Series 353, Journal of Physics, pp. 1-10.

CAFLISCH, R. E., 1998, “Monte Carlo and quasi-Monte Carlo Methods”. In: Acta Numerica, Vol. 7, pp. 1-49, UK.

CALMON, P. JENSON, F., REBOUD, C., 2015, “Simulated probability of detection maps in case of non-monotonic signal response”, In: AIP Conference Proceedings, v. 1650, pp. 1933, USA.

CARBONI, M., CANTINI, S., 2012, “A “Model assisted probability of detection” approach for ultrasonic inspection of railways axles”, In: 18th World Conference on Nondestructive Testing, pp. 2457-2466, South Africa.

CHAPIUS, B., JENSON, F., CALMON, P., DiCRISCI, G., HAMILTON, J., POMIÉ, L., 2014, “Simulation supported PoD curves for automated ultrasonic testing of pipeline girth welds”. In: Welding in the World. Vol. 58, Issue 4, pp 433-441, Springer Link (last viewed: May-28th-2018).

CHAPIUS, B., CALMON, P., JENSON, F., 2018, Best Practices for the Use of Simulation in POD Curves Estimation – Application to OU Weld Inspection. 1 ed. Switzerland, IIW-Springer.

CHIOU, C., MARGETAN, F., THOMPSON, R. B., 1995, "Ultrasonic Signal Characterization of Flat-Bottom Holes in Titanium Alloys: Experiment and Theory". Review of Progress in Quantitative Nondestructive Evaluation, pp. 2121-2128, USA.

CHIOU, C., MARGETAN, F., THOMPSON, R. B., 1996, "Modeling of Ultrasonic Signals from Weak Inclusions". Review of Progress in Quantitative Nondestructive Evaluation, pp. 49-55, USA.

DEMEYER, S., JENSON, F., DOMINGUEZ., N., IAKOVLEVA, E., 2012, "Transfer Function Approach Based on Simulations Results for the Determination of POD Curves". Review of Progress in Quantitative Nondestructive Evaluation, pp. 1757-1764, USA.

FERTIG, K.W., RICHARDSON, J.M., 1983, "Computer Simulation of Probability of Detection", Review of Progress in Quantitative Nondestructive Evaluation, pp. 147-169, New York, USA.

GEORGIOU. G., 2006, Probability of Detection (POD) Curves – Derivation, applications and limitations. UK, Health and Safety Executive.

HARDING, C.A., HUGO, G. R., BOWLES, S. L., 2009, "Application on Model-Assisted POD Using a Transfer Function Approach". Review of Progress in Quantitative Nondestructive Evaluation, pp. 1792-1799, USA.

HONEYWELL, J., 2009. "How sensitive is pressure drop due to friction with roughness factor?" Campbell online Tip of the Month, Mar 2009: http://www.jmcampbell.com/tip-of-the-month/2009/03/how-sensitive-is-pressure-drop-due-to-friction-with-roughness-factor/

KANZLER, D., MULLER, C., ROSENTHAL, M., EWERT, U., PITKANEN, J., 2013, "An Approach to the POD Based on Real Defects Using Destructive Testing and Bayesian Statistics". In 9th International Conference on NDE in Relation to Structural Integrity for Nuclear and Pressurized Components, pp. 191-199, USA.

KRAUTKRAMER, J. and KRAUTKRAMER, H, 1990, "Ultrasonic Testing of Materials", 4th/revised edition, Springer Verlag.

MARK, A. F., FAN, Z., AZOUGH, F., LOWE, M. J. S. WITHERS, P. J., 2014, "Investigation of the Elastic/Crystallographic Anisotropy of Welds for Improved Ultrasonic Inspections". In: Material Characterization, Vol. 98, pp. 47-53, USA.

MATZKANIN, G., YOLKEN, T., 2001, A Technology Assessment of Probability of Detection (POD) for Nondestructive Evaluation (NDE), 1 Ed, NTIAC/Defense Technical Information Center, USA.

MEEKER, W. Q., JENG, S., CHIOU, C., THOMPSON, R. B., 1998, "Improved Methodology for Inspection Reliability Assessment for Detecting Synthetic Hard Alpha Inclusions in Titanium". Review of Progress in Quantitative Nondestructive Evaluation, pp. 2061-2068, USA.

MEYER, R. M., CRAWFORD, S. L., LAREAU, J. P., ANDERSON, M. T., 2014, Review of Literature for Model Assisted Probability of Detection. Pacific Northwest National Laboratory for U.S. Nuclear Regulatory Commission, USA.

MIL-HDBK-1823A, 2009, Nondestructive Evaluation System Reliability Assessment. USA, US Department of Defense.

NAKAGAWA, N., BEISSNER, R. E., 1990, "Probability of Tight Crack Detection Via Eddy-Current Inspection", Review of Progress in Quantitative Nondestructive Evaluation, pp. 893 - 899, New York, USA.

OGILVT, J. A., 1993, "Model for Predicting Ultrasonic Pulse-Echo Probability of Detection". NDT&E International, vol. 26, no. 1, Butterworth-Heinemann LTD., pp. 19-29, UK.

RAJESH, S. N., UDPA, L. and UDPA, S. S., 1993, "Estimation of Eddy Current Probability of Detection (POD) Using Finite Element Method". Review of Progress in Quantitative Nondestructive Evaluation, pp. 2365-2372, New York, USA.

REBOUD, C., PINECHOT, G., PAILLARD, S., JENSON, F., 2010, “Statistical study of ECT detection around fasteners using simulation based PoD curves”, In: AIP Conference Proceedings, v. 1211 - 1903, USA.

REVERDY, F. DOMINGUEZ, N., 2013, “NDT Modeling tools applied to the aeronautic industry: examples in CIVA”, In: 5th International Symposium on NDT in Aerospace, Singapore.

SCHMERR Jr., LESTER W. and THOMPSON, D. O., 1997, “The Role of Modeling in NDE Standards”. The Center for Nondestructive Evaluation, Iowa State University, pp. 25, USA.

SIMOLA, K., PULKKINEN, U., 1998, “Models for Non-destructive Inspection Data," Reliability Engineering and System Safety, pp. 1 – 52, USA.

SMITH, K., THOMPSON, B., MEEKER, B., GRAY, T., BRASCHE, L., 2007, “Model-Assisted Probability of Detection Validation for Immersion Ultrassonic Application”. Review of Progress in Quantitative Nondestructive Evaluation, pp. 1816-1822, USA.

THOMPSON, D. O., SCHMEER, Jr., LESTER W., 1993, "Uses for Model-Based Probability of Detection Curves". Nondestructive Inspection of Aging Aircraft, SPIE, pp. 121- 132, USA.

THOMPSON, R. B., BRASCHE, L. J., FORSYTH, D., LINDGREN, E. A., SWINDELL, P., WINFREE, W., 2009, “Recent Advances in Model-Assisted Probability of Detection”. Presented at 4th European-American Workshop of Reliability of NDE, Germany.

TOW, D. M., REUTER, W. G., 1998, "Probabilistic Model for Pressure Vessel Reliability Incorporating Fracture Mechanics and Nondestructive Examination ". Nondestructive Evaluation of Utilities and Pipelines II, SPIE, pp. 168-176, USA.

WALL, M., WEDGWOOD, F. A., 1994, "NDT - Value for Money". Insight, vol. 36, no. 10, British Institute of Nondestructive Testing, pp. 782-790, UK.

WALL, M., 1997, "Modelling of NDT Reliability and Applying Corrections for Human Factors", European-American Workshop, Determination of Reliability and Validation Methods of NDE, pp. 87-98, Germany.